Bernadette Reiter, BSc

Determination of eicosanoids in dOFM samples by HPLC-MS

MASTER'S THESIS

to achieve the university degree of

Diplom-Ingenieurin

Master's degree programme: Technical Chemistry

submitted to

Graz University of Technology

Supervisor

Univ.-Prof. Mag. Dr.rer.nat. Kevin Francesconi

Institute of Chemistry
University of Graz

DI Dr. Anita Eberl
JOANNEUM RESEARCH Forschungsgesellschaft mbH - HEALTH, Graz

Graz, September 2015

AFFIDAVIT

I declare that I have authored this thesis independently, that I have not used other than the declared sources/resources, and that I have explicitly indicated all material which has been quoted either literally or by content from the sources used. The text document uploaded to TUGRAZonline is identical to the present master‘s thesis dissertation.

Date

Signature

Danksagung

An dieser Stelle möchte ich mich bei all jenen Personen bedanken, die durch ihre fachliche und persönliche Unterstützung zum Gelingen meiner Diplomarbeit beigetragen haben.

Mein Dank gilt Herrn Univ.-Prof. Mag. Dr.rer.nat. Kevin Francesconi für das Übernehmen der universitären Betreuung, kompetente Beratung und für dessen Hilfsbereitschaft, die er mir stets entgegenbrachte.

Ebenso danke ich Frau DI^{in} Dr.^{in} Anita Eberl für ihre stetige Unterstützung, ohne ihre Bemühungen wäre diese Arbeit nicht zustande gekommen. Weiterhin danke ich Herrn Mag. Dr. Christoph Magnes für die Bereitstellung des spannenden Forschungsthemas. Bedanken möchte ich mich auch bei allen anderen Mitarbeitern und meinen liebgewonnenen KollegInnen der Joanneum Research Forschungsgesellschaft mbH für die Hilfsbereitschaft und gute Zusammenarbeit.

Ein ganz besonderer Dank gilt meiner Familie, meinen Eltern und Geschwistern, die mir mein Studium ermöglicht haben. Sie haben mich immer wieder ermutigt und mich stets in all meinen Entscheidungen unterstützt.

Abschließend möchte ich noch all meinen FreundInnen danken, die mir immer mit Rat und Tat zur Seite gestanden haben und dank denen ich auf eine äußerst schöne Studienzeit zurückblicken kann.

Danke!

Abstract

Eicosanoids represent a large class of bioactive lipid mediators. As such they are involved in numerous physiological processes where they play an important role especially in inflammation. The usually very low in vivo concentrations of eicosanoids require highly sensitive analytical methods. The aim of this thesis was to develop a multi-analyte HPLC-MS method for the quantification of important eicosanoids in diluted interstitial fluid. It deals with the development, optimisation and also critical evaluation of the whole analytical process, from sampling to measurement with the focus on mass spectrometric detection. Additionally, a comparison of the developed high resolution MS method with triple quadrupole MS was performed and discussed.

Analytes were extracted by solid phase extraction in 96-well-plate format. An HPLC method was developed to separate 10 representatives of prostaglandins, thromboxanes, hydroxyeicosapentaenoic and hydroxyeicosatetraenoic acids in a 16 min run prior to MS detection. Because all eicosanoids contain a carboxyl-group, charged molecules were formed by electrospray ionisation in negative mode. Analytes were qualified and quantified via fragmentation on a high resolution Q Exactive™ MS. Method development was focused on sensitivity improvement. The resulting method enables qualification and quantification of eicosanoids in ng/ml or even pg/ml range, depending on the analyte.

The developed high resolution MS method was then used to analyse interstitial fluid samples, obtained via dermal open-flow microperfusion, from healthy as well as psoriatic skin. Most of the 10 analytes could be quantified or at least shown qualitatively to be present in the samples. Time-concentration-profiles for each of the analytes were created and influencing factors on these profiles discussed.

Table of contents

1. Introduction

1.1. Eicosanoid-background information

Bioactive mediators have always been an interesting field of research. One important compound class from these bioactive substances is the eicosanoids, also known as prostanoids. Their name derives from the Greek word “eicos”, which means 20 because of their important precursor molecule arachidonic acid (AA), a C:20 fatty acid with four non-conjugated unsaturated double-bonds (Figure 1).

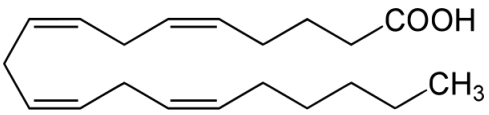

Figure 1: Structure of arachidonic acid

Nowadays, eicosanoids are known to be involved in numerous important biological and physiological processes (Buczynski et al., 2009) such as pain, regulation of blood pressure, blood coagulation, muscle constriction, and, of course, inflammation. As such, they play an important role in diseases like for instance arthritis, asthma, atherosclerosis and cancer (Harizi et al., 2008).

The effects of eicosanoids were firstly discovered in the 1930s by Lieb and Kurzrok (1930), who were doing research on artificial insemination. They observed different pharmacological effects of uterine tissue after interacting with seminal fluid: depending on whether the uterine tissue was taken from sterile or from formerly pregnant women, it responded either by contraction or by relaxation. At that time, they thought acetylcholine to be responsible for this reaction (Kurzrok & Lieb, 1930). In subsequent related studies similar results were achieved (Goldblatt, 1933). Euler (1934) later was able to extract and characterize the responsible active compound. He described the unsaturated acidic lipid properties of the substance, which indicated a new active compound class. Because the compound was originally identified from prostate extracts and believed to originate from the prostate gland, Euler referred to them as “prostaglandins”. Although it was later realized that the extracts were originally produced by the vesicular glands (Bergström et al., 1963), the meanwhile well-established name of prostaglandins remained unchanged.

Research on eicosanoids has come a long way since then; their involvement has been proven in a vast number of biological processes, and over a hundred different types of eicosanoids have been identified so far.

1.2. Biological relevance

Eicosanoids can be counted as members of the lipid family of compounds. In contrast to fats, waxes or phospholipids, eicosanoids are non-hydrolysable lipids. They possess various signalling functions, which is probably one of their most important features. These bioactive lipids have great influence on a vast number of physiological processes such as control of smooth muscle activity, platelet aggregation, bronchoconstriction and inflammation (Marks, 1999). Eicosanoids interact with G-protein-coupled transmembrane receptors, also referred to as 7-transmembrane domain receptors (7TM receptors) due to their seven transmembrane helices (Voet & Voet, 2011). The 7TM receptors represent a big group of membrane proteins that function as signal transduction sites. After sensing extracellular messenger molecules they activate signal transduction pathways inside the cell which ultimately lead to respective cellular responses (Trzaskowski et al., 2012).

Eicosanoids are also referred to as lipid mediators that have hormone-like biological principles of operation. Unlike hormones, however, eicosanoids are not produced by glands but rather by many different cell-types. They are not stored but formed ad hoc to trigger signalling cascades locally already in very low concentrations in the respective area of formation. After formation, prostanoids can affect either neighbouring cells (paracrine signalling) or the producing cell itself (autocrine signalling). Either way, they have only a restricted radius of action, limited by fast (metabolic) breakdown (Koolman & Röhm, 1998). Their inactivation happens within seconds either by double-bond-reducing enzymes or via dehydrogenation of hydroxyl groups.

1.3. Pathways and classification systems

Almost all types of mammalian tissue or cell possess the ability to produce eicosanoids. The essential ω6–fatty acid arachidonic acid (AA; 20:4; 5,8,11,14), which has to be taken in through food, serves as the most prevalent precursor of eicosanoid synthesis. It can also be formed out of the essential fatty acids linoleic acid (18:2; 9,12) or α-linoleic acid (18:3; 9,12,15) enzymatically by different desaturases, elongases and synthases. These synthetic pathways also lead to the formation of dihomo-γ-linoleic acid (DGLA; 20:3, 8,11,14) and eicosapentaenoic acid (EPA; 20:5; 5,8,11,14,17), two ω3–fatty acids, which can serve as eicosanoid precursors as well (Voet & Voet, 2011). ω6–derived eicosanoids have more pro-inflammatory properties in contrast to ω3–derived eicosanoids, which show anti-inflammatory activity (Schmitz & Ecker, 2008).

Arachidonic acid is stored at the Sn-2 position of glycerol-phospholipids in the phospholipid-bilayer which builds up cell membranes. After stimulation AA is extracted by phospholipase A_2 (= PLA_2), which accounts the rate-limiting step in the metabolism of arachidonic acid. Depending on the enzyme-environment of the respective cell, AA can then undergo two different pathways leading to the formation of different eicosanoid classes in further reaction steps (Marks, 1999), which are shown in excerpts in Figure 2:

- Cyclic pathway: leading to the formation of the highly unstable (due its containing a peroxide group) precursor molecule PGH_2 with the cyclopentane ring moiety, which is characteristic for prostaglandins.
    - Cyclooxygenases (COX): prostaglandins (PGs) and thromboxanes (TXs); these are collectively also known as prostanoids
- Linear pathway: leading to linear basic structures
    - Lipoxygenases (LOX): hydroperoxyeicosatetraenoic acids (HPETEs), lipoxins (LXs), leukotrienes (LTs)
    - Cytochrome P-450 (CYP) dependent monooxygenases: hydroxyeicosatetraenoic acids (HETEs)
    - Non-enzymatic lipid oxidation: isoprostanes (IsoPs)

Parts of these pathways can be inhibited by drugs. Corticosteroids, for instance, lower PLA_2 activity. They inhibit AA-release from cell membranes and thus lead to inhibited formation of eicosanoids. The effects of aspirin–intake can also be explained: acetylsalicylic acid inhibits COX–activity by covalently binding to the active site of the enzyme which consequently lowers the production of

prostaglandins (Voet & Voet, 2011). This leads to antipyretic (fever-reducing), analgesic (pain-relieving) and anti-inflammatory effects.

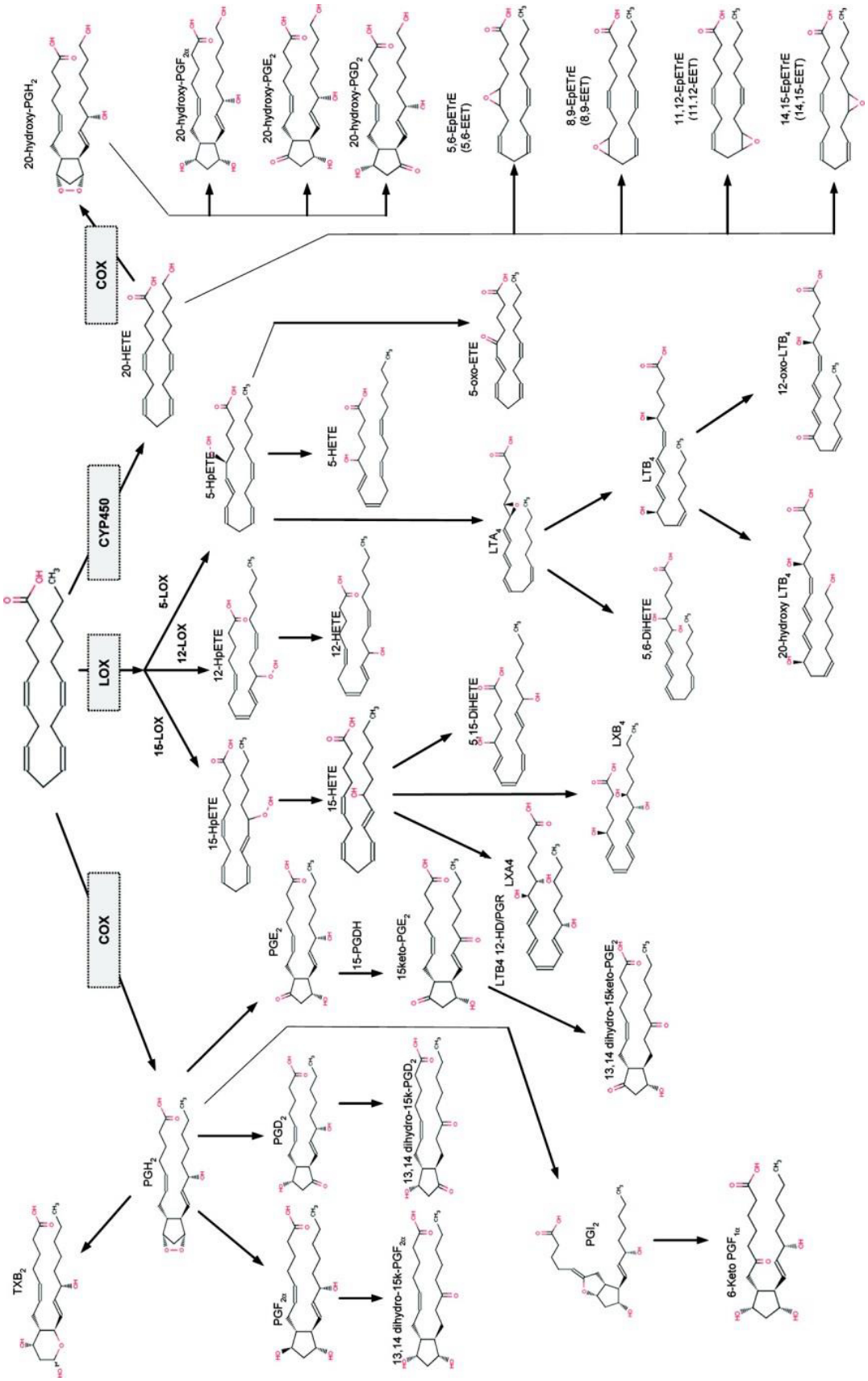

Figure 2: Arachidonic acid – cascade (Masoodi et al., 2010)

Further classification system of prostaglandins

Prostaglandins (PGs) can be roughly classified into three groups (Voet & Voet, 2011):

- Series-1 PGs: synthesized from DGLA
- Series-2 PGs: synthesized from AA
- Series-3 PGs: synthesized from EPA

The series number signifies the amount of double bonds in the side chain. As arachidonic acid is considered to be the most abundant precursor in humans, series-2 prostaglandins are currently the most investigated PGs. The ω3–FA products of series-1 and series-3 (derived from DGLA and EPA) are generally regarded as primarily anti–inflammatory compounds, while series-2 PGs have mostly pro-inflammatory properties (Schmitz & Ecker, 2008).

Prostaglandins can be further characterized and classified by the substituents on their cyclopentane ring which leads to their nomenclature: PGx_y, where PG stands for Prostaglandin, x=structure of prostane ring, and y= number of double bonds in the main side chains (which are bonded to the carbon atoms 8 and 12).

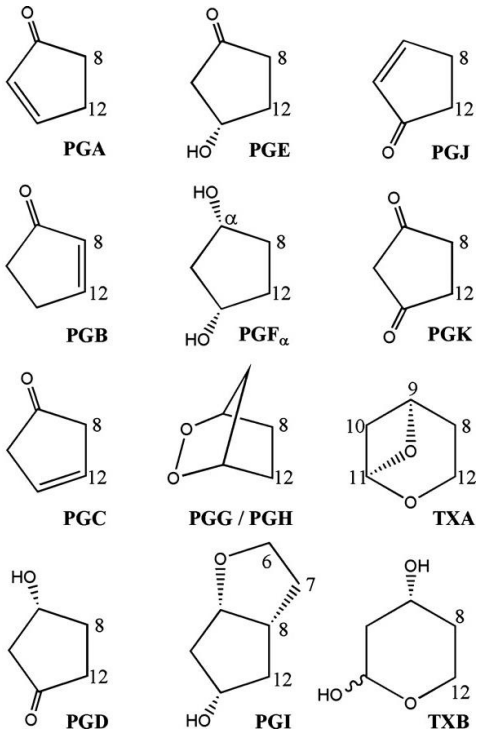

Figure 3: Nomenclature and respective structures of the ring system in prostaglandins (Buczynski et al., 2009)

1.4. Analyte-specific information

1.4.1. Prostaglandins

The prostaglandins are probably the best investigated eicosanoid class in terms of biochemistry, mass spectrometry and pharmacology. They are unsaturated, hydroxylated carboxylic acids. Their chemical structure includes a cyclopentane ring attached to two side chains; one of these has a carboxyl group ending while the other terminates with a simple methyl group derived from arachidonic acid. Due to the carboxylic acid group, ionisation in negative mode is preferred in ESI–MS/MS analysis, yielding relatively stable carboxylate anions $[M-H]^-$ (Murphy et al., 2005)[1].

Prostaglandins are generally synthesized by the COX-pathway and the respective synthase enzyme present at the production site. In vivo, the four most abundant ubiquitously produced PGs are PGE_2, PGD_2, PGI_2 and $PGF_{2\alpha}$. Usually one or two of these are produced dominantly depending on the respective cell-type. Inflammatory responses result in a drastic change of PG production (Ricciotti & FitzGerald, 2011). PG levels in uninflamed tissues are usually very low but in acute inflammation, levels immediately increase, even before the intervention of immune cells or leukocytes.

PGE_2

PGE_2 shows numerous biological activities. It mediates many biological functions such as regulation of blood pressure and immune response. A wide range of pathological conditions can be associated with disregulated PGE_2 cata- or anabolism. PGE_2 plays a prominent role specifically in inflammation. Many classic signs of inflammation can be linked to PGE_2. It mediates increased arterial dilatation and microvascular permeability which promotes higher blood pressure, redness and swelling (Funk, 2001). Pain-sensation can be rooted back to an interaction of PGE_2 with peripheral sensory neurons and with central sites within the brain and the spinal cord (Ricciotti & FitzGerald, 2011). PGE_2 is also regarded as an important regulator of cellular reactions in homeostasis like proliferation and apoptosis of keratinocytes (Pilkington et al., 2014).

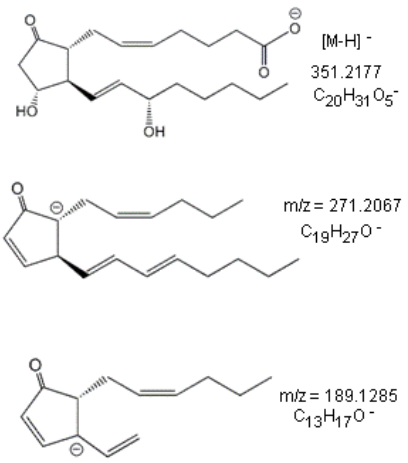

Figure 4: Structures of PGE_2 parent and its most abundant fragment ions for MS/MS detection in negative ionization mode.[1]

[1] Structures of parent and its most abundant fragment ions of the prostaglandin, thromboxane & leukotriene analytes in section 1.4 were obtained from *The LIPID MAPS Lipidomics Gateway*; Available at: http://www.lipidmaps.org/ [Accessed June 11, 2015]

PGD_2

PGD_2 is a structural isomer of PGE_2 showing the same fragment ions in MS/MS analysis. It is often further metabolized to, for instance, $PGF_{2\alpha}$ or PGs of the J series like PGJ_2. It is mainly synthesized in peripheral tissue and the central nervous system. PGD_2 has inflammatory and homeostatic properties, but is presumed to possess anti-inflammatory mediating properties as well. It is involved in regulating processes of sleep, pain perception and other central nervous system activities in the brain (Eguchi et al., 1999). In peripheral tissue, PGD_2 is mainly synthesized by mast cells, but other leukocytes are involved as well. It is also proven that mast cells produce PGD_2 as the predominant PG within allergic reactions. Studies show that PGD_2 levels are also increased during an allergic asthma attack (Ricciotti & FitzGerald, 2011) inter alia causing bronchoconstriction.

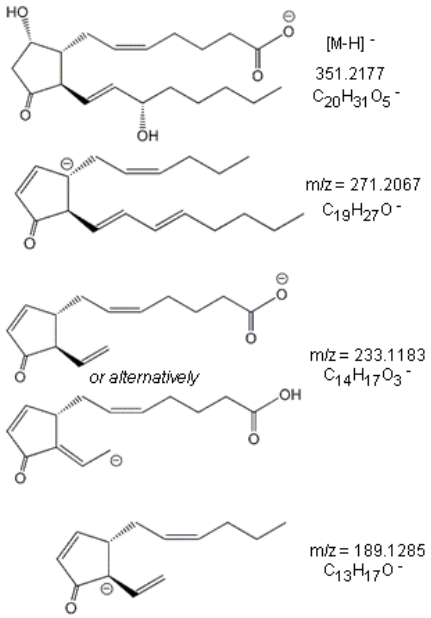

Figure 5: Structures of PGD_2 parent and its most abundant fragment ions for MS/MS detection in negative ionization mode.[1]

$PGF_{2\alpha}$

$PGF_{2\alpha}$ interacts with a so called "FP" receptor, which is typical for eicosanoid receptors coupled to a G-protein regulating intracellular free calcium concentration (Ricciotti & FitzGerald, 2011). In the female reproductive system, $PGF_{2\alpha}$ plays a fundamental role in luteal regression, ovulation, smooth muscle contraction of the uterus (Saito et al., 2003) and consequently in the initiation of parturition (Veitch et al., 2002). In vitro and in vivo studies (Sugimoto et al., 1997) have shown that acute inflammation is induced after administration of $PGF_{2\alpha}$. After giving NSAIDs (nonsteroidal anti–inflammatory agents) biosynthesis of $PGF_{2\alpha}$ was inhibited.

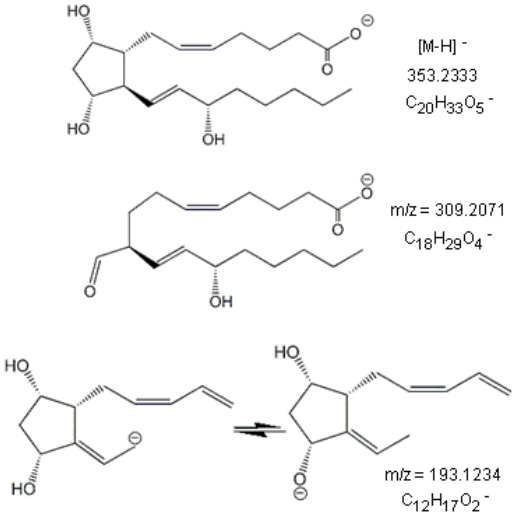

Figure 6: Structures of $PGF_{2\alpha}$ parent and its most abundant fragment ions for MS/MS detection in negative ionization mode[1]

6-keto- $PGF_{1\alpha}$

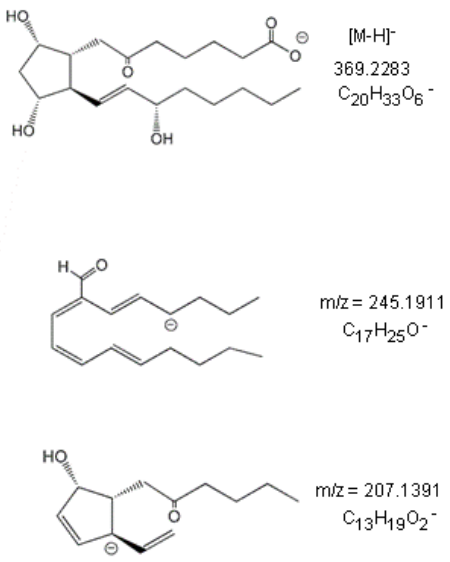

Figure 7: Structures of 6-keto-$PGF_{1\alpha}$ parent and abundant fragment ions for MS/MS detection in negative ionization mode.[1]

6–keto-$PGF_{1\alpha}$ is the biologically inactive product of non-enzymatic PGI_2 hydrolysis. PGI_2 operates very locally and has a short half-life. Therefore, most analytical methods are designed to measure the decomposition product 6-keto-$PGF_{1\alpha}$ instead of PGI_2 (Ricciotti & FitzGerald, 2011). PGI_2 is known for its vasodilatory effects and is considered to be the most significant prostanoid responsible for regulation of cardiovascular homeostasis. It inhibits adhesion of leukocytes, proliferation of vascular smooth muscle cells (VSMC) and aggregation of platelets (Noda et al., 2007). In VSMC, PGI_2 further counteracts mitosis and consequently acts as an inhibitor against DNA synthesis (Libby et al., 1988). Despite its cardiovascular effects, PGI_2 also plays a vital part in mediating pain and edema formation in acute inflammation processes. It is synthesized fast as a consequence of tissue injury, and occurs at relatively high concentrations in inflamed areas (Bombardieri et al., 1981).

1.4.2. Thromboxanes

Thromboxanes are, as well as prostaglandins, synthesized by the COX–pathway and are also secondary products of PGH_2. PGH_2 is metabolized by rearrangement of a peroxide group into the highly unstable precursor TXA_2. In aqueous solutions, TXA_2 has a half-life of ~ 30 s at 37 °C (Hamberg et al., 1975). A characteristic structural feature of thromboxane is a 6-member ring-system which is connected between C-12 and C-8 atom of the structural precursor arachidonic acid.

TXB_2

The cyclic endoperoxide group present in TXA_2 is easily and non-enzymatically metabolized into the more stable TXB_2. Thus TXB_2 is usually the analyte of choice in analytical method development aiming for thromboxane related information. The biologically active TXA_2 serves as a very important inducer of platelet aggregation and vasoconstriction (Murphy et al., 2005). It is predominantly produced by blood platelets, but can also be synthesized by other types of cells like macrophages. TXA_2 interacts with the "TP" receptor (Ricciotti & FitzGerald, 2011) and consequently mediates different pathophysiological and physiological responses like contraction and proliferation of smooth muscles, aggregation and adhesion of platelets, or activation of inflammatory response in the endothelium.

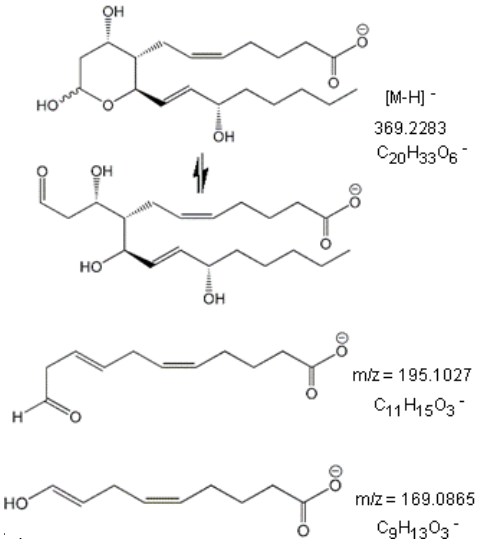

Figure 8: Structures of TXB_2 parent and abundant fragment ions for MS/MS detection in negative ionization mode.[1]

1.4.3. Leukotrienes

Leukotrienes are products of the 5-LOX-pathway. Their chemical structure characteristically contains three conjugated double bonds. Different substituents are positioned allylic to these double bonds. LTs (except for LTA_2) can roughly be separated into two groups (Murphy et al., 2005): sulfidopeptide LTs (also known as Cys-LTs) binding a substituent over a sulfur atom which is linked allylicly to the main chain; and the dihydroxy LTs whose conjugated triene group is positioned between two allylicly-bound hydroxyl groups.

LTB_4

The light sensitive LTB_4 is widely known to be the most important activator of leukocytes and has potent chemoattractant properties. It promotes a number of leukocyte functions including chemotaxis, adhesion of leucocytes to endothelial cells, the activation of granulocytes, monocytes, macrophages, eosinophils and T cells as well as the activation of natural killer cells. In the respiratory system LTB_4 is often linked with bronchial asthma and the constriction of lung parenchymal (Yokomizo et al., 2001). It is also involved into pathophysiological processes like melanocyte pigmentation of the skin (Yokomizo et al., 2001). In allergic skin inflammation neutrophil-derived LTB_4 promotes itching and scratching (Oyoshi et al., 2012).

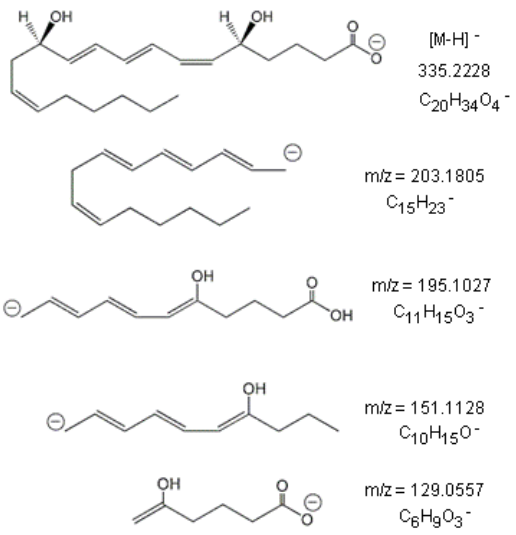

Figure 9: Structures of LTB_4 parent and abundant fragment ions for MS/MS detection in negative ionization mode.[1]

1.4.4. Hydroxyeicosatetraenoic acids

The chemical structure of HETEs is characterized by four double bonds and one hydroxyl-group substituted somewhere along the main chain. HETEs are mainly produced by the LOX pathway of AA metabolism. Arachidonic acid is thereby converted by the regio- and stereo-specific LOX enzyme into hydroperoxyeicosatetraenoic acid (HPETE). This enzyme reaction produces mainly the respective S-enantiomer, but sometimes also R-enantiomers (Marks, 1999). HPETEs are rapidly reduced in cells to become the respective monohydroxy compounds (HETE). HPETEs can also be converted into HETEs via nonspecific lipid oxidation leading to racemic compounds. A further, very important pathway to synthesize HETEs out of arachidonic acid involves cytochrome P-450-dependent monooxygenases which, in contrast to LOX-derived HETE production, does not form hydroperoxides as intermediates.

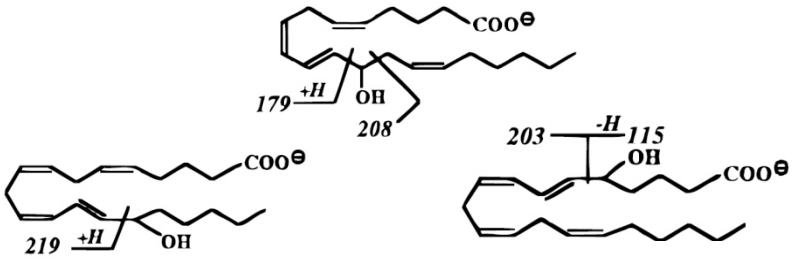

Figure 10: Isobaric structures of 15-HETE (left), 12-HETE (middle) and 5-HETE (right) with abundant fragment ion masses for MS/MS detection in negative ionization mode; all having the same chemical formula $C_{20}H_{31}O_3^-$ and parent mass $[M-H]^- = 319$ (figure adapted from Nakamura et al. 1997)

15-HETE, 12-HETE and 5-HETE, the three major HETEs produced by the widely spread lipoxygenase enzymes, are very sensitive to oxygen and light. All of them can be further metabolized to other biologically active compounds. Their biological functions have not yet been fully explored. HETEs are often studied together with their respective hydroperoxy-precursors (HPETEs) because of their direct LOX-pathway linkage. However, because there are other possible synthetic pathways leading to HETEs, their concentration cannot directly be attributed to the respective HPETEs.

15-HETE

15-HETE is the predominant HETE produced by human cells (Moreno, 2009). It can serve as a precursor for lipoxins and can be produced by for instance the respiratory epithelium, leukocytes, and reticulocytes. 15-HETE is implicated in metastasis, cell proliferation, cell-adhesion and -accumulation. It is therefore assumed that 15-HETE is involved in the development of different types of cancer like in colon, lymph nodes and many other tissues (Schneider & Pozzi, 2011). Contrary to those properties, 15-HETE activates nuclear transcription factors which are integrated in epithelial differentiation; a possible explanation of anti-proliferative action in terms of prostate cancer cells[2]. 15-HETE further takes part in carcinogenesis, asthma, atherogenesis, asthma, cell differentiation and inflammation. It can also counteract 12-HETE derived cell infiltration. 15-HETE further acts conversely to 12-HETE in terms of carcinogenesis (Kendall & Nicolaou, 2013); while 12-HETE shows tumor-promoting activity, 15-HETE operates against proliferation.

12-HETE

12-HETE possesses chemotactic properties that influence cells of the human immune system (leucocytes, neutrophils, eosinophils) and tumor cells. It stimulates tumor cell adhesion to endothelial and subendothelial cells, for instance. 12-HETE can also function as a modulator of membrane properties and is able to excite for example melatonin synthesis. 12-HETE can deactivate the enzyme prostacyclinsynthase, and thus is possibly able to counteract synthesis of pro-inflammatory PGs. At the same time it has been shown to attract inflammatory cells like neutrophils and macrophages, and thus act pro inflammatory to the skin (Kendall & Nicolaou, 2013). It is believed that the usually scarce 12(R)-HETE enantiomer form is involved in skin diseases, especially in psoriasis. In fact, 12–HETE has already been detected in large amounts in psoriatic skin (Marks, 1999).

[2] Christie, W.W., 2014. *Hydroxyeicosatetraenoic acids and related compounds - Chemistry and Biology*, pp.1–8. Available at: http://lipidlibrary.aocs.org/Lipids/eic_hete/file.pdf [Accessed June 9, 2015]

5-HETE

5-HETE serves as a potent precursor for lipoxins and leukotrienes. Although its metabolites show more biological activity than 5-HETE itself, it possesses biological functions as well. 5-HETE is often found in leucocytes[3]. It is known for increasing vascular permeability as well as recruiting and activating inflammatory cells, two potent steps in tumorigenesis. It stimulates cancer proliferation comparable to certain leukotrienes, and can be found in brain tumor tissue in elevated amounts (Schneider & Pozzi, 2011).

1.4.5. Hydroxyeicosapentaenoic acids

HEPEs are products of the LOX pathway and are derived from eicosapentaenoic acid (EPA) instead of AA. Their characteristic structure consequently contains five double bonds and one hydroxyl-group substituted along the main chain. Eicosanoids derived from ω3–fatty acid are generally counted as anti-inflammatory mediators. Higher dietary intake of those fatty acids are beneficial in many inflammatory disorders (Kubota et al., 2014). This effect may result from different mechanisms (Schmitz & Ecker, 2008), either by serving as an alternative compound for forming less potent products instead of pro-inflammatory AA-derived eicosanoids, or by being transformed into active anti-inflammatory mediators.

12-HEPE

12-HEPE is produced via the 12-LOX enzyme. Compared to its AA derived counterpart, 12-HETE, there are still many questions concerning the particular biological functions of 12-HEPE. It is one of the most prevalent eicosanoids in skin (Kendall & Nicolaou, 2013). As well as 12-HETE, it can act as inhibitor of platelet aggregation (Takenaga et al., 1986).

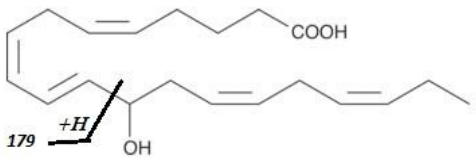

Figure 11: Structure of 12-HEPE parent with fragment ion masse for MS/MS detection in negative ionization mode; parent mass $[M-H]^-$ = 317

[3] Christie, W.W., 2014. *Hydroxyeicosatetraenoic acids and related compounds - Chemistry and Biology*, pp.1–8. Available at: http://lipidlibrary.aocs.org/Lipids/eic_hete/file.pdf [Accessed June 9, 2015]

1.5. Skin: biology and functions

The skin is the largest organ of the human body and possesses numerous important functions. One of its most important tasks is serving as an effective barrier against physical, chemical or microbial assaults of all kinds like mechanical injury, UV-radiation, allergens, and bacteria. It also plays a crucial role in the immune system, sensation of pain, touch or temperature, and also in water-loss- and thermo-regulation (Proksch et al., 2008). The basic skin structure consists of three main layers: epidermis, dermis and hypodermis:

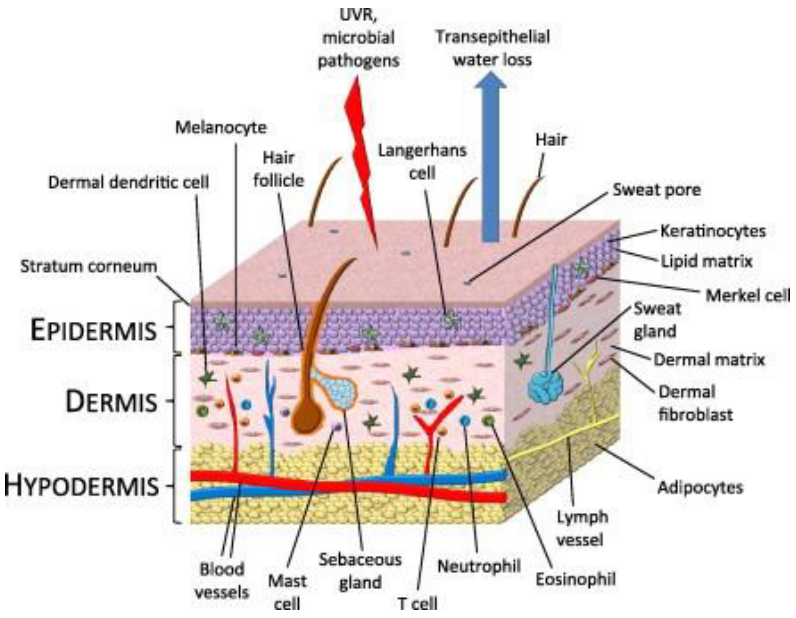

Figure 12: Schematic skin structure (Kendall & Nicolaou, 2013)

- Epidermis: it mainly consists of keratinocytes embedded into extracellular lipid-enriched matrix. These cells migrate during cell-maturation from the dermis to the outer surface of the skin. There they form a tight, protein-enriched layer which is about 20 µm thick, the so called stratum corneum. It is continuously built-up by aging, upwards migrating keratinocytes that transform into flat and anucleated cells termed corneocytes. The stratum corneum represents the outer skin layer, and functions as the main barrier against mechanical assaults and percutaneous penetration of microbes and chemicals. The epidermis also contains unique cutaneous antigen-presenting immune-cells called Langerhans cells which respond to foreign stimuli. It also contains Merkel cells, which are believed to play a role in the development of cutaneous nerves and further in skin homeostasis (Kendall & Nicolaou, 2013). Pigment-producing melanocytes are also placed in the bottom region of the epidermis.

- Dermis: the dermis is separated from the epidermis through a basal membrane. It contains sweat glands, hair follicles, sensory nerves and smaller blood vessels. The dermal matrix consists of collagen, elastic fibres, fibroblasts and numerous immune cells. Important immune cells like neutrophils, macrophages/monocytes, B cells, T cells, eosinophils, dendritic and mast cells undergo routine surveillance processes in the dermis. During inflammation, resident and other immune cells also infiltrate the cutaneous tissue triggered by inflammatory mediator stimulation (e.g.: cytokines, bioactive lipids) (Kendall & Nicolaou, 2013) consequently leading to a notably increased population of cutaneous immune cells.

- Hypodermis: below the epidermis and dermis lays the hypodermis, also known as reticular dermis or subcutaneous tissue. Adipocytes form adipose tissue in which blood and lymph vessels are embedded. These vessels allow migration and constant flux of (immune) cells out of and into the skin, depending on the respective demands of the cutaneous immune and inflammatory system. The main function of adipose tissue is to serve as a lipid reserve for energy generation. But the adipocytes range of duty also involves the production of important bioactive lipid mediators consequently influencing other cutaneous cells (Kendall & Nicolaou, 2013).

1.6. Psoriasis

Psoriasis is one of the most prevalent skin diseases (=dermatoses) in humans, affecting 120-180 million people worldwide (Pietrzak et al., 2010). Despite the widespread occurrence of psoriasis, its etiology is still not completely understood (Kendall & Nicolaou, 2013). Its prevalence is believed to be mainly influenced by genetic, environmental, immunological, infectious, biochemical and physiological factors, but can also be related to alcohol and drugs. Psoriasis can be described as a multifactorial immunometabolic disease, which involves inflammation of the skin.

1.6.1. Disease pattern

Psoriasis can be described as an organ-specific autoimmune disease triggered by activation of the cellular immune system. An autoimmune disease is defined as "a clinical syndrome caused by the activation of T cells or B cells, or both, in the absence of an ongoing infection or other discernible cause" (Davidson & Diamond, 2001). Hence psoriasis can be related to other immune-mediated diseases like rheumatoid arthritis, multiple sclerosis or diabetes. It can accompany a broad variety of multi-organ abnormalities and dysfunctions (Pietrzak et al., 2010). Patients suffering from psoriasis have been reported to show increased risk of other diseases like hypertension, diabetes, obesity, dyslipidemia, atherosclerosis, cerebral stroke, cardiovascular disease, osteoporosis, depression and also cancer.

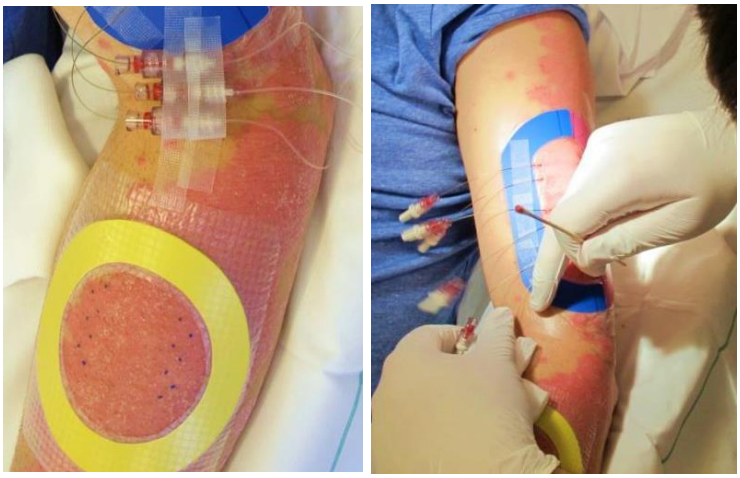

Figure 13: Lesional psoriatic skin from analysed subject in this thesis; pictures include parts of dOFM-sampling equipment

Psoriasis is characterized by highly distinct proliferation of keratinocytes in comparison to healthy skin. This excessive growth of keratinocytes leads to the formation of raised, itchy, red and scaly inflammation plugs or lesions which are believed to be triggered by auto-immune responses of the cellular immune system (Lowes et al., 2007). The epidermis is thereby thickened markedly. The pathogenesis involves altered activity of T cells, dendritic cells and diverse chemokines and cytokines related to the immune system.

Figure 14 shows a histological and schematic comparison between healthy and psoriatic skin. Abnormal stacking of cells in the stratum corneum leads to the formation of scales. Epidermal rete ridges (thickenings which are extended in the direction of the dermal papillary dermis) are significantly elongated. Also blood vessels located in the dermis are enlarged leading to increased blood flow causing the red colour of psoriatic plaques. Psoriatic skin is also highly enriched in trafficking and resident immune cells, such as excessive T cell activity, compared to healthy skin (Figure 14). Numerous pathways related to immune-responses are activated, and the amount of leukocytes is markedly increased in psoriatic lesions.

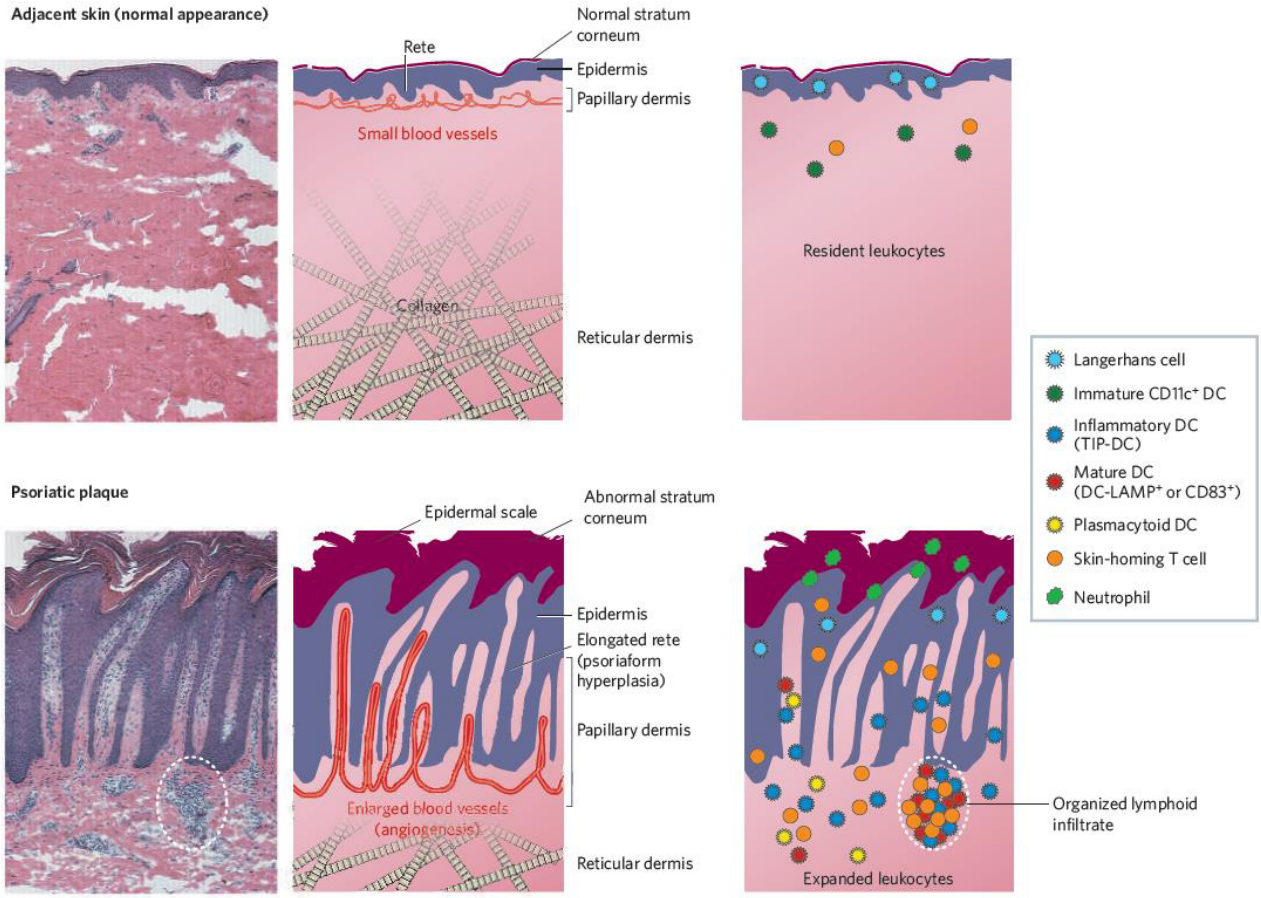

Figure 14: Skin histology and scheme in normal, healthy skin (above) compared to psoriatic analogues (below) (Lowes et al., 2007)

1.6.2. Eicosanoids in psoriasis

Because eicosanoids are important fatty acid-derived messenger and marker substances involved in inflammation, they are suspected to play an important role in the pathogenesis of the inflammatory skin disease psoriasis.

Among other symptoms, psoriatic patients demonstrate altered lipid metabolism, which represents one of the key metabolic pathways in skin pathology. Hence the composition of fatty acids in psoriatic skin differs from that in healthy skin. Altered lipid metabolism consequently leads to changes in eicosanoid synthesis. One crucial factor in eicosanoid-regulation is the release of polyunsaturated fatty acids from cell membranes, a process carried out enzymatically by PLA_2. Different types of the AA-releasing PLA_2 are altered and partly up-regulated in psoriasis (Kendall & Nicolaou, 2013). Levels of AA-derived HETEs and also, to a lesser extent, PGE_2 and $PGF_{2\alpha}$ have already been reported to be increased in psoriatic skin (Hammarström et al., 1975).

12-HETE, generally a very prominent eicosanoid in skin, is believed to be one of the eicosanoids most affected by psoriasis. Owing to its chemotactic properties, 12-HETE is suspected to attract immune cells like neutrophils and hence promote the development of an inflammatory milieu. These neutrophils are suspected to synthesize LTs and general eicosanoic 5-LOX products. The leukotrienes such as LTB_4 play an important role in psoriatic pathogenesis. LTB_4 stimulates neutrophil activity such as aggregation, chemokinesis and degranulation by receptor binding. LTB_4 is further able to stimulate changes of the dermis and epidermal hyperproliferation. Products of the 5-LOX pathway like LTB_4, its precursor 5-HETE and also cys-LTs like LTC_4 and LTD_4 have already been shown multiple times to be elevated in psoriatic patients (Ikai, 1999) in various sample types, e.g. from epidermis, scales to suction blister fluid sampled from psoriatic lesions, and many others.

15-HETE is one of the predominant LOX-products in normal dermis where it inhibits chemotactic and pro-inflammatory enzyme activities like those of 5-LOX and 12-LOX. 15-HETE can counteract 12-HETE (Ikai, 1999). Studies have already shown lower 15-HETE content of psoriatic compared to normal skin; simultaneously, 12-HETE showed an opposite trend by increased levels in psoriatic skin (Kragballe & Voorhees, 1987).

The roles of other eicosanoids in psoriasis are still not clarified. For instance PGE_2 can cause vasodilation and increased blood flow in the already enlarged blood vessels of psoriatic dermis while at the same time it can act as an anti-inflammatory agent due to its potential immunosuppressive properties (e.g.: inhibition of lymphocytes and monocytes). Therefore, in psoriasis the role of PGE_2 in psoriasis is still controversial (Ikai, 1999).

1.7. Analytical methods

The fast growing interest in the resolution of lipid mediator pathways has created an urgent need for efficient analytical qualification and quantification methods of eicosanoids. These should be highly sensitive, selective, accurate and time efficient.

Because eicosanoids are so widely distributed, they are studied in various types of sample-matrices: blood, serum, plasma, urine, suction blister fluid, exhaled breath condensate, different kinds of tissues and many more. To purify the analyte and minimise interfering matrix components, various "clean-up" procedures can be used. Protein precipitation (PP), liquid-liquid-extraction (LE) or immunoaffinity chromatography (IA) are sometimes used as a clean-up step prior to eicosanoid measurement (Martin-Venegas et al., 2014), sample preparation is mostly done with solid phase extraction (SPE). It is relatively simple and shows a broad field of application with sufficiently high extraction efficiency.

Currently used measurement approaches for eicosanoids are briefly described here. Radioimmunoassays and enzyme-linked immunosorbent assays are commonly used (D. Wang & DuBois, 2007), but these methodologies possess several drawbacks: they measure only one substance at a time, they show cross-reactivity, are only available for particular analytes, and sometimes lack selectivity. Gas chromatography (GC) with mass spectrometry (MS) or tandem mass spectrometry (MS/MS) is also used (Hughes et al., 1988). Derivatisation is necessary for GC-analysis to form volatile species; this additional sample preparation step and the GC-separation are limited to thermally stable analytes and their corresponding derivatives.

Although the above methods are still commonly used and have particular applications, state of the art methods for measuring eicosanoids are based on high performance liquid chromatography (HPLC) combined with MS or MS/MS detection (Massey & Nicolaou, 2013). Only the most relevant key data common for most analytical approaches concerning eicosanoids are discussed in this paragraph; a more detailed description and discussion of these methods can be found later on in the introduction section: Quantification is mostly performed using deuterated analytes as internal standards. In order to improve selectivity, the various acidic/lipoid eicosanoids extracted by SPE are separated chromatographically, mostly on reversed-phased C-18 columns, prior to measurement. Analytes are usually ionised in negative ionisation mode, which is preferred due to the carboxyl group in eicosanoids. Identification and detection is often performed by fragmentation with MS/MS devices; the superior speed of triple quadrupole mass spectrometers enables fast detection of various eicosanoids, usually at very low concentrations (in pg/ml range).

1.7.1. Sampling of dermal interstitial fluid: dermal open-flow microperfusion (dOFM)

Dermal interstitial fluid, which was analysed in this thesis, was sampled by dermal open-flow microperfusion (dOFM). dOFM is a novel, minimally invasive sampling technique that allows continuous and membrane-free access to the interstitial fluid of the dermis (Bodenlenz et al., 2013). The technique was developed for in vivo dermatological drug testing and pharmacodynamic/ pharmacokinetic studies.

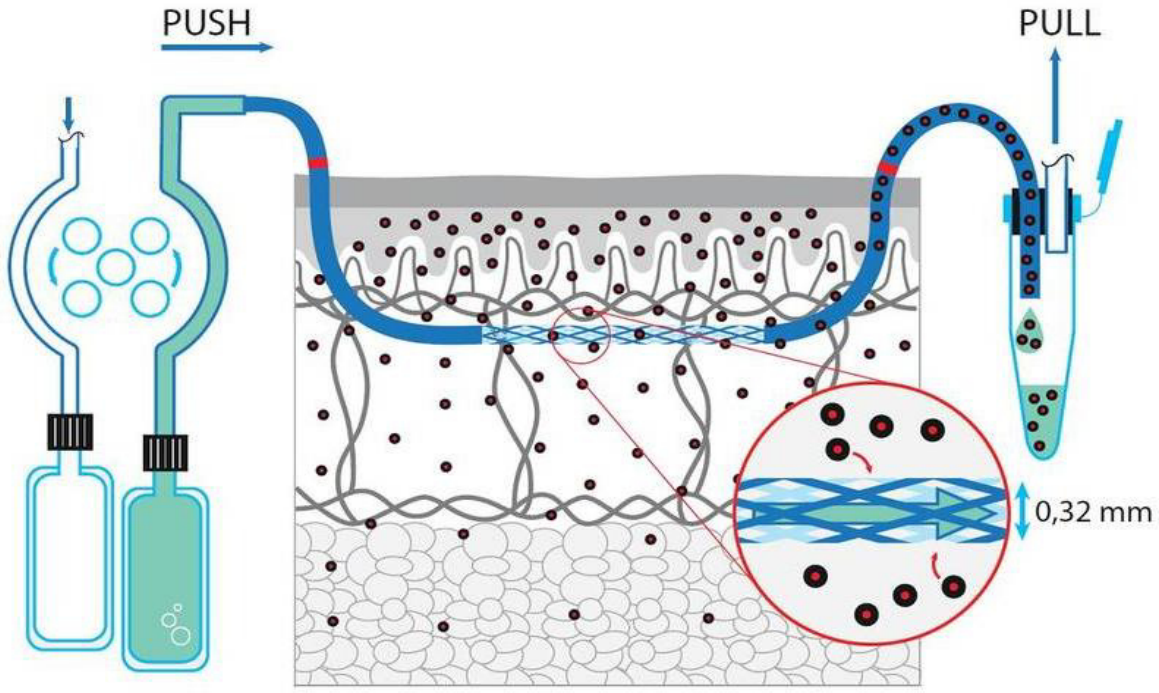

Figure 15: Scheme of dOFM sampling with a sampling-probe located in the dermis, connected to one push-pull-system pump; perfusate is pushed through the probe and on the probe´s outlet pulled by evacuation by the pump system. This setup allows fractionised sampling and hence enables time resolved analyte profiles (Bodenlenz et al., 2013).

The flexible, linear dOFM sampling probe is membrane-free and possesses a braided sampling section that is permeable to all molecules of interest in the interstitial area of the respective target tissue. The probe is inserted into the dermis with a thin needle and then attached to a pump at the inlet side of the probe. At the outlet side it is connected to a PCR (polymerase chain reaction) sampling tube, which is again connected to the same sampling pump. The probe is continuously perfused by a push-pull system with a sterile perfusate. The push-pull system enables controlled flow rates in the µl/min range during the sampling process. The depth of the dOFM probe can be assessed by ultrasound.

The interstitial fluid samples collected by dOFM can be used to measure inflammation markers, like eicosanoids, and further investigate their role in various kinds of inflammatory diseases of the skin.

1.7.2. MS detection

This section briefly describes the basic setup and functions of the two different types of mass spectrometers (i) Q Exactive™ MS and (ii) triple quadrupole MS. Further discussion and comparison of these two detectors concerning the measurement of eicosanoids can be found in section 3.5.

Q Exactive™ MS

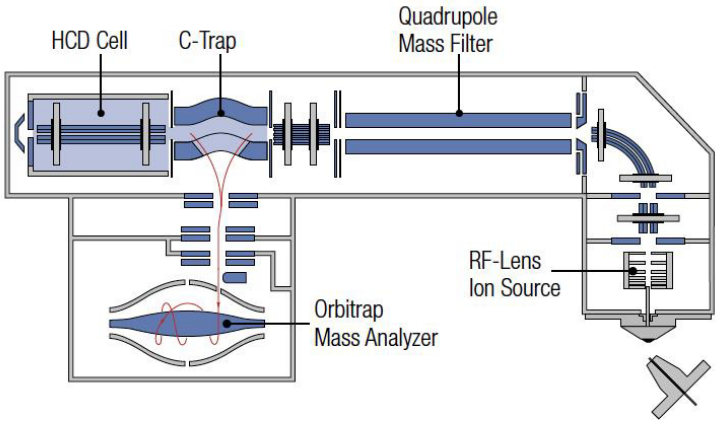

Figure 16: Scheme[4] of the high resolution Q Exactive™ MS

Figure 16 shows the basic components of the high resolution Q Exactive™ MS: a lens system at the entrance where neutral compounds are separated and the remaining ions are focused to an ion-beam. Ions are formed by for instance electrospray ionisation (ESI), a soft (low energy) ionisation technique applicable also to biomolecules and substances with limited stability, forms + or - charged molecules; negative ESI-ionisation usually leads to poorer ionisation efficiency and hence to lower overall-sensitivity compared to positive mode. The ion-beam coming from the ionisation source enters a quadrupole mass filter, where ions can be sorted by their m/z ratio. The resulting ions are transferred via a transfer multipole into the C-trap. The C-trap functions as ion collector; from there the ions can either directly be sent into the orbitrap mass analyser or otherwise into the HCD cell (high-energy collisional dissociation). In the HCD cell, the prior selected ions are broken up into fragments by excitation with a high radiofrequency voltage. These fragments are then sent back, via the C-trap, either into the orbitrap analyser or back again into the quadrupole mass filter for further selection. This series quadrupole → C-trap → HCD and back can be repeated multiple times in order to gain more information about the structural-composition of the analyte (MS^n); it has to be

[4] Scheme obtained from *ThermoFisherScientific*:
http://planetorbitrap.com/data/fe/image/QEFocusScheme.jpg [Accessed March 7, 2015]

considered that every additional “n” lowers overall signal-intensity, due to ion-loss, and thus lowers sensitivity. Eventually fragments and ions are sent into the electrostatic field of the orbitap mass analyser, where they move along the axis of an inner electrode due to simultaneous centrifugal forces and electrostatic attraction. The ions circulate around the electrode in a manner dependent on their m/z value, and they induce different frequency signals which are then detected. This design is highly selective and responsible for the high resolving power of the orbitrap mass analysers. Compared with most other detectors they are able to distinguish ions with extremely small mass differences leading to very clean mass traces with minimal background (Gross, 2013).

Triple quadrupole MS

A quadrupole mass analyser consists of four parallel electrode rods. An electric field is created by supplying them with alternating AC/DC voltage (always two opposing rods having the same polarity). Hence the normally straight movement of passing ions can be influenced: they oscillate between the quadrupoles due to alternating electrostatic attraction and repulsion. The degree of influence is determined by the mass-to-charge ratio of the respective ion. Hence separation of charged molecules is possible.

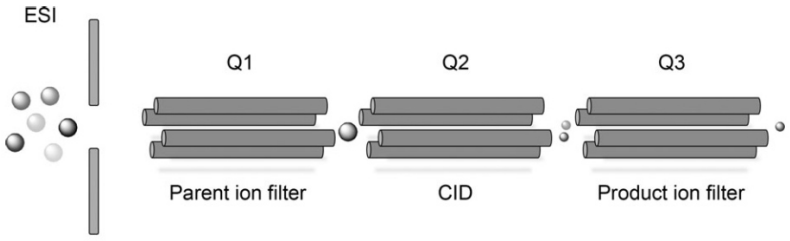

Figure 17: Scheme of a triple quadrupole mass analyser (Balgoma et al., 2013)

Figure 17 shows the main components of a triple quadrupole mass analyser. The ions originating from the source are focused by a lens-system into the first quadrupole (Q1), where they can be separated and sent into the second one (Q2). This second quadrupole contains an inert gas and functions as a collision cell; the ions selected by Q1 collide with the inert gas leading to fragmentation. These fragments can then be further separated in a third mass analyser (Q3), which is connected to a detection system. A major advantage of this MS system is its speed - numerous m/z values can be scanned in a very short time, which makes quadrupoles perfectly suitable for multi-analyte eicosanoid-analysis.

1.8. Objectives

The aim of this thesis was the development of a multi-analyte method for qualitative and quantitative determination of eicosanoids in human dermal interstitial fluid. The method should be applicable to the small sample volumes (~60 µl) available from sampling with dermal open flow microperfusion (dOFM). With this method, eicosanoid levels in dermal interstitial fluid from healthy and psoriatic skin will be measured to assess the potential use of eicosanoids as inflammation markers.

The analytical approach, aimed at the measurement of 10 representatives of the eicosanoid class, involved (i) sample preparation based on SPE; (ii) separation based on RP-HPLC; and (iii) the development of a highly sensitive mass spectrometric detection method. In addition, the HR-MS detection was compared to triple quadrupole MS detection.

2. Experimental

2.1. Chemicals

2.1.1. Standards

(±)12-HEPE	*(5Z,8Z,10E,14Z,17Z)-12-Hydroxy-5,8,10,14,17-icosapentaenoic acid*	25 µg, 100 µg/ml solution in ethanol (Cayman CHEMICAL, Ann Arbor, Michigan, USA)
(±)12-HETE	*(5E,8E,10E,14E)-12-Hydroxy-5,8,10,14-icosatetraenoic acid*	25 µg, 100 µg/ml solution in ethanol (Cayman CHEMICAL, Ann Arbor, Michigan, USA)
(±)15-HETE	*(5Z,8Z,11Z,13E)-15-Hydroxy-5,8,11,13-icosatetraenoic acid*	25 µg, 100 µg/ml solution in ethanol (Cayman CHEMICAL, Ann Arbor, Michigan, USA)
(±)5-HETE	*(5S,6E,8Z,11Z,14Z)-5-Hydroxy-6,8,11,14-icosatetraenoic acid*	25 µg, 100 µg/ml solution in ethanol (Cayman CHEMICAL, Ann Arbor, Michigan, USA)
6-keto-$PGF_{1\alpha}$	*(9α,11α,13E,15S)-9,11,15-Trihydroxy-6-oxoprost-13-en-1-oic acid*	1 mg, ≥98 % Purity, crystalline solid (Cayman CHEMICAL, Ann Arbor, Michigan, USA)
LTB_4	*(5S,6Z,8E,10E,12R,14Z)-5,12-Dihydroxy-6,8,10,14-icosatetraenoic acid*	25 µg, 100 µg/ml solution in ethanol (Cayman CHEMICAL, Ann Arbor, Michigan, USA)
PGD_2	*(5Z,9α,13E,15S)-9,15-Dihydroxy-11-oxoprosta-5,13-dien-1-oic acid*	1 mg, ≥98 % Purity, crystalline solid (Cayman CHEMICAL, Ann Arbor, Michigan, USA)
PGE_2	*(5Z,11α,13E,15S)-11,15-Dihydroxy-9-oxoprosta-5,13-dien-1-oic acid*	1 mg, ≥98 % Purity, crystalline solid (Cayman CHEMICAL, Ann Arbor, Michigan, USA)
$PGF_{2\alpha}$	*(5Z,8β,9β,11β,12α,13E,15S)-9,11,15-Trihydroxyprosta-5,13-dien-1-oic acid*	1 mg, ≥98 % Purity, crystalline solid (Cayman CHEMICAL, Ann Arbor, Michigan, USA)
TXB_2	*(5Z,9β,13E,15S)-9,11,15-Trihydroxythromboxa-5,13-dien-1-oic acid*	1 mg, ≥99 % Purity, crystalline solid (Cayman CHEMICAL, Ann Arbor, Michigan, USA)

Internal standards

12(S)-HETE-d_8	*(5Z,8Z,10E,12S,14Z)-12-Hydroxy(5,6,8,9,11,12,14,15-$^2H_8$)-5,8,10,14-icosatetraenoic acid*	25 µg, 100 µg/ml solution in acetonitrile (Cayman CHEMICAL, Ann Arbor, Michigan, USA)
15(S)-HETE-d_8	*(5Z,8Z,11Z,13E,15S)-15-Hydroxy(5,6,8,9,11,12,14,15-$^2H_8$)-5,8,11,13-icosatetraenoic acid*	25 µg, 100 µg/ml solution in acetonitrile (Cayman CHEMICAL, Ann Arbor, Michigan, USA)
5(S)-HETE-d_8	*(5S,6E,8Z,11Z,14Z)-5-Hydroxy(5,6,8,9,11,12,14,15-$^2H_8$)-6,8,11,14-icosatetraenoic acid*	25 µg, 100 µg/ml solution in acetonitrile (Cayman CHEMICAL, Ann Arbor, Michigan, USA)
6-keto-$PGF_{1\alpha}$-d_4	*(9α,11α,13E,15S)-9,11,15-Trihydroxy-6-oxo(3,3,4,4-$^2H_4$)prosta-13-en-1-oic acid*	25 µg, 100 µg/ml solution in methyl acetate (Cayman CHEMICAL, Ann Arbor, Michigan, USA)
LTB_4-d_4	*(6Z,8E,10E,14Z)-5,12-Dihydroxy(6,7,14,15-$^2H_4$)-6,8,10,14-icosatetraenoic acid*	25 µg, 100 µg/ml solution in acetonitrile (Cayman CHEMICAL, Ann Arbor, Michigan, USA)
PGD_2-d_4	*(5Z,9α,13E,15S)-9,15-Dihydroxy-11-oxo(3,3,4,4-$^2H_4$)prosta-5,13-dien-1-oic acid*	25 µg, 100 µg/ml solution in methyl acetate (Cayman CHEMICAL, Ann Arbor, Michigan, USA)
PGE_2-d_4	*(5Z,11α,13E,15S)-11,15-Dihydroxy-9-oxo(3,3,4,4-$^2H_4$)prosta-5,13-dien-1-oic acid*	50 µg, 500 µg/ml solution in methyl acetate (Cayman CHEMICAL, Ann Arbor, Michigan, USA)
$PGF_{2\alpha}$-d_4	*(5Z,9α,11α,13E,15S)-9,11,15-Trihydroxy(3,3,4,4-$^2H_4$)prosta-5,13-dien-1-oic acid*	50 µg, 500 µg/ml solution in methyl acetate (Cayman CHEMICAL, Ann Arbor, Michigan, USA)
TXB_2-d_4	*(5Z,8α,9α,13E,15R)-9,11,15-Trihydroxy(2,2,3,3-$^2H_4$)thromboxa-5,13-dien-1-oic acid*	25 µg, 100 µg/ml solution in methyl acetate (Cayman CHEMICAL, Ann Arbor, Michigan, USA)

2.1.2. Reagents

2-Propanol	LC-MS CHROMASOLV® (Sigma Aldrich, St. Louis, USA)
Acetonitrile	CHROMASOLV® gradient grade, for HPLC, ≥99.9 % (Sigma Aldrich, St. Louis, USA)
Ammonia	puriss. p.a., reag. ISO, reag. Ph. Eur., ~25 % NH_3 basis (Sigma Aldrich, St. Louis, USA)
Ethanol	puriss. p.a., absolute, ≥99.8 % (Sigma Aldrich, St. Louis, USA)
Formic acid	puriss., p. a., 98.0-100 % (Sigma Aldrich, St. Louis, USA)
Human serum albumin	Albunorm, 20 % (Octapharma, Vienna, AUT)
Methanol	CHROMASOLV®, for HPLC, ≥99.9 % (Sigma Aldrich, St. Louis, USA)
Water	18.2 MΩ*cm, Milli-Q® Academic water purification system (Millipore GmbH, Vienna, AUT)
Phosphoric acid	for HPLC, 85-90 % (Fluka, Buchs, CHE)
Physiological saline	Elo-Mel isoton, infusion solution, (Fresenius Kabi, Graz, AUT)

2.2. Equipment

Centrifuge	Centrifuge 5415 D	(Eppendorf, Hamburg, DEU)
Vortexer	Reax top	(Heidolph, Schwabach, DEU)
Microplate evaporator	MiniVap with with 96 needle head	(Porvair Sciences, Wales, UK)
96-Wellplate vortexer	Signature™ Pulsing Vortex Mixer	(VWR, Vienna, AUT)
µl pipettes	Reference	(Eppendorf, Hamburg, DEU)
Ultrasonic bath	RK 100	(Bandelin, Berlin, DEU)

Consumables

HPLC vials	Verex vial, 9 mm screw, 2 ml, amber	(Phenomenex, California, USA)
Vial caps	Verex cap, 9 mm, PTFE/silicone septa, blk	(Phenomenex, California, USA)
Vial inserts	Vial insert, 250 µL, pulled point glass	(Agilent Technologies, Waldbronn, Ger)
0.5 ml protein lobind tubes	Protein LoBind tubes, 0.5 ml, PCR clean	(Eppendorf, Hamburg, DEU)
0.2 ml PCR tubes	0.2 ml PCR tube, flat cap	(VWR, Vienna, AUT)
SPE collection plates	96-well sample collection plate, 800 µL	(Waters, Massachusetts, USA)
Sealing mats	Sealing mats 96-well deepwell plates, 1.2 ml	(Eppendorf, Hamburg, DEU)

Solid phase extraction

Solid phase extraction of the weakly acidic analytes was performed with Oasis MAX 96-well µElution plates, 2 mg Sorbent per Well, 30 µm particle size (Waters, Massachusetts, USA) on an extraction plate manifold for OASIS 96-well-plates (Waters, Massachusetts, USA) equipped with a type N811K18 diaphragm pump (Neuberger, Freiburg, Germany) with a possible operating pressure range from 0.24–2 bar.

HPLC column

Atlantis® T3, 3 µm, 2.1 x 150 mm (Waters, Massachusetts, USA)

HPLC – MS/MS system

HPLC:	Ultimate 3000	(Thermo Scientific, Rockford, USA)
ESI-MS:	TSQ Quantum Access MAX	(Thermo Scientific, Rockford, USA)

U-HPLC/high resolution MS system

U-HPLC:	UHPLC^{+} Focused	(Thermo Scientific, Rockford, USA)
HR-ESI-MS:	Q Exactive™	(Thermo Scientific, Rockford, USA)

Evaluation software

Xcalibur 2.2 SP1.48 (Thermo Scientific, Rockford, USA)

2.3. Procedures

2.3.1. Sample collection

Diluted interstitial fluid investigated in this thesis was sampled by dOFM[5]. Samples were collected from one healthy subject ("Set 11"; 12 probes: 1-6 arm, 7-12 leg) and from one subject suffering from psoriasis ("Set 12"; 12 probes: 1-3 non-lesional skin from leg, 4-12 lesional skin from arm). Physiological saline with 1 % human serum albumin (HSA) was taken as perfusate. Both sets were sampled hourly (nominal sample volume 60 µl) over a 12 h period with an applied flow rate of 1 µl/min. Samples were immediately stored at -80 °C. The sampling procedure of Set 12 included two additional steps: the sampling vials were flushed with Ar prior to sampling and the samples overlaid with Ar prior to freezing in order to minimise loss of oxygen-sensitive analytes.

2.3.2. Preparation of standards

After handling, prior to re-storing, all of the stocks and prepared solutions were overlaid with N_2 or, later, Ar, due to limited oxygen stability of some of the analytes. All prepared standard solutions were stored at -80 °C.

A-stocks

A-stocks of the five analytes 5-HETE, 15-HETE, 12-HETE, 12-HEPE, LTB_4 and of all nine internal standards 12(S)-HETE-d_8, 15(S)-HETE-d_8, 5(S)-HETE-d_8, 6-keto-$PGF_{1\alpha}$-d_4, LTB4-d_4, PGD_2-d_4, PGE_2-d_4, $PGF_{2\alpha}$-d_4, TXB_2-d_4) were the solutions in their original containers with their respective concentrations (see 2.1.1). A-stocks of the five analytes 6-keto-$PGF_{1\alpha}$, PGD_2, PGE_2, $PGF_{2\alpha}$ and TXB_2 were prepared by directly dissolving each substance in ethanol and transferring the solution to a 10 ml volumetric flask, which was filled with ethanol to reach a respective concentration of 100 µg/ml. The stocks were aliquoted into amber glass HPLC vials, overlaid with N_2, sealed and stored at -80 °C.

[5] Sampling of dermal interstitial fluid was carried out by the Biomedical Engineering and Monitoring group of HEALTH – Institute for Biomedicine and Health Sciences, Joanneum Research Forschungsgesellschaft m.b.H., Graz, Austria.

B-stocks

B-stocks of all 10 analytes and 9 internal standards were prepared by dilution in ethanol of the respective A-stock amounts to reach a concentration of 10 µg/ml:

- B-stocks of 6-keto-$PGF_{1\alpha}$-d_4 and PGE_2-d_4: 10 µl A-stock (500 µg/ml) were diluted in 490 µl ethanol in an amber glass HPLC vial and vortexed. The solutions were aliquoted into HPLC vials with glass insert, overlaid with Ar, sealed and stored at -80 °C.
- B-stocks of the remaining eight analytes and nine internal standards: 10 µl A-stock (100 µg/ml) were diluted in 90 µl ethanol in an amber glass HPLC vial with glass insert and vortexed. The solutions were overlaid with Ar, sealed and stored at -80 °C.

Calibration standard solutions

For quantification, calibration standards were prepared in water according to Table A 1 (see Appendix).

Internal standard solution

For quantification of the 10 analytes in dOFM samples, a 10 ng/ml internal standard mix was prepared: in an amber glass HPLC vial 10 µl of each of the nine internal standard B-stock solutions (10 µg/ml) were added to 910 µl ethanol. The mixture (= internal standard C-stock with 100 ng/ml) was sealed and vortexed. An aliquot (150 µl) of the internal standard C-stock (100 ng/ml) was further diluted in water (1350 µl) in an amber glass HPLC vial (= internal standard mix for sample preparation with 10 ng/ml).

2.3.3. Preparation of samples

Preparation of dOFM samples

Samples had to be pooled in order to get enough sample volume for triple determinations. Thus after thawing to room temperature, the samples from the psoriatic and the healthy subjects (three probes each, complete 1-12 h) were vortexed, shortly centrifuged and then pooled as follows: samples from the same sampling time of three different probes were pooled resulting in 12 time-resolved sample-pools per subject. These 24 samples were then further treated following the standard extraction procedure and then measured via HPLC–MS/MS on the Q Exactive™ MS.

Standard extraction procedure

After several preliminary experiments, the following extraction procedure was adopted as the "standard extraction procedure". Samples were prepared in replicate (n=3). 40 µl of sample[6] or 20 µl of calibration solution were transferred to a 0.2 ml PCR tube, and 20 µl of internal standard mix (10 ng/ml) and 20 µl of H_3PO_4 (4 % aq. solution) were added. The resulting solution, termed "SPE–mixture", was vortexed and briefly centrifuged by pulse function.

Solid phase extraction was performed with mixed-mode anion exchange 96-well µElution Plates from Waters (Figure 18). The SPE-cartridges were conditioned with 200 µl of methanol and then 200 µl of water. Afterwards the SPE-mixture was loaded quantitatively onto the SPE cartridge and washed with 200 µl of NH_4OH (5 % aq. solution) and 200 µl of methanol. Analytes were then eluted into a 96-well-collection plate with 2 x 50 µl of acetonitrile:methanol (60:40, v:v) containing 2 % of formic acid. The cartridges were reconditioned with 200 µl of methanol and 200 µl of water.

The extracts were then dried under a N_2 stream at room temperature with a microplate evaporator. Afterwards they were re-dissolved in 40 µl of mobile phase A (H_2O:ACN:formic acid, 63:37:0.02, v:v:v), overlaid with Ar and shaken at RT with a vortex mixer (45 min, 2000 rpm) prior to HPLC–MS/MS analysis.

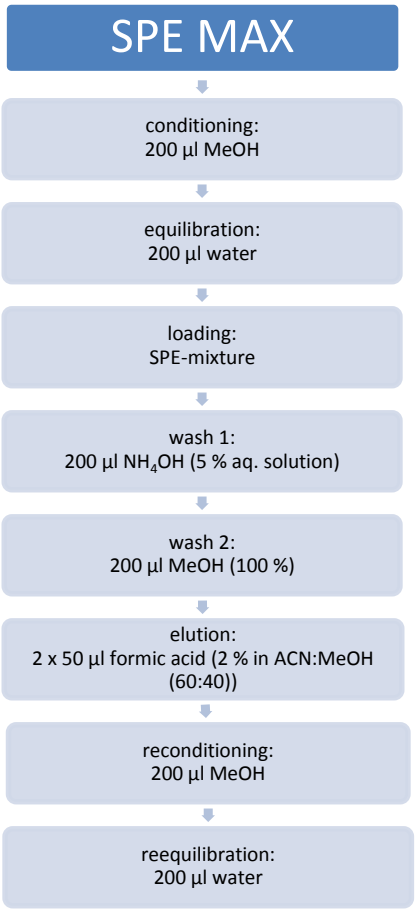

Figure 18: Mixed-mode anion exchange (=MAX) SPE–protocol

[6] Investigated extraction volume of dOFM-samples was 40 µl due to their very low analyte concentration; 20 µl of sample were extracted to determine the hemolytic impact, method recovery, accuracy and inter–day precision.

Determination of hemolytic impact

A further centrifugation step was introduced into the sample preparation procedure to evaluate the influence of hemolytic effects on the results. One sample pool was prepared out of the probe samples from a former dOFM–sampling set (set 09; 1-6 h samples from probe 5), which were selected based on their very reddish colour. Samples were pooled in a 0.5 ml protein lobind tube, vortexed and divided into two aliquots. Aliquot 1 was centrifuged (10 min, 13000 rpm) prior to extraction and the supernatant was transferred to a 0.2 ml PCR tube. The supernatant of aliquot 1 and all of aliquot 2 were extracted separately (3 times per aliquot, n=3) in the same batch by the standard extraction procedure and measured by HPLC–MS/MS on the Q Exactive™ MS.

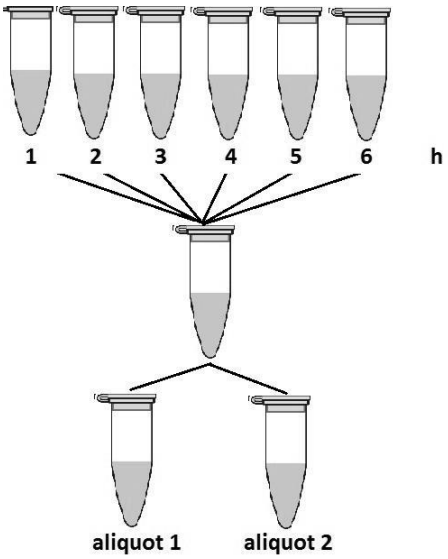

Figure 19: Scheme of sample-pooling for the determination of hemolytic impact

Determination of inter-day precision

Precision represents the repeatability of an experiment. The inter-day precision in this thesis was defined as the relative standard deviation (RSD) of the measured concentrations of an analyte-spiked dOFM sample (worked-up in triplicate and measured, each on two separate days). For the mathematical definition of inter-day precision see Appendix (Table A 16).

For determination of inter-day precision of the analytical method, two dOFM-sample-pools spiked with different amounts of analyte solution were prepared and worked up on two different days.

- Solution 1 (10.0 ng/ml): sample pool (set 09; 7-12 h samples from probe 5) was prepared in a 0.5 ml protein lobind tube. After vortexing the sample, 20 µl of calibration solution (10A C-stock in water, 100 ng/ml) were added to 180 µl of sample pool in a 2.0 ml amber glass HPLC vial with glass insert, and the solution was vortexed again.
- Solution 2 (1.00 ng/ml): sample pool (set 11; 7-12 h samples from probe 12) was prepared in a 0.5 ml µl protein lobind tube. After vortexing, 20 µl of calibration solution (10A 10.0, 10.0 ng/ml) were added to 180 µl of sample pool in a 2.0 ml amber glass HPLC vial with glass insert, and the solution was vortexed again.

Both solutions were worked up in triplicate and measured on two different days by HPLC–MS^2 on the Q Exactive™ MS to determine the variation range of the analytical method.

Determination of accuracy

In quantitative research of biomarkers in endogenous samples like dermal interstitial fluid (where no certified reference material is available) accuracy is usually determined by spiking a matrix-blank (also referred to as "surrogate matrix") with a known amount of analyte (Shaik et al., 2014); the resulting spike-concentration is defined as "true concentration" which is then compared with the measured concentration (Y. Wang et al., 2014). For the mathematical definition of accuracy see Appendix (Table A 16).

The accuracy of this analytical method for eicosanoids was determined by a spiked perfusate solution (10 ng/ml). Thus, 20 µl of calibration solution (10A C-stock in water, 100 ng/ml) were added to 180 µl of dOFM–perfusate (physiological saline, 1 % HSA) in a 2.0 ml amber glass HPLC vial with glass insert, and the solution was vortexed. The solution was worked up in quadruplicate and measured by HPLC-MS/MS on the Q Exactive™ MS.

Determination of recovery

To determine the recovery of the solid phase extraction, two solutions were prepared:

- Internal standard solution (5 ng/ml): internal standard C-stock (100 ng/ml) was diluted in mobile phase A (H_2O:ACN:formic acid, 63:37:0.02, v:v:v) in a 2.0 ml amber glass HPLC vial to a concentration of 5 ng/ml. This solution was not further extracted prior to measurement.
- Internal standard solution (10 ng/ml): internal standard C-stock (100 ng/ml) was diluted in dOFM–perfusate (physiological saline, 1 % HSA) in a 2.0 ml amber glass HPLC vial to a concentration of 10 ng/ml. This solution was extracted in triplicate using the standard extraction procedure except for one difference in the SPE-mix composition: instead of internal standard mix (20 µl, 10 ng/ml), water (20 µl) was added to the sample (20 µl) and 4 % aq. H_3PO_4 (20 µl) solution.

Both solutions were then measured by HPLC–MS/MS on the Q Exactive™ MS, and the resulting areas were compared for recovery determination.

2.3.4. Chromatographic separation

Prior to detection by MS systems (triple quadrupole MS and Q Exactive™ MS) chromatographic separation of the analytes was performed according to Table 1. Because of the partly lipid structure of the analytes, the C18 column Atlantis® T3 from Waters was chosen.

Table 1: Gradient elution conditions for chromatographic separation at 25 °C; solvent A was H_2O:ACN:formic acid (63:37:0.02, v:v:v), solvent B was ACN:2-propanol (50:50, v:v); constant flow rate of 300 µl/min (Deems et al., 2007); 10 µl injection volume

time [min]	A [%]	B [%]
0	100	0
6	100	0
6.5	45	55
10	45	55
12	0	100
13	0	100
13.5	100	0
16	100	0

2.3.5. Determination of eicosanoids by HPLC with TSQ Quantum™ Access MAX Triple Quadrupole MS detection

After HPLC separation, identification and quantification was performed on a TSQ Quantum™ Access MAX Triple Quadrupole (referred to hereafter as TSQ). In this section, only the main features of the TSQ instrument method are mentioned; for complete method settings see Appendix (Table A 6).

Analytes were ionised by an ESI (electrospray ionisation) source with an integrated regular flow needle operated in negative ion mode. Detection of the 10 analytes was carried out by single reaction monitoring (SRM). SRM-transitions used for identification are listed in Table 2. The respective MS instrument method was divided into six scan segments based on the retention times of the analytes (and their respective internal standard). To optimise sensitivity, no parallel full MS scan was performed.

Table 2: SRM-transitions used for identification and quantification; ESI was operated in negative mode.

analyte	parent $[M-H]^-$	fragment 1	fragment 2	internal standard	parent $[M-H]^-$	fragment 1	fragment 2
6-keto-$PGF_{1\alpha}$	369	163	245	6-keto-$PGF_{1\alpha}$-d4	373	167	249
TXB_2	369	195	169	TXB_2-d4	373	173	199
$PGF_{2\alpha}$	353	193	247	$PGF_{2\alpha}$-d4	357	197	251
PGE_2	351	189	271	PGE_2-d4	355	193	275
PGD_2	351	189	271	PGD_2-d4	355	193	275
LTB_4	335	195	-	LTB_4-d4	339	197	-
12-HEPE	317	179	-	12(S)-HETE-d8 used as internal standard			
15-HETE	319	219	175	15(S)-HETE-d8	327	226	182
12-HETE	319	179	135	12(S)-HETE-d8	327	184	140
5-HETE	319	115	-	5(S)-HETE-d8	327	116	-

Analytes and internal standards were tuned with a 1 µg/ml solution of each analyte to determine optimal fragment mass, collision energy, tube lens and skimmer offset settings. Optimal spray settings were determined with a 1 µg/ml $PGF_{2\alpha}$ solution in solvent A (see Table A 5) prior to measurement.

Mixed analyte standard solutions, diluted in mobile phase A in concentrations ranging from 0.50-100 ng/ml, were measured directly for comparison of sensitivity to the Q Exactive™ MS measurements.

2.3.6. Determination of eicosanoids by U-HPLC with Q Exactive™ MS detection

Identification and quantification of eicosanoids was achieved by combining U-HPLC with a high resolution Q Exactive™ mass spectrometer. In this section, only the main features of the Q Exactive™ MS instrument method are mentioned; further information on exact instrument settings (Table A 2), inclusion list settings (Table A 3), and exact parent and fragment masses (Table A 4) can be found in the Appendix.

The selected scan mode was targeted MS^2 in combination with an inclusion list, containing exact analyte and internal standard parent masses (isolation window was set to ± 0.4 m/z) including respective retention time windows and normalized collision energies. The same transitions for identification and absolute quantification were used as in TSQ–analysis (section 2.3.5).

Analytes and internal standards were tuned with a 1 µg/ml solution of each analyte to determine optimal collision energy and fragment mass settings. Analytes were ionised in negative mode by an ESI source with an integrated regular flow needle, installed at the MS inlet. Optimal spray settings were determined with a 1 µg/ml $PGF_{2\alpha}$ solution in solvent A prior to measurement.

Only the Q Exactive™ MS method was used to measure eicosanoids in dOFM samples. External calibration with internal standard normalization was carried out with mixed analyte standard solutions diluted in mobile phase A in concentrations ranging from 0.01-100 ng/ml.

3. Results & discussion

3.1. Time-resolved eicosanoid levels in interstitial fluid of psoriatic and healthy subjects

During the thesis an analytical method was developed to measure 10 representatives of the eicosanoid class. The method was implemented and optimised on a high resolution Q Exactive™ and then additionally adapted to a triple quadrupole MS for qualitative comparison of the two detector types. The optimised method on the Q Exactive™ MS was used to determine eicosanoid levels in interstitial fluid of the skin, sampled by minimally invasive dermal open flow microperfusion (dOFM). As eicosanoids are important markers for inflammation in various physiological processes and diseases, samples were taken from dermis of healthy and psoriatic lesional skin. Samples were prepared in triplicate in one batch for statistical purposes (see section 2.3.). As dOFM sampling enables time-resolved concentration profiling, analyte trends corresponding to sampling time could be observed. In this section, examples of the measured eicosanoid levels, more specifically their time-concentration-curves are listed and discussed; for all original data see Appendix, Table A 7 and Table A 8. It can be summarised that many analytes showed higher concentration levels in interstitial fluid of psoriatic skin compared to healthy samples, which supports the view that eicosanoids can be used to monitor states of inflammation. However, in most cases, and contrary to expectations, the concentration differences did not occur in a multiple range.

Moreover, a statement has to be made concerning the statistical significance of these results: only one healthy and one psoriatic subject have been analysed owing to a lack of sampling-slots and subject availability. Outcomes are likely to vary considerably from subject to subject. Further problems arise in terms of sampling and sample preparation, the analytical implications of which will be discussed in sections 3.1.1. & 3.1.2.

A general observation was made: the 9 h sample of Set12 appeared to be out of line throughout all 10 measured eicosanoids, and some of these seemed to be more affected than others in terms of their respective time-concentration-profiles. This may be reasoned by possible complications during sampling - perhaps this sample was not immediately frozen like the others leading to further enzymatic reactions and changes in eicosanoid production. Analyte concentrations could also have been increased by argon-overlaying steps during sample-handling prior to extraction: for example, higher gas-flow leads to more solvent evaporation resulting in pseudo-higher analyte concentrations in the sample. For these reasons, the 9 h sample was regarded as an outlier and will not be discussed further during the following sections.

Prostaglandins

Since PLA_2 enzyme activity is higher during inflammation (Grimminger & Mayser, 1995), it was expected that AA release would increase in psoriatic samples, which would in turn lead to higher levels of eicosanoids, especially prostaglandins. PGE_2, an important mediator for increasing microvascular permeability and blood flow, also functions as a signalling molecule for proliferation and apoptosis of keratinocytes. All of these effects are very prominent in psoriasis, which is why PGE_2 levels are elevated in affected subjects. Indeed, levels of PGE_2 and also $PGF_{2\alpha}$ continuously showed higher concentrations in every psoriatic sample compared to healthy interstitial fluid (Figure 20).

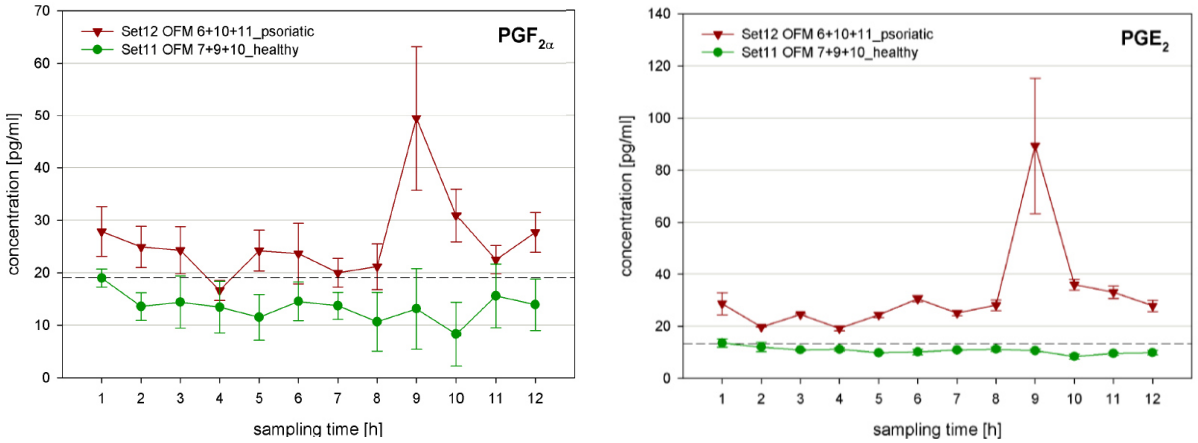

Figure 20: Time-resolved concentration profiles of $PGF_{2\alpha}$ and PGE_2 from two sample pools: "Set11" samples were taken from a healthy subject, "Set12" samples were taken from lesional plaques of a psoriatic subject; the dashed black line marks the LOQ.

Because these prostaglandins are usually produced relatively fast in vivo after irritation by foreign stimuli, a higher amount of PGs was expected especially at the first few sampling hours due to insertion of the probe into the dermis: although dOFM sampling represents a minimally invasive sampling technique, particularly compared to common biopsy, the skin is still injured to some extent. Such an injury was expected to promote acute immune responses and consequently also to enhance ad hoc production of substances mediating inflammation. Interestingly, the obtained concentration-profiles of $PGF_{2\alpha}$ and PGE_2, however, stayed within a similar concentration range throughout the whole duration of sampling. Hence the data-set supports the statement of dOFM being minimally invasive - $PGF_{2\alpha}$ and PGE_2 levels do not seem to be affected by the insertion of the sampling-probe.

Thromboxanes

The biologically inactive TXB_2 is the chemically stable metabolite of TXA_2 (Murphy et al., 2005). In contrast to the PG results, TXB_2 production actually seemed to increase in response to the sampling procedure (Figure 21). This result supports the assumption that probe insertion into the dermis immediately promotes production of inflammatory mediators like TXA_2, responsible for symptoms like blood coagulation. As TXA_2 is predominantly produced by blood platelets, a different interpretation could also be made: the first few samples could have been subject to in vitro hemolysis. Rupturing of red blood cells (erythrocytes) would lead to highly increased amounts of TXA_2 and TXB_2 in the sample, resulting in higher concentrations in the interstitial fluid. Hemolysis could also explain higher TXB_2 levels in the 6 h sample of Set12. For more detailed discussion see section 3.1.2.

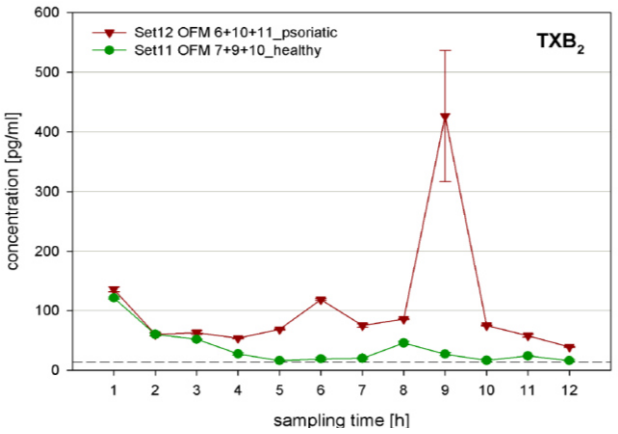

Figure 21: Time-resolved concentration profiles of TXB_2 from two sample pools: "Set11" samples were taken from a healthy subject, "Set12" samples were taken from lesional plaques of a psoriatic subject; the dashed black line marks the LOQ.

Hydroxyeicosapentaenoic acids

12-HEPE was present well above the limits of quantification (Figure 22); it could reliably be quantified in the sub ng/ml range with excellent precision. The results indicated that the levels of 12-HEPE also increased in response to the insertion of the sampling-probe, although the effect was considerably more marked for the psoriasis samples. According to these results one may assume that an injury induced by probe-insertion is more traumatizing for psoriatic than healthy skin in terms of 12-HEPE production. Further investigations have to be made in order to gain more insight into the actual biological response of 12-HEPE.

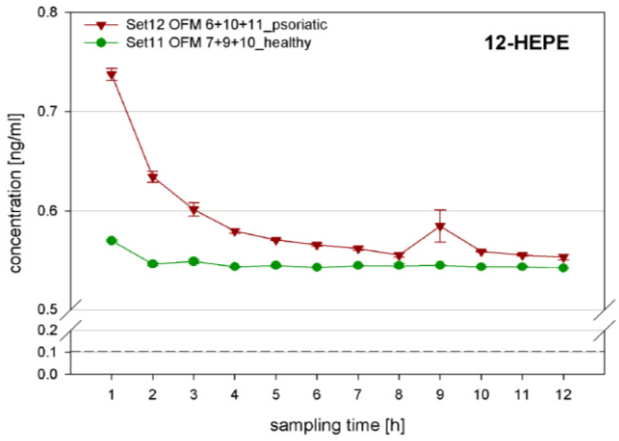

Figure 22: Time-resolved concentration profiles of 12-HEPE from two sample pools: "Set11" samples were taken from a healthy subject, "Set12" samples were taken from lesional plaques of a psoriatic subject; the dashed black line marks the LOQ.

Hydroxyeicosatetraenoic acids

15-HETE, 12-HETE and 5-HETE were all quantifiable with good precision (Figure 23). The obtained profiles of 15-HETE and 5-HETE showed no large differences in concentration between psoriatic and healthy interstitial fluid samples. 15-HETE seems to slightly respond to the probe-insertion, whereas 5-HETE does not seem to be affected at all. However, the amount of 12-HETE increased in response to the insertion of the sampling-probe; the effect was considerably more marked for the psoriasis samples. Interestingly, the obtained concentration-profile of 12-HETE (Figure 23b) shows a similar trend as the related EPA derived 12-HEPE (Figure 22). This similarity reflects the strong affinity of these two compounds due to their common pathway. In contrast to 15- and 5-HETE, 12-HETE was more concentrated in almost every psoriatic sample compared to healthy skin. Highly elevated levels of 12-HETE in psoriasis have been often reported (Hammarström et al., 1975); according to stereochemical analysis, the 12(R)-HETE enantiomer, possessing higher chemotactic properties than 12(S)-HETE, is elevated in psoriatic lesions (Woollard, 1986).

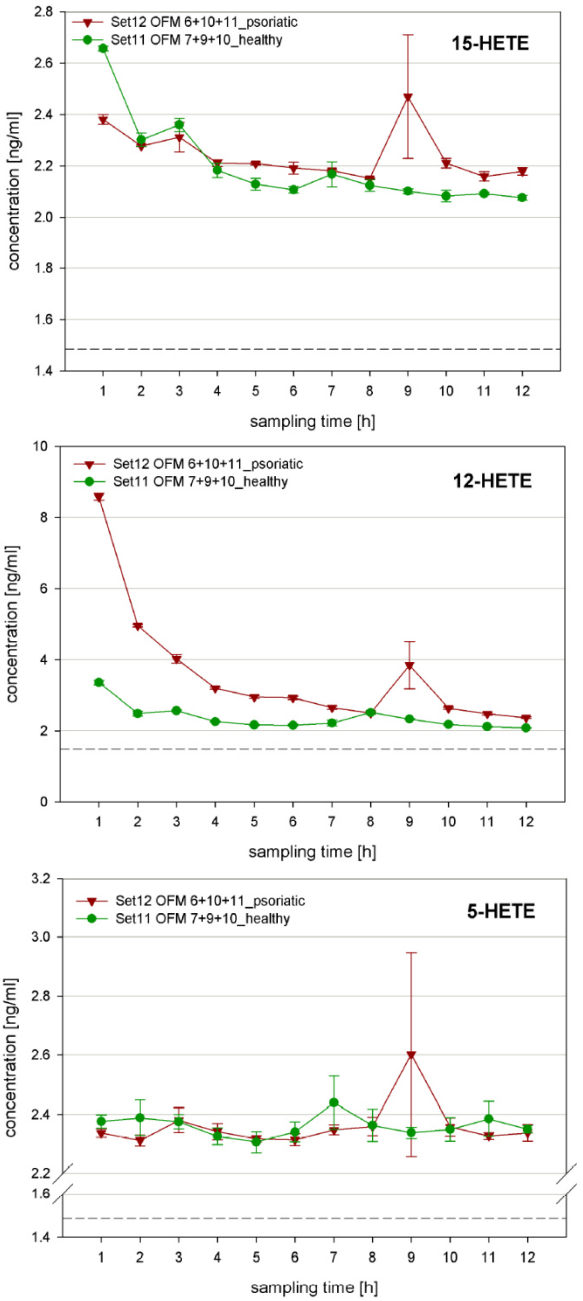

Figure 23a+b+c: Time-resolved concentration profiles of 15-HETE (a), 12-HETE (b) and 5-HETE (c) from two sample pools: "Set11" samples were taken from a healthy subject, "Set12" samples from lesional plaques of a psoriatic subject; the dashed black line marks the LOQ.

Leukotrienes

LTB_4, as representative of the leukotriene group, was not quantifiable by the developed analytical method in either the healthy or psoriatic sample-set. Improvement in the measurement of LTB_4 thus serves as a subject of further method development. Based on the existing data, no statement can be made concerning the biological concentration levels and differences of LTB_4 in dermal interstitial fluid samples of psoriatic and healthy dermis.

3.1.1. Challenges in dOFM sampling

Dermal open-flow microperfusion is a sampling technique that gives the possibility of monitoring analytes in vivo directly at the dermal target tissue. Sampling by dOFM is optimised for application in pharmacological and pharmacokinetic in vivo investigations (Bodenlenz et al., 2013). It has several advantages in comparison to sampling via common dermal microdialysis: utilisation of membrane-free macroscopically fenestrated probes leads to a wider range of accessible analytes in terms of analyte size and lipophilic properties; and a wearable multi-channel pump enables simultaneous sampling from multiple probes over longer periods of time.

But in terms of measuring endogenous analytes, especially eicosanoids, in dermal interstitial fluid by HPLC-MS, there are still some challenges to be further investigated or optimised. Starting with the differing probe depth - the sampling probe is usually inserted manually into the dermis of the skin by a physician. Although probe depth is measured by ultrasound after the sampling period, the thickness of the different layers of the skin can vary a lot between subjects, especially if diseases are involved. Analyte concentrations can vary hugely depending on the exact sampling position of respective probes. In psoriatic sampling during this study, for example, exact probe insertion into the dermis appeared much more difficult in comparison to healthy subjects due to the distinctive thickened stratum corneum. Because the epidermis in psoriatic skin is thicker and irregularly distributed compared to healthy epidermis, probes can easily be misplaced in superior layers rather than in the dermis, where analyte levels can be totally different. Many eicosanoids analysed in this thesis for instance have been reported to have higher abundance in the epidermis than in the dermis (Kendall et al., 2015), making it difficult to compare analyte levels from probes within one subject let alone from different subjects.

A further challenge for the development of an analytical method for dOFM samples was the very low sample volume per probe and period (~60 µl per hour). In addition, these interstitial fluid samples are highly diluted with perfusate. The occurrence of probe-clogging by precipitated proteins, tissue components or blood clots leads to reduced sample flow and consequently decreased analyte amount. During method development, it was decided to pool samples in order to increase the amount of analytes and consequently the sensitivity of the analytical method.

Another point which has to be optimised is the flushing-step of the probes prior to sampling. In dOFM sampling, the probes are flushed with perfusate after insertion in order to establish equal pumping conditions and to flush interfering compounds like blood platelets out of the probes to get clear, perfusate-diluted interstitial fluid. Usually four pumps, each connected to three probes, are installed. Every pump is set to flush-mode right after probe-connection and set-up. But inserting the

probes and connecting them to the pumps takes time leading to varying flushing-times and volumes between probes. Eicosanoids, which are produced very quickly after an acute injury, are possibly flushed out of the system even sampling begins, leading to distorted concentration profiles. For analysing the impact of probe insertion and resultant inflammation development, an equalised (fast) flushing–process has to be designed.

Air, or more correctly oxygen, can also have an impact on the value obtained for an in vivo analyte measured ex vivo. Many eicosanoids, especially HETEs, are oxygen-sensitive and partly light-sensitive owing to the presence of several double bonds. Therefore, to minimise analyte decomposition through oxidation, a further step was introduced into the dOFM sampling procedure: the flushing with argon of empty sampling tubes prior to sampling and overlaying samples after sampling with argon.

3.1.2. Hemolytic effects

One difficulty encountered when using dermal open-flow microperfusion is represented by hemolytic effects. Hemolysis refers to the rupture of red blood cells, the erythrocytes, which is followed by release of the cytoplasm into its surrounding fluid. Hence the actual analyte concentration changes, due either to dilution by cytoplasm or from higher analyte concentrations in cells. Additionally, the enzymatic composition inside these cells can differ widely from its surroundings, leading to further unwanted reactions and transformations resulting in increases or decreases of the analyte. TXB_2 for instance is primarily produced by blood platelets and is heavily involved in the cascade of blood clotting (Yin et al., 2013); hence TXB_2 amounts can be greatly influenced by hemolysis. Rupturing of erythrocytes can be promoted by many factors: in vivo either by disease or ex vivo by stress factors such as too harsh mechanical shear forces, freeze-thaw-cycles, and chemical treatments.

Figure 24: Analysed dOFM samples of Set11 (left) and Set12 (right) after thawing, prior to pooling and extraction; hemolysis is a likely explanation for the high amounts of many analytes in the 9h sample pool of Set12 visible in the time-concentration profiles.

Hemolysis leads to release of hemoglobin, an important iron-containing protein responsible for oxygen transport. Its cofactor heme is responsible for the red colour. Hemoglobin and its degradation products like bilirubin can already be detected visually. Hemolysis is thereby often measured via spectrometric measurements; for instance its absorbance at 410 nm can be used as an index for hemolysis (Nakamura et al., 1997). But spectrometric analysis is unsuitable for dOFM samples due to very small sample volume. Although theoretically dOFM sampling excludes sampling of erythrocytes and should give clear diluted interstitial fluid samples, it often occurs that blood platelets are sampled as well. These usually accumulate at the bottom of the sampling tube during the one hour sampling period, visible as a red dot overlayed with clear interstitial fluid. It is also possible that the whole sample appears to have a homogenous red colour as a clear sign of hemolysis. Usually only the first few sampling hours are affected, although later samples can also show this effect; due to factors like subject movement, small changes in interior flow rate and pump pressure, or clogging of the sample probe consequently leading to increasing shearforces.

Usually after samples were collected, they were overlayed with argon and stored at -80 °C. After thawing, samples were mixed by vortexing in order to avoid inhomogenous distribution in the sample caused by for instance adhesion to the wall of the tube. To test, whether the hemolytic impact could be decreased after thawing, a further centrifugation step was introduced into the sample preparation prior to extraction, and compared to “normal” sample preparation (for exact procedure see 2.3.3). Blood platelets were thereby anticipated to be separated, due to higher density, leaving the supernatant free of blood platelets. Despite centrifugation there was no visible pellet and the fluid was still red. The results of the corresponding HPLC-MS/MS measurement after extraction exhibited no significant concentration difference for most analytes (for data see Table A 9). Hence, a further centrifugation step was not incorporated into the sample preparation. The erythrocytes are probably already ruptured by freezing and thawing. For further investigations it is therefore suggested to centrifuge and separate the supernatant from intact blood platelets directly after sampling in order to achieve clear interstitial dOFM samples.

3.2. Recovery

In eicosanoid-analysis there are several possibilities for sample-clean-up like liquid-liquid extraction, solid phase extraction, immunoaffinity chromatography (IAC) or protein precipitation (PP). Each of the clean-up methods comes with different advantages and drawbacks; the decision of which method to use should consider various factors such as ease-of-use, cost, specificity and sensitivity. PP, for example, usually provides high extraction efficiencies (Martin-Venegas et al., 2014) but, as eicosanoids can bind unspecifically to proteins and co-precipitate, it is not suitable for samples with very low concentrations of analyte.

For sample preparation, solid phase extraction with SPE MAX mixed mode ion exchange material obtained from Waters was chosen. These extraction cartridges feature reversed-phase and anion exchange retention mechanisms enabling them to extract a broad range of eicosanoids, which possess both acidic as well as lipid character. SPE is therefore very suitable for the development of multi-analyte analytical methods. The SPE MAX cartridges are available inter alia in a 96-well-plate µElution format enabling them to extract analytes efficiently from very small sample volumes like dOFM samples. By using 96-well-plates, time-efficient parallel workup of several different samples is possible[7].

Table 3: SPE-recovery of deuterated analytes (n=3); for data and calculation see Table A 10 & Table A 16

analyte	recovery [%]	RSD [%]
6-keto-$PGF_{1\alpha}$-d4	103.2	4.5
TXB_2-d4	85.1	2.4
$PGF_{2\alpha}$-d4	87.1	3.8
PGE_2-d4	88.9	4.8
PGD_2-d4	71.6	8.9
LTB_4-d4	37.7	1.5
15(S)-HETE-d8	30.2	1.5
12(S)-HETE-d8	36.7	2.1
5(S)-HETE-d8	37.6	2.8

Table 3 shows the results from the recovery experiment. These results were comparable to other current analytical methods for eicosanoids (Massey & Nicolaou, 2013). In the SPE procedure, samples were first mixed with internal standard and then acidified in order to disrupt protein binding and improve flow through the SPE-device. After conditioning and equilibration of the SPE-material, samples were loaded onto the medium, and suctioned carefully through it. This step must be performed slowly to avoid major analyte loss due to insufficient anionic exchange and binding of the analytes. Washing with aq. NH_4OH promotes charging of the acidic analytes leading to better binding to the stationary phase, while at the same time other neutral and basic compounds are washed out. The following wash-step with MeOH leads to elution of non-polar components bound by reversed-phase interactions. Although some eicosanoid groups with higher lipid-character may be partly eluted by this step, the separation of the

[7] *Waters Corporation*, 2015. Sample preparation. pp.23–78.
Available at: http://www.waters.com/webassets/cms/library/docs/lcSP.pdf [Accessed July 31, 2014]

target analytes from MS–interfering compounds was prioritised. Afterwards, a solution of formic acid diluted in ACN/MeOH was used to elute the target eicosanoids. Subsequently, solvent–evaporation was done with N_2, not air, in order to minimise analyte loss through oxidation of sensitive analytes. Oxidation in air and also decomposition by light while sample processing could be reasons for the relatively low recovery of the HETEs and LTB_4.

3.3. Accuracy & precision

Table 4: Results of accuracy determination (n=4); for data & calculation see Table A 11 & Table A 16

analyte	accuracy [%]	RSD [%]
6-keto-$PGF_{1\alpha}$	100.4	2.6
TXB_2	101.0	2.6
$PGF_{2\alpha}$	102.6	2.1
PGE_2	100.7	1.5
PGD_2	98.3	1.2
LTB4	99.7	2.3
12-HEPE	62.8	1.2
15-HETE	121.7	1.5
12-HETE	128.0	1.5
5-HETE	125.5	4.3

The accuracy represents the correspondence between a measured sample-concentration and its true concentration. As already stated in section 2.3.3, the accuracy in quantitative research of biomarkers in endogenous samples is determined by spiking a matrix-blank (Shaik et al., 2014); the resulting spike-concentration is defined as "true concentration". This solution was prepared by spiking a perfusate-blank sample to get a reference concentration of 10 ng/ml. Accuracy, especially for the five "main analytes" (four PGs and TXB_2) that were prioritised throughout the development and optimisation processes of method development, were quite acceptable (Table 4). These eicosanoids are also the first eluting analytes during the chromatographic separation. LTB_4 also showed good results similar to those for the five main analytes; measured values for all six analytes were within 3 % of the spiked (true) concentration.

The remaining representatives of other eicosanoid groups, 12-HEPE and the three HETEs, showed poorer accuracy with values ranging from 62.8 % to 128 % of the spiked concentrations, even though deuterated internal standards for each compound (except for 12-HEPE, which was quantified by related 12(S)-HETE-d8) were added directly before sample-workup. Because their chemical structures are equivalent, except for partial replacement of hydrogen with deuterium, these internal standards have chemical properties and behaviour equal to those of the naturally occurring analytes. Hence, uncertainties in the analytical method resulting from variations in sample extraction and measurement should be compensated for and not affect the concentration results.

A possible explanation for the poor accuracy values for the three HETEs is carryover effects and increasing background. During later-phase method development, it became clear that for these less polar analytes, repeated use of the same SPE-cartridge-slots led to background-noise and carryover signals, which were both absent in new SPE-cartridges. This effect was not observed for the more polar analytes. For the accuracy (and precision) experiments, both performed in earlier stages of method development, SPE clean-up was performed with already used SPE-material (whereas extraction of psoriatic and healthy samples from section 3.1. was performed with new and unused SPE-cartridges, and no background problems occurred). Thus, measured concentrations for HETEs are high as a result of contamination. This effect was also apparent for the precision experiments,

which showed similar trends of high HETE values (Table 5). These carryover and high background problems for HETEs must be addressed by further optimisation of the SPE-procedure in future development of the method.

Table 5: Results of inter-day precision determination (3-fold workup per concentration & day → n=6); for data & calculation see Table A 12 & Table A 16. The measured recovery of the HETEs is high as a result of carry over effects and resultant high (uncorrected) background

analyte	x̄ [ng/ml] (10 ng/ml)	RSD [%] (10 ng/ml)	x̄ [ng/ml] (1 ng/ml)	RSD [%] (1 ng/ml)
6-keto-$PGF_{1\alpha}$	10.5	2.1	1.01	1.5
TXB_2	9.80	1.7	0.963	3.1
$PGF_{2\alpha}$	10.4	1.6	0.994	3.3
PGE_2	10.1	2.0	0.946	4.3
PGD_2	7.98	7.1	0.612	30.8
LTB_4	10.7	3.1	1.06	3.1
12-HEPE	6.06	6.3	1.43	15.5
15-HETE	13.7	6.6	4.96	5.0
12-HETE	15.6	4.5	5.10	6.2
5-HETE	14.0	5.6	4.86	5.1

Precision data was obtained by measuring two dOFM sample-pools, each spiked with either 1 ng/ml or 10 ng/ml of the analytes; the two samples were extracted in triplicate and measured on two different days; the inter-day precision was defined as the relative standard deviation of the respective measured concentrations. Results show that the five main analytes (except PGD_2) and LTB_4 eluting first from the HPLC column again show better precision compared to the others (Table 5). The PGD_2 peak of the resulting chromatogram has often to be integrated manually due to insufficient automatic processing of the software (as a consequence of slight retention time shifts), which could be an explanation for the high value of PGD_2. In addition, the raw data shows that the PGD_2-concentrations of the 1 ng/ml sample were considerably lower on day 2 compared to day 1 (Table A 12); a possible cause is analyte degradation due to too long handling at room temperature during sample workup; PGD_2 exhibits low stability at temperatures >4 °C (Maddipati & Zhou, 2011). According to current studies, general accuracy and precision can be improved by handling samples and stock-solutions on ice (Kamlage et al., 2014; Martin-Venegas et al., 2014). Thereby risk of primarily thermal but also enzymatic changes in analyte concentrations can be minimised.

Precision can be influenced by variation during sample processing, so called random errors, prior to the addition of internal standard; for example pipetting-errors or slightly different degrees of solvent evaporation due to inert-gas overlay. Generally, the lower the measured concentration range, the less precise was the measurement.

3.4. Chromatographic separation

The extracted samples were separated by high performance liquid chromatography prior to mass spectrometric detection. For the separation of eicosanoids, which possess both lipid as well as acidic character, an Atlantis T3 column from Waters was chosen. Its proprietary silica-based C_{18} reversed-phase stationary material is optimised for separating a wide range of neutral, hydrophobic and also polar compounds[8]; thus it was suitable for development of a multi-analyte analytical method. Eicosanoids were well resolved by using gradient elution (Figure 25).

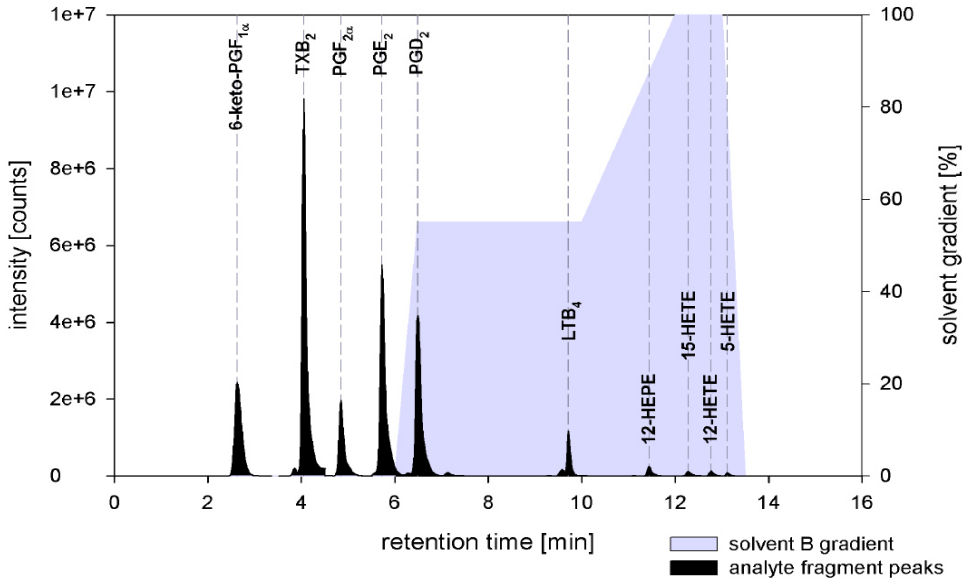

Figure 25: U–HPLC/targeted MS^2 of an extracted 100 ng/ml calibration solution; solvent A was H_2O:ACN:formic acid (63:37:0.2, v:v:v), solvent B was ACN:2-propanol (50:50, v:v); the chromatogram shows the separation of the 10 analytes; the elution conditions are based on those reported by Deems et al (2007).

The polar PGs elute first with the partly aqueous mobile phase, followed by LTB_4 and eventually 12-HEPE and the three HETEs which elute at pure organic conditions due to their higher hydrophobic character. Clear chromatographic separation was especially important for compounds with the same molecular mass and MS-fragmentation pattern like PGE_2 and its structural isomer PGD_2. The resulting chromatogram showed adequate separation (improving method selectivity) of the 10 eicosanoid analytes along with sharp peak shapes (improving sensitivity). Chromatographic separation was not optimised further: sharper peaks would also require faster detectors to give improved method sensitivity otherwise signal-output is lost. Given that scan time is kept the same, the total amount of scans per peak decreases with narrower peak width which results in poor peak shape; this effect is accompanied by an increasing risk of intensity loss (cf. section 3.5) and hence reduced sensitivity.

[8] *Waters Corporation*, 2007. ATLANTIS T3 AND ACQUITY UPLC HSS T3 COLUMNS. pp.1-6.
Available at: http://www.waters.com/webassets/cms/library/docs/720001887en.pdf [Accessed July 20, 2014].

3.5. Comparison of Q Exactive™ MS with triple quadrupole MS

Most reported methods for measuring eicosanoids use triple quadrupole mass analysers to detect the analytes because of their enhanced detection speed. Therefore the method developed for the Q Exactive™ MS was adapted for use with an HPLC/TSQ Quantum™ Access MAX Triple Quadrupole MS system in order to compare these two detector types.

3.5.1. Scan mode: targeted MS^2 versus SRM

Q Exactive™ MS

The Q Exactive™ MS offers various different scan types and combinations from which the targeted MS^2 mode was selected for this study. Depending on an inclusion list, where retention time range, polarity and parent mass of the respective analytes have to be provided, the MS selects the respective parent ions in the quadrupole mass filter and transfers them to the HCD cell (via the C-trap) for fragmentation. All fragments are then sent back into the C-trap which is filled until sending them into the orbitrap, where all fragment ions are detected with high resolution of the fragment ions (→ a full MS scan of the fragments in a prior selected m/z range is recorded). This scan type was chosen because detection can be focused on the parent ion of choice during the already known retention time ranges while MS interfering compounds causing background noise are split off right at the first mass filtering step. The retention time windows were circumscribed as narrow as possible during method development in order to enhance the number of scans per analyte and its internal standard to obtain maximal signal intensity. This step was critical during method development: the narrower the retention time window was set in the inclusion list, the higher was the risk of partial or even complete loss of analyte signals due to slight retention time shifts. Such shifts can be caused by small changes in mobile phase composition, formic acid evaporation out of solvent A for instance. Hence the decision was made to let retention time windows of some analytes overlap partially, even though overlapping leads to only half the number of scans per analyte per overlapping section (or even fewer, depending on the number of overlapping analytes and internal standards).

Scan time generally was a highly limiting factor during method development; short scan times raise the number of total scans and make it possible to detect substances, even at trace levels, which are only briefly eluted, but this is accompanied by a loss of signal intensity because smaller numbers of ions are detected. Vice versa, if scan times are chosen too wide, higher intensity but lesser scan-signals are produced, resulting in poor peak shape. Also signals of very low concentrated substances, which elute only in a short time span, can be lost due to growing background-noise. Scan time is

influenced and increased by several instrument settings: (i) resolution: the higher it is, the longer the scan; (ii) AGC target (automatic gain control): gives the limiting amount of ions in the C-trap before directly sending them into the orbitrap; the higher the setting, the longer it takes till the limit is reached, hence the longer the scan; (iii) maximal inject time: after this time ion injection from the C-trap into the orbitrap is triggered, regardless of whether the AGC target was reached or not. During method development the optimal settings for all these factors were found in order to balance the scan duration/amount and signal intensity.

In order to push sensitivity for most analytes, not only signals from one but two characteristic fragments were summed by the evaluation software in order to further increase the respective signal intensity. Ultimately the developed method combining HPLC–separation and high resolution Q Exactive™ MS produced good quality chromatograms (Figure 26).

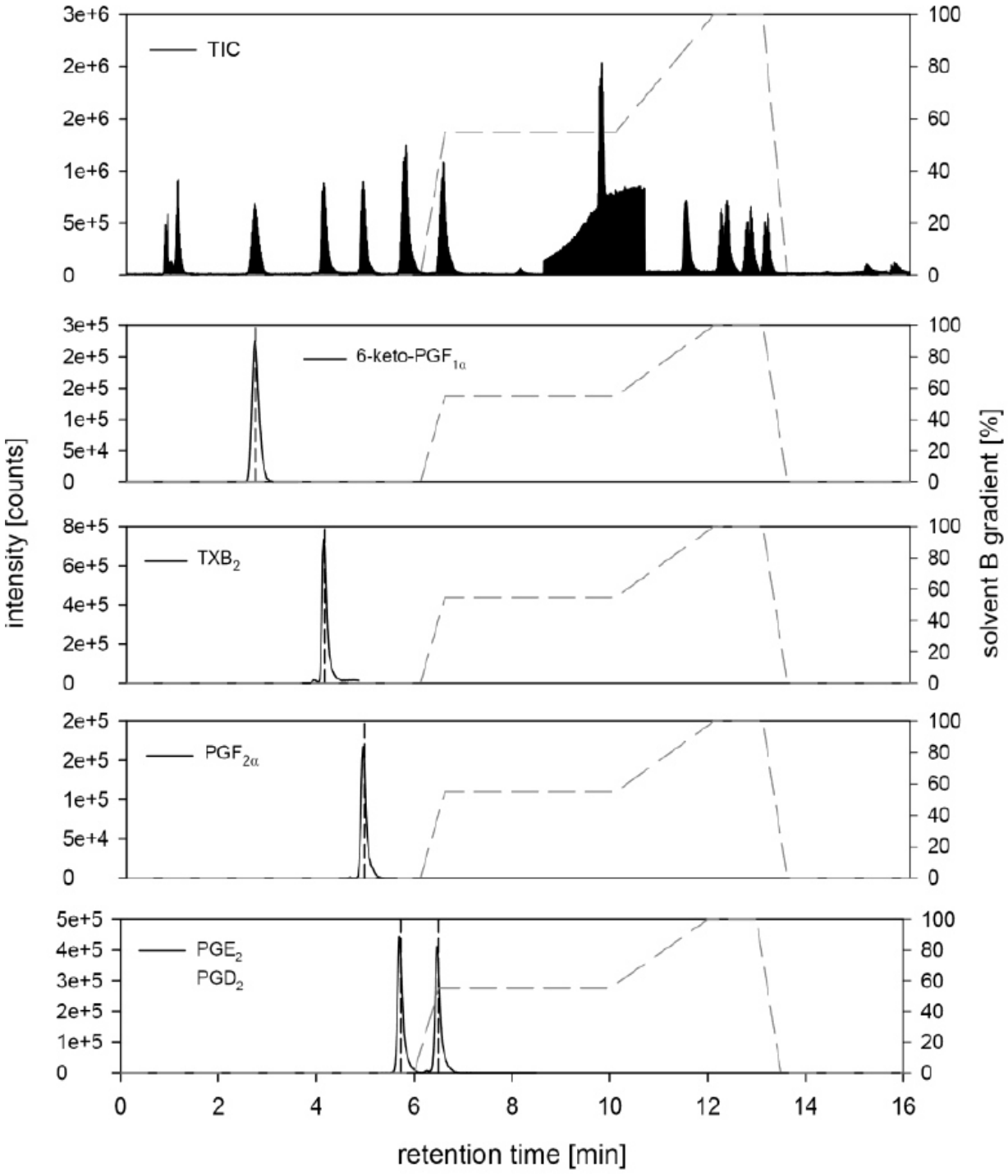

Figure 26a: U–HPLC/targeted MS² fragment chromatograms of a 5 ng/ml analyte solution detected with a Q Exactive™ MS; shown are the total ion current (TIC) and the five first eluting analytes; exact instrumental settings are listed in Table A 2 and Table A 3.

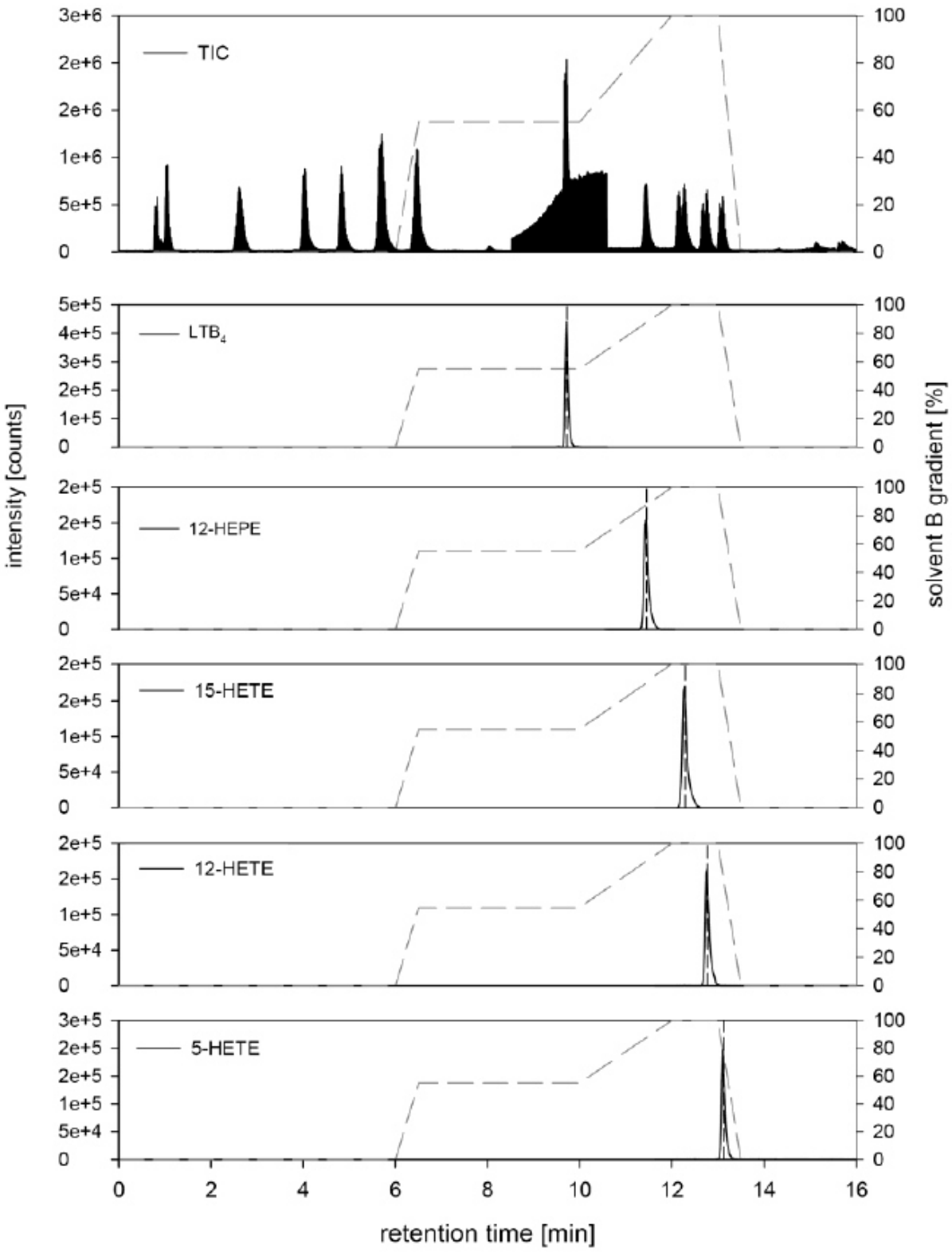

Figure 26b: U–HPLC/targeted MS² fragment chromatograms of a 5 ng/ml analyte solution detected with a Q Exactive™ MS; shown are the total ion current (TIC) and the five later eluting analytes; exact instrumental settings are listed in Table A 2 and Table A 3.

Triple quadrupole MS

A major advantage of this MS system is its speed. Numerous m/z values can be scanned in very short time, which makes them perfectly applicable for sensitivity- and speed-requiring multi-analyte eicosanoid-analysis. These very short scan times are also the reason why tandem MS systems are mostly preferred in mass spectrometric eicosanoid analysis (Balgoma et al., 2013). Literature research also indicated that most studies in this field do not use triple quadrupoles from Thermo Fisher Scientific, but rather from AP SCIEX or Waters. Hence it was suspected that triple quadrupole MS instruments from Thermo Scientific lack sensitivity. To test this assumption and to determine sensitivity of triple quadrupole detection, the method developed for the Q Exactive™ MS was transferred and adjusted to a SRM-method (single reaction monitoring: parent ions are selected in Q1, fragmented in Q2 and via selection in Q3 only preselected fragments are detected in the end, hence making detection fast and sensitive) on a TSQ Quantum™ Access MAX Triple Quadrupole MS. The method was partitioned into 6 scan-segments according to the respective retention times of the analytes and internal standards. During these segments only the given fragments are scanned - no full scan over a certain m/z range was made (compared to the Q Exactive™ MS method), and hence detection was expected to exceed the Q Exactive™ MS method in terms of speed and sensitivity. The respective instrumental settings are listed in Table A 5 and Table A 6. Figure 27 shows the results of a 5 ng/ml analyte solution measured with the TSQ–method.

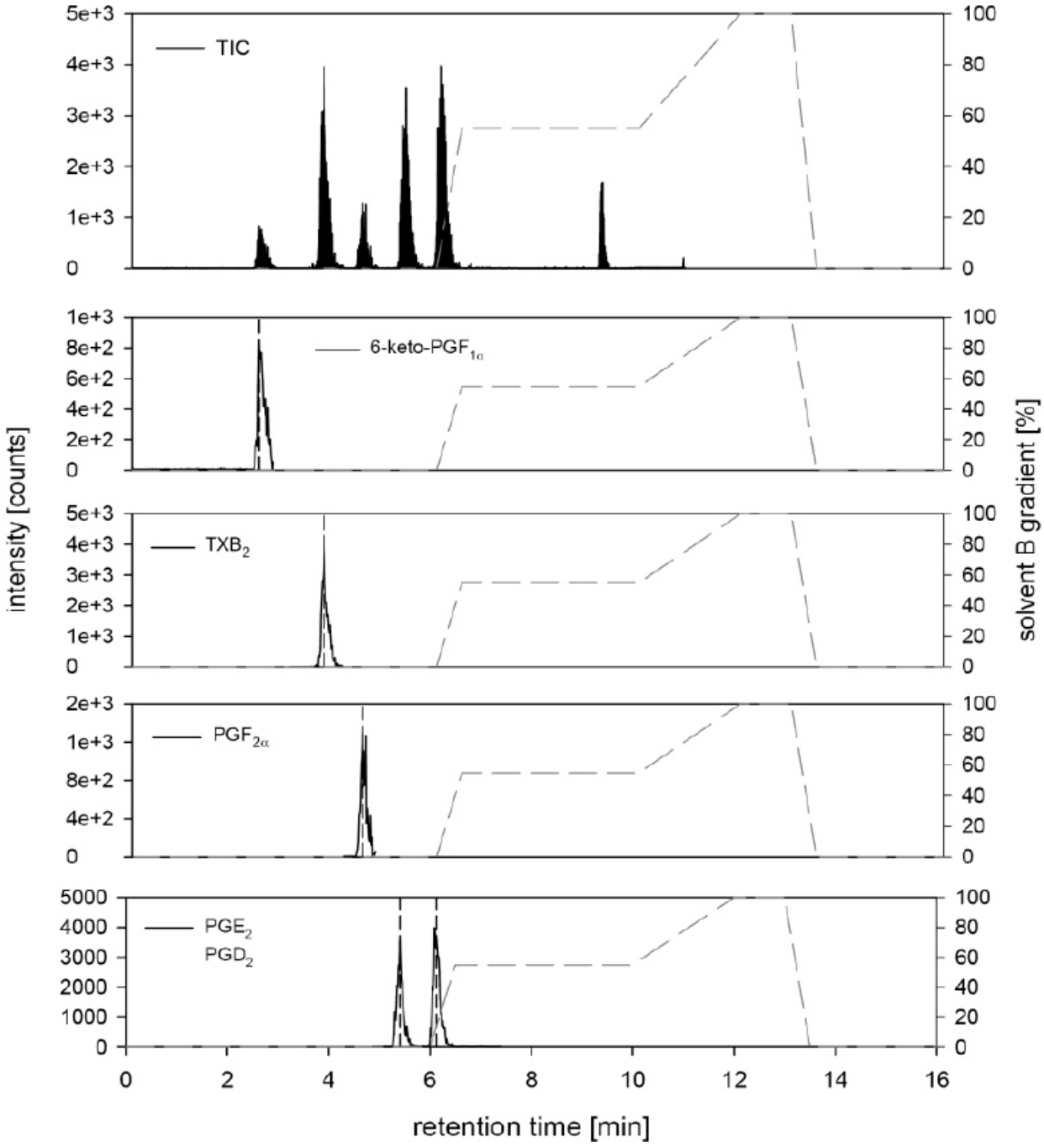

Figure 27a: HPLC/SRM triple quadrupole MS fragment chromatograms of a 5 ng/ml analyte solution; shown are the total ion current (TIC) and the five first eluting analytes; exact instrumental settings are listed in Table A 5 and Table A 6.

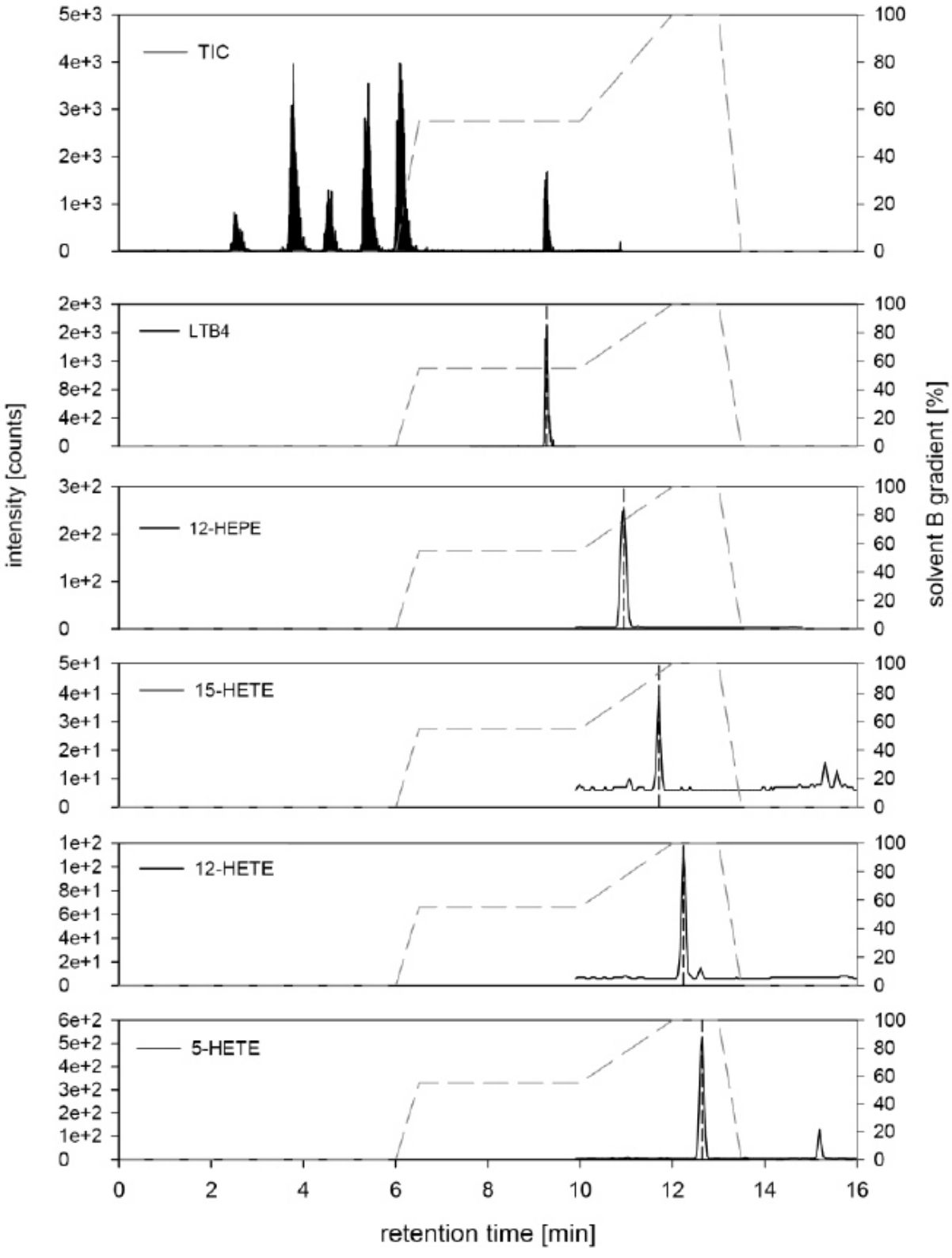

Figure 27b: HPLC/SRM triple quadrupole MS fragment chromatograms of a 5 ng/ml analyte solution; shown are the total ion current (TIC) and the five later eluting analytes; exact instrumental settings are listed in Table A 2 and Table A 3.

3.5.2. Sensitivity

The obtained results comparing measurements are shown in Figure 26 (Q Exactive™) and Figure 27 (TSQ). Peaks of the Q Exactive™ have a nice, sharp shape with relatively high intensities compared to the TSQ measurements; the peak shapes in the chromatograms of the triple quadrupole detection are less sharp, show higher background noise, and the overall intensities are very poor, especially those of HETEs. One factor for poor detection of HETEs with TSQ is reasoned by the respective scan-segment in the instrument method: there was only one section for measuring 12-HEPE and all HETEs (fragments of analytes as well as internal standards). This setting greatly decreases the total number of scans per analyte resulting in poor peak shape.

Sensitivity is a major requirement in the determination of very low concentrated analytes such as eicosanoids. Although signal intensity and sensitivity are related, a direct comparison of sensitivity between Q Exactive™ and TSQ by means of area under the curve is difficult due to their totally different detector design. The Q Exactive™ possesses a C-trap which collects ions prior to the finally detecting orbitrap. The trap is only triggered if either a certain inject time or amount of ions has been reached. This means that signals are only produced after reaching a certain threshold value; these signals already possess relatively high intensity (depending on the respective threshold settings), which leads to high areas under the curve. A triple quadrupole MS, however, detects continuously; there is no trap for prior ion-collection and intensity-pushing. Hence very low ion-amounts can already produce a signal but with low intensity. In summary this means that the Q Exactive™ generally produces peak-signals with higher intensities. Hence the produced areas under the curve of the same solution cannot be compared directly in terms of sensitivity. For an exact comparison of sensitivity, further experiments with different setups have to be made. Nevertheless, Figure 28 can already give a qualitative feel for signal differences between Q Exactive™ and TSQ; it visualizes the area differences in log scale between the two measurements from Figure 26 (Q Exactive™) and Figure 27 (TSQ). Detection by TSQ continuously showed lower signals in a multiple range for all measured eicosanoids compared to the Q Exactive™. As already mentioned, sensitivity should theoretically follow

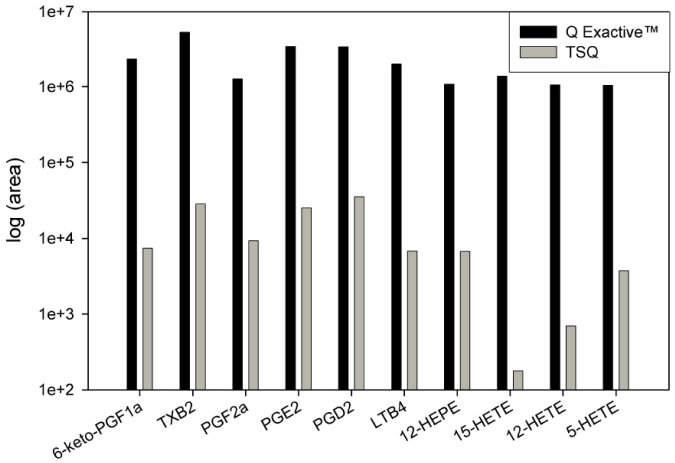

Figure 28: Area comparison between Q Exactive™ MS and triple quadrupole MS by a 5 ng/ml analyte solution in log scale

quite an opposite trend; detection with the TSQ should exhibit better sensitivity because of faster detection due to only scanning specific fragments instead of a wider m/z range, as performed by the high resolution Q Exactive™ MS. But a likely major reason for such a large difference in the sensitivities is the age of the utilised instruments; while the Q Exactive™ was a relatively new device, the TSQ Quantum™ Access MAX Triple Quadrupole was several years older and its performance compromised by numerous previous routine analyses. Newer, state of the art triple quadrupole detectors possess speed and sensitivity properties far superior to the TSQ, with LOQs in the pg-range (Y. Wang et al., 2014). Thus new triple quadrupole mass spectrometers might be expected to outperform the Q Exactive in terms of sensitivity for the determination of eicosanoids.

3.6. Outlook

The developed analytical method for qualification and quantification of eicosanoids was optimised for measuring diluted interstitial fluid sampled by dermal open-flow microperfusion (dOFM). A combination of high performance liquid chromatography and high resolution mass spectrometry with a Q Exactive™ MS detection was used for the measurements. The obtained results look promising but there is still considerable room for improvement. Some of the factors open for optimisation include the sampling process, sample handling, extraction and last but not least sample measurement. In this section one promising possibility, which has not been mentioned before, is shortly presented, namely derivatisation.

Due to low eicosanoid concentrations, especially in highly diluted interstitial fluid, the current developed method struggles in terms of sensitivity, especially for analysis of PGD_2, LTB_4 and HETEs. Addition of further analytes into this method is limited by the scan speed of the Q Exactive™ MS, and also by the low ionisation efficiency when ESI is used in negative mode. Sensitivity could be increased by forming a cationic derivative and operating the ESI in positive ion mode. The derivatising agent, called N-(4-aminomethylphenyl)pyridinium (AMPP) (Bollinger et al., 2010), reacts with the carboxyl terminus of the eicosanoid leading to an AMPP-eicosanoid derivative linked via an amide bond.

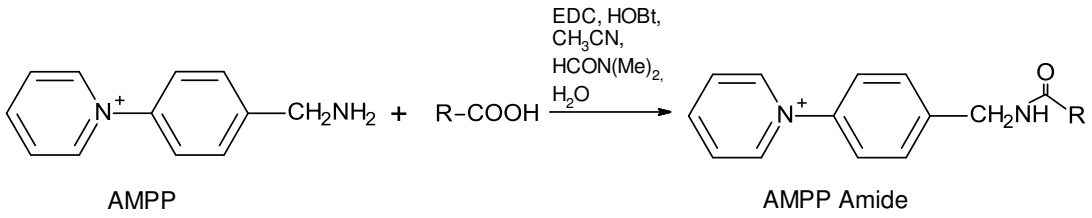

Figure 29: Derivatisation reaction of AMPP with carboxyl-group of eicosanoids (Bollinger et al., 2010)

The cationic derivatives can be detected in positive instead of negative ionisation mode, thereby benefitting from better ionisation efficiency and sensitivity. The derivatisation itself is also simply performed; the derivatisation mixture is just added and mixed with the extracted dry sample, incubated for 30 min at 60 °C and the resulting solution can be measured directly without any further purification (Liu et al., 2013). Introduction of derivatisation into the existing analytical method would probably significantly enhance the sensitivity of the method for the current 10 analytes.

4. Concluding comments

This thesis describes the development and evaluation of an analytical method to determine 10 representatives of prostaglandins, thromboxanes, hydroxyeicosapentaenoic and hydroxyeicosatetraenoic acids, collectively known as eicosanoids. Through combination of solid phase extraction, high performance liquid chromatography and high resolution mass spectrometry it was possible to successfully qualify and quantify these eicosanoids in the ng/ml or even pg/ml range. Nevertheless, accuracy and repeatability in such low concentration ranges have to be optimised further, specifically for highly sensitive hydroxyeicosatetraenoic acids.

As eicosanoids are vital markers in inflammation, the developed multi-analyte method was used to create time-concentration profiles of eicosanoids in diluted interstitial fluid from human dermis. Samples from one healthy subject and one suffering from psoriasis were obtained via dermal open-flow microperfusion in order to compare their eicosanoid levels. Most of the analytes were successfully quantified in psoriatic and at least detected in healthy samples. However the analytical method lacked sensitivity for measuring in vivo concentrations of PGD_2 and LTB_4 in the sampled interstitial fluid.

Further optimisation of the existing sampling procedure and analytical method especially in terms of sensitivity is necessary in order to qualify and quantify all 10 selected eicosanoids in diluted dermal interstitial fluid. It is suggested as well to add further eicosanoids to the analytical panel to gain better knowledge of in vivo pathways during inflammation.

Also, further sampling has to be done in order to elucidate and consolidate differences of concentration levels and trends from eicosanoids. Only then will it be possible to give a clear statement concerning differences of in vivo concentrations and pathways of eicosanoids between health and sickness.

5. References

Balgoma, D., Checa, A., Sar, D. G., Snowden, S., & Wheelock, C. E. (2013). Quantitative metabolic profiling of lipid mediators. *Molecular Nutrition & Food Research*, *57(8)*, 1359–1377.

Bergström, S., Ryhage, R., Samuelsson, B., & Sjövall, J. (1963). Prostaglandins and Related Factors. *The Journal of Biological Chemistry*, *238(11)*, 3555–3564.

Bodenlenz, M., Aigner, B., Dragatin, C., Liebenberger, L., Zahiragic, S., Höfferer, C., Sinner, F. et. al. (2013). Clinical applicability of dOFM devices for dermal sampling. *Skin Research and Technology*, *0*, 1–10.

Bollinger, J. G., Thompson, W., Lai, Y., Oslund, R. C., Hallstrand, T. S., Sadilek, M., Gelb, M. H. et. al. (2010). Improved sensitivity mass spectrometric detection of eicosanoids by charge reversal derivatization. *Analytical Chemistry*, *82(16)*, 6790–6796.

Bombardieri, S., Ciabattoni, G., Munno, D. I., Pasero, G., Pinca, E., & Pugliese, F. (1981). The synovial prostaglandin system in chronic inflammatory arthritis: differential effects of steroidal and nonsteroidal anti-inflammatory drugs. *British Journal of Pharmacology*, *73*, 893–901.

Buczynski, M. W., Dumlao, D. S., & Dennis, E. A. (2009). Thematic Review Series: Proteomics. An integrated omics analysis of eicosanoid biology. *Journal of Lipid Research*, *50(6)*, 1015–38.

Davidson, A., & Diamond, B. (2001). Autoimmune Diseases. *The New England Journal of Medicine*, *345*, 340–350.

Deems, R., Buczynski, M. W., Bowers-Gentry, R., Harkewicz, R., & Dennis, E. A. (2007). Detection and quantitation of eicosanoids via high performance liquid chromatography-electrospray ionization-mass spectrometry. *Methods in Enzymology*, *432*, 59–82.

Eguchi, N., Minami, T., Shirafuji, N., Kanaoka, Y., Tanaka, T., Nagata, A., Hayaishi, O. et. al. (1999). Lack of tactile pain (allodynia) in lipocalin-type prostaglandin D synthase-deficient mice. *Proceedings of the National Academy of Sciences of the United States of America.*, *96,* 726–730.

Funk, C. D. (2001). Prostaglandins and Leukotrienes : Advances in Eicosanoid Biology. *Science*, *294*, 1871–1876.

Goldblatt, M. W. (1933). A depressor substance in seminal fluid. *J. Soc. Chem. Ind.*, *52*, 1056–1057.

Grimminger, F., & Mayser, P. (1995). Lipid mediators, free fatty acids and psoriasis. *Prostaglandins, Leukotrienes and Essential Fatty Acids*, *52(1)*, 1–15.

Gross, J. H. (2013). *Massenspektrometrie - Ein Lehrbuch*. Berlin Heidelberg: Springer.

Hamberg, M., Svensson, J., & Samuelsson, B. (1975). Thromboxanes: a new group of biologically active compounds derived from prostaglandin endoperoxides. *Proceedings of the National Academy of Sciences*, *72(8)*, 2994–2998.

Hammarström, S., Hamberg, M., Samuelsson, B., Duell, E. A., Stawiski, M., & Voorhees, J. J. (1975). Increased concentrations of nonesterified arachidonic acid , 12L-hydroxy-5,8,10,14-eicosatetraenoic acid, prostaglandin E2, and prostaglandin F2α in epidermis of psoriasis. *Proceedings of the National Academy of Sciences of the United States of America*, *72(12)*, 5130–5134.

Harizi, H., Corcuff, J.-B., & Gualde, N. (2008). Arachidonic-acid-derived eicosanoids: roles in biology and immunopathology. *Trends in Molecular Medicine*, *14(10)*, 461–469.

Hughes, H., Nowlin, J., Gaskelli, S. J., & Parr, V. C. (1988). Selected Reaction Monitoring During Gas Chromatography / Mass Spectrometry of Eicosanoids. *Biomedical and Environmental Mass Spectrometry*, *16*, 409–413.

Ikai, K. (1999). Psoriasis and the arachidonic acid cascade. *Journal of Dermatological Science*, *21(3)*, 135–146.

Kamlage, B., Maldonado, S. G., Bethan, B., Peter, E., Schmitz, O., Liebenberg, V., & Schatz, P. (2014). Quality markers addressing preanalytical variations of blood and plasma processing identified by broad and targeted metabolite profiling. *Clinical Chemistry*, *60(2)*, 399–412.

Kendall, A. C., & Nicolaou, A. (2013). Bioactive lipid mediators in skin inflammation and immunity. *Progress in Lipid Research*, *52(1)*, 141–164.

Kendall, A. C., Pilkington, S. M., Massey, K. a, Sassano, G., Rhodes, L. E., & Nicolaou, A. (2015). Distribution of Bioactive Lipid Mediators in Human Skin. *The Journal of Investigative Dermatology*, *135*(6), 1510–1520.

Koolman, J., & Röhm, K.-H. (1998). *Taschenatlas der Biochemie*. Stuttgart: Thieme.

Kragballe, K., & Voorhees, J. J. (1987). Eicosanoids in Psoriasis – 15-HETE on the Stage. *Dermatologica*, *174*, 109–213.

Kubota, T., Arita, M., Isobe, Y., Iwamoto, R., Goto, T., Yoshioka, T., Arai, H. et. al. (2014). Eicosapentaenoic acid is converted via ω-3 epoxygenation to the anti-inflammatory metabolite 12-hydroxy-17,18-epoxyeicosatetraenoic acid. *FASEB Journal*, *28(2)*, 586–593.

Kurzrok, R., & Lieb, C. C. (1930). Biochemical Studies of Human Semen. II. The Action of Semen on the Human Uterus. *Experimental Biology and Medicine*, *28(3)*, 268–272.

Libby, P., Wamer, S. J. C., & Friedman, G. B. (1988). Interleukin 1 : a Mitogen for Human Vascular Smooth Muscle Cells That Induces the Release of Growth-inhibitory Prostanoids. *Journal of Clinical Investigation*, *81*, 487–498.

Liu, X., Moon, S. H., Mancuso, D. J., Jenkins, C. M., Guan, S., Sims, H. F., & Gross, R. W. (2013). Oxidized fatty acid analysis by charge-switch derivatization, selected reaction monitoring, and accurate mass quantitation. *Analytical Biochemistry*, *442(1)*, 40–50.

Lowes, M. a, Bowcock, A. M., & Krueger, J. G. (2007). Pathogenesis and therapy of psoriasis. *Nature*, *445(7130)*, 866–873.

Maddipati, K. R., & Zhou, S.-L. (2011). Stability and analysis of eicosanoids and docosanoids in tissue culture media. *Prostaglandins & Other Lipid Mediators*, *94*, 59–72.

Marks, F. (1999). *Prostaglandins, Leukotrienes and Other Eicosanoids*. (G. Fürstenberger, Ed.). Weinheim: Wiley-VCH.

Martin-Venegas, R., Jáuregui, O., & Moreno, J. J. (2014). Liquid chromatography-tandem mass spectrometry analysis of eicosanoids and related compounds in cell models. *Journal of Chromatography. B, Analytical Technologies in the Biomedical and Life Sciences*, *964*, 41–49.

Masoodi, M., Eiden, M., Koulman, A., Spaner, D., & Volmer, D. A. et. al. (2010). Comprehensive lipidomics analysis of bioactive lipids in complex regulatory networks. *Analytical Chemistry*, *82(19)*, 8176–8185.

Massey, K. A, & Nicolaou, A. (2013). Lipidomics of oxidized polyunsaturated fatty acids. *Free Radical Biology & Medicine*, *59*, 45–55.

Moreno, J. J. (2009). New aspects of the role of hydroxyeicosatetraenoic acids in cell growth and cancer development. *Biochemical Pharmacology*, *77(1)*, 1–10.

Murphy, R. C., Barkley, R. M., Zemski Berry, K., Hankin, J., Harrison, K., Johnson, C., Zarini, S. et. al. (2005). Electrospray ionization and tandem mass spectrometry of eicosanoids. *Analytical Biochemistry*, *346(1)*, 1–42.

Nakamura, T., Bratton, D. L., & Murphy, R. C. (1997). Analysis of Epoxyeicosatrienoic and Monohydroxyeicosatetraenoic Acids Esterified to Phospholipids in Human Red Blood Cells by Electrospray Tandem Mass Spectrometry. *Journal of Mass Spectrometry*, *32*, 888–896.

Noda, M., Kariura, Y., Pannasch, U., Nishikawa, K., Wang, L., Seike, T., Wada, K. et. al. (2007). Neuroprotective role of bradykinin because of the attenuation of pro-inflammatory cytokine release from activated microglia. *Journal of Neurochemistry*, *101(2)*, 397–410.

ÖNORM-DIN-32645. (2011). ÖNORM DIN 32645 - Chemische Analytik - Nachweis-, Erfassungs- und Bestimmungsgrenze unter Wiederholbedingungen. *ÖNORM*, *2011-0401*, 1–28.

Oyoshi, M. K., He, R., Li, Y., Mondal, S., Yoon, J., Miller, L. S., Geha, R. S. et. al. (2012). Leukotriene B4-driven neutrophil recruitment to the skin is essential for allergic skin inflammation. *Immunity*, *37(4)*, 747–758.

Pietrzak, A., Michalak-Stoma, A., Chodorowska, G., & Szepietowski, J. C. (2010). Lipid disturbances in psoriasis: an update. *Mediators of Inflammation*, *2010*, 1-13.

Pilkington, S. M., Rhodes, L. E., Al-Aasswad, N. M. I., Massey, K. A., & Nicolaou, A. (2014). Impact of EPA ingestion on COX- and LOX-mediated eicosanoid synthesis in skin with and without a pro-inflammatory UVR challenge - Report of a randomised controlled study in humans. *Molecular Nutrition and Food Research*, *58(3)*, 580–590.

Proksch, E., Brandner, J. M., & Jensen, J. M. (2008). The skin: An indispensable barrier. *Experimental Dermatology*, *17(12)*, 1063–1072.

Ricciotti, E., & FitzGerald, G. A. (2011). Prostaglandins and inflammation. *Arteriosclerosis, Thrombosis, and Vascular Biology*, *31(5)*, 986–1000.

Saito, O., Guan, Y., Qi, Z., Davis, L. S., Ko, M., Sugimoto, Y., Breyer, M. D. et. al. (2003). Expression of the prostaglandin F receptor (FP) gene along the mouse genitourinary tract. *American Journal of Physiology - Renal Physiology*, *284(6)*, 1164–1170.

Schmitz, G., & Ecker, J. (2008). The opposing effects of n-3 and n-6 fatty acids. *Progress in Lipid Research*, *47(2)*, 147–155.

Schneider, C., & Pozzi, A. (2011). Cyclooxygenases and lipoxygenases in cancer. *Cancer Metastasis Reviews*, *30*, 277–294.

Shaik, J. S. B., Miller, T. M., Graham, S. H., Manole, M. D., & Poloyac, S. M. (2014). Rapid and simultaneous quantitation of prostanoids by UPLC-MS/MS in rat brain. *Journal of Chromatography. B, Analytical Technologies in the Biomedical and Life Sciences*, *945-946*, 207–216.

Sugimoto, Y., Yamasaki, A., Segi, E., Tsuboi, K., Aze, Y., Nishimura, T., Narumiya, S. et. al. (1997). Failure of parturition in mice lacking the prostaglandin F receptor. *Science (New York, N.Y.)*, *277(5326)*, 681–683.

Takenaga, M., Hirai, A., Terano, T., Tamura, Y., Kitagawa, H., & Yoshida, S. (1986). Comparison of the in vitro effect of eicosapentaenoic acid (EPA)-derived lipoxygenase metabolites on human platelet function with those of arachidonic acid. *Thrombosis Research*, *41(3)*, 373–384.

Trzaskowski, B., Latek, D., Yuan, S., Ghoshdastider, U., Debinski, A., & Filipek, S. (2012). Action of Molecular Switches in GPCRs - Theoretical and Experimental Studies. *Current Medicinal Chemistry*, *2(19)*, 1090–1109.

Veitch, C., Brown, L., Sernia, C., & Gemmell, R. T. (2002). Role of PGF 2a and oxytocin in parturition in the brushtail possum (Trichosurus vulpecula). *Reproduction*, *123*, 429–434.

Voet, D., & Voet, J. G. (2011). *Biochemistry* (4th ed.). Hoboken, NJ: Wiley.

Wang, D., & DuBois, R. N. (2007). Measurement of eicosanoids in cancer tissues. *Methods in Enzymology*, *433*, 27–50.

Wang, Y., Armando, A. M., Quehenberger, O., Yan, C., & Dennis, E. A. (2014). Comprehensive ultra-performance liquid chromatographic separation and mass spectrometric analysis of eicosanoid metabolites in human samples. *Journal of Chromatography. A*, *1359*, 60–69.

Woollard, P. M. (1986). Stereochemical difference between 12-hydroxy-5,8,10,14-eicosatetraenoic acid in platelets and psoriatic lesions. *Biochemical and Biophysical Research Communications*, *136(1)*, 169–176.

Yin, P., Peter, A., Franken, H., Zhao, X., Neukamm, S. S., Rosenbaum, L., Lehmann, R. et. al. (2013). Preanalytical aspects and sample quality assessment in metabolomics studies of human blood. *Clinical Chemistry*, *59(5)*, 833–845.

Yokomizo, T., Izumi, T., & Shimizu, T. (2001). Leukotriene B4: metabolism and signal transduction. *Archives of Biochemistry and Biophysics*, *385(2)*, 231–241.

6. Appendix

Table A 1: Preparation of calibration standards

10A C-stock in Milli-Q (100 ng/ml)	900	µl water
in HPLC vial without glas insert	10	µl B-stock PGE_2
	10	µl B-stock PGD_2
	10	µl B-stock TXB_2
	10	µl B-stock 6k-$PGF_{1\alpha}$
	10	µl B-stock PGF_2
	10	µl B-stock 12-HEPE
	10	µl B-stock 15-HETE
	10	µl B-stock 12-HETE
	10	µl B-stock 5-HETE
	10	µl B-stock LTB_4
10A 50.0 (50.0 ng/ml)	100	µl water
in HPLC vial with glas insert	100	µl 10A C-stock
10A 10.0 (10.0 ng/ml)	180	µl water
in HPLC vial with glas insert	20	µl 10A C-stock
10A 5.00 (5.00 ng/ml)	180	µl water
in HPLC vial with glas insert	20	µl 10A 50.00
10A 1.00 (1.00 ng/ml)	180	µl water
in HPLC vial with glas insert	20	µl 10A 10.00
10A 0.50 (0.50 ng/ml)	180	µl water
in HPLC vial with glas insert	20	µl 10A 5.00
10A 0.10 (0.10 ng/ml)	180	µl water
in HPLC vial with glas insert	20	µl 10A 1.00
10A 0.05 (0.05 ng/ml)	180	µl water
in HPLC vial with glas insert	20	µl 10A 0.50
10A 0.02 (0.02 ng/ml)	160	µl water
in HPLC vial with glas insert	40	µl 10A 0.10
10A 0.01 (0.01 ng/ml)	180	µl water
in HPLC vial with glas insert	20	µl 10A 0.10

Table A 2: Instrumental settings for Q Exactive™ MS detection

ESI-Settings	
Spray voltage [V]	negative 3750
Capillary temperature [°C]	320
Sheath gas pressure [arbitrary units]	30
Auxiliary gas pressure [arbitrary units]	13
Spare gas [arbitrary units]	0
Probe Heater Temp. [°C]	30
S-Lens RF Level	60

targeted MS^2 settings	
Scan type	targeted MS^2
Runtime [min]	15.99
Polarity	negative
Default charge state	1
Inclusion MS^2	on
MS^2 microscans	1
Resolution	35000
AGC target	2E+05
max inject time [ms]	200
MSX count	1
Isolation window [m/z]	0.8

Table A 3: Inclusion list settings for Q Exactive™ MS detection; general settings: negative polarity, species = –H, CS = 1 [z]

mass [m/z]	formula [M]	start [min]	end [min]	NCE	comment
369.22826	$C_{20}H_{34}O_6$	0.00	3.50	38%	6-keto-$PGF_{1\alpha}$
373.25337	$C_{20}H_{30}D_4O_6$	0.00	3.50	38%	6-keto-$PGF_{1\alpha}$-d4
369.22826	$C_{20}H_{34}O_6$	3.51	4.75	20%	TXB_2
373.25337	$C_{20}H_{30}D_4O_6$	3.51	4.75	20%	TXB_2-d4
353.23335	$C_{20}H_{34}O_5$	4.47	5.55	39%	$PGF_{2\alpha}$
357.25845	$C_{20}H_{30}D_4O_5$	4.47	5.55	39%	$PGF_{2\alpha}$ -d4
351.21770	$C_{20}H_{32}O_5$	5.25	8.50	18%	PGE_2 / PGD_2
355.24280	$C_{20}H_{28}D_4O_5$	5.25	8.50	18%	PGE_2-d4 / PGD_2-d4
335.22278	$C_{20}H_{32}O_4$	8.51	10.60	20%	LTB_4
339.24789	$C_{20}H_{28}D_4O_4$	8.51	10.60	20%	LTB_4-d4
317.21222	$C_{20}H_{30}O_3$	10.51	12.07	20%	12-HEPE
319.22787	$C_{20}H_{32}O_3$	11.60	end	22%	15-HETE / 12-HETE / 5-HETE
327.27808	$C_{20}H_{24}D_8O_3$	11.60	end	22%	15-HETE-d8 / 12-HETE-d8 / 5-HETE-d8

Table A 4: Exact parent and fragment masses used for identification and quantification for Q Exactive™ MS

Analyte	parent $[M-H]^-$	fragment 1	fragment 2	internal standard	parent $[M-H]^-$	fragment 1	fragment 2
6-keto-$PGF_{1\alpha}$	369.22826	163.11139	245.19110	**6-keto-$PGF_{1\alpha}$-d4**	373.25337	167.13625	249.21664
TXB_2	369.22826	195.10168	169.08559	**TXB_2-d4**	373.25337	173.11120	199.12726
$PGF_{2\alpha}$	353.23335	193.12240	247.20644	**$PGF_{2\alpha}$-d4**	357.25845	197.14758	251.23122
PGE_2	351.21770	189.12850	271.20621	**PGE_2-d4**	355.24280	193.15240	275.23215
PGD_2	351.21770	189.12850	271.20621	**PGD_2-d4**	355.24280	193.15240	275.23215
LTB4	335.22278	195.10198	-	**LTB_4-d4**	339.24789	197.11395	-
12-HEPE	317.21222	179.10672	-	*12(S)-HETE-d8 used as internal Standard*			
15-HETE	319.22787	219.13840	175.14806	**15(S)-HETE-d8**	327.27808	226.18243	182.19183
12-HETE	319.22787	179.10668	135.11624	**12(S)-HETE-d8**	327.27808	184.13814	140.14266
5-HETE	319.22787	115.03851	-	**5(S)-HETE-d8**	327.27808	116.04482	-

Table A 5: Instrumental settings for TSQ Quantum Ultra™ Triple Quadrupole MS detection

ESI settings	
Capillary voltage [V]	negative 3000
Capillary temperature [°C]	320
Sheath gas pressure [arbitrary units]	25
Auxiliary gas pressure [arbitrary units]	12

Method settings for all scan segments/events	
Mode	SRM
Isolation width [m/z]	0.800
Scan time	0.200
Peak width Q1	0.70
Peak width Q3	0.70
Q2 gas pressure [mTorr]	1.5
MS runtime [min]	15.99
Skimmer offset [V]	0

Table A 6: Segment and scan settings for TSQ Quantum Ultra™ Triple Quadrupole MS detection

Scan event parameters						
Segment	**segment duration [min]**	**parent [m/z]**	**fragment [m/z]**	**collision energy [eV]**	**tube lens offset [V]**	**analyte**
1	3.10	369.228	163.21	31	139	6-keto-$PGF_{2\alpha}$
		369.228	245.05	31	139	6-keto-$PGF_{2\alpha}$
		373.253	167.136	31	139	6-keto-$PGF_{2\alpha}$-d4
		373.253	249.216	31	139	6-keto-$PGF_{2\alpha}$-d4
2	1.05	369.228	169.140	19	102	TXB_2
		369.228	195.110	19	102	TXB_2
		373.253	173.111	19	102	TXB_2-d4
		373.253	199.127	19	102	TXB_2-d4
3	0.70	353.233	193.220	24	129	$PGF_{2\alpha}$
		353.233	247.080	24	129	$PGF_{2\alpha}$
		357.258	197.148	24	129	$PGF_{2\alpha}$-d4
		357.258	251.231	24	129	$PGF_{2\alpha}$-d4
4	2.75	351.218	189.140	21	90	PGE_2 / PGD_2
		351.218	271.250	21	90	PGE_2 / PGD_2
		355.243	193.153	21	90	PGE_2-d4 / PGD_2-d4
		355.243	275.232	21	90	PGE_2-d4 / PGD_2-d4
5	2.30	335.223	195.070	20	125	LTB_4
		339.248	197.114	20	125	LTB_4-d4
6	6.09	317.212	179.120	18	113	12-HEPE
		319.227	115.150	20	107	5-HETE
		319.227	135.120	21	93	12-HETE
		319.227	175.460	23	137	15-HETE
		319.227	179.120	21	93	12-HETE
		319.227	219.500	23	137	15-HETE
		327.278	116.045	20	107	5-HETE-d8
		327.278	140.148	21	93	12-HETE-d8
		327.278	182.192	23	137	15-HETE-d8
		327.278	184.138	21	93	12-HETE-d8
		327.278	226.182	23	137	15-HETE-d8

Table A 7a: Measured concentrations (c), mean (x̄) and relative standard-deviation (RSD) of the first 5 eluting analytes 6-keto-$PGF_{1\alpha}$, TXB_2, $PGF_{2\alpha}$, PGE_2 and PGD_2 from the sample pool of "Set12" (probes 6, 10, 11); concentration values were obtained via Thermo Xcalibur Quanbrowser software; to get the actual sample concentrations, and respective mean and standard-deviation, these values were multiplied by 2 regarding the applied sample volume (40 µl) and internal standard volume (20 µl)

	6-keto-$PGF_{1\alpha}$			TXB_2			$PGF_{2\alpha}$			PGE_2			PGD_2		
sampling	c [ng/ml]	x̄ [ng/ml]	RSD [%]	c [ng/ml]	x̄ [ng/ml]	RSD [%]	c [ng/ml]	x̄ [ng/ml]	RSD [%]	c [ng/ml]	x̄ [ng/ml]	RSD [%]	x̄ [ng/ml]	x̄ [ng/ml]	RSD [%]
1	2.252E-02	4.006E-02	45.67	2.622E-01	2.711E-01	2.86	6.635E-02	5.570E-02	16.95	6.684E-02	5.734E-02	14.95	2.706E-02	2.733E-02	3.13
	3.864E-02			2.764E-01			4.837E-02			5.020E-02			2.665E-02		
	5.902E-02			2.746E-01			5.236E-02			5.497E-02			2.829E-02		
2	3.843E-02	3.640E-02	48.44	1.154E-01	1.203E-01	4.61	5.092E-02	4.982E-02	15.82	3.967E-02	3.951E-02	0.56	NF	2.289E-02	-
	5.293E-02			1.263E-01			4.144E-02			3.961E-02			2.289E-02		
	1.784E-02			1.192E-01			5.709E-02			3.926E-02			NF		
3	2.427E-02	2.362E-02	24.35	1.194E-01	1.260E-01	4.96	4.399E-02	4.855E-02	18.53	4.951E-02	4.908E-02	1.75	2.279E-02	2.290E-02	0.67
	2.901E-02			1.319E-01			5.891E-02			4.964E-02			2.301E-02		
	1.757E-02			1.267E-01			4.274E-02			4.810E-02			NF		
4	1.328E-02	1.659E-02	47.38	1.044E-01	1.067E-01	1.93	2.990E-02	3.325E-02	11.46	3.882E-02	3.838E-02	4.69	NF	2.293E-02	-
	1.093E-02			1.074E-01			3.246E-02			3.991E-02			2.293E-02		
	2.557E-02			1.084E-01			3.739E-02			3.639E-02			NF		
5	3.795E-02	3.093E-02	28.78	1.356E-01	1.369E-01	1.11	4.033E-02	4.842E-02	16.12	5.068E-02	4.868E-02	4.35	NF	2.391E-02	-
	3.393E-02			1.365E-01			4.902E-02			4.889E-02			2.391E-02		
	2.092E-02			1.386E-01			5.590E-02			4.646E-02			NF		
6	2.986E-02	2.389E-02	33.08	2.337E-01	2.369E-01	1.27	3.551E-02	4.730E-02	24.59	6.372E-02	6.100E-02	3.87	2.520E-02	2.450E-02	4.08
	2.688E-02			2.397E-01			5.877E-02			5.947E-02			NF		
	1.493E-02			2.373E-01			4.761E-02			5.981E-02			2.379E-02		
7	1.440E-02	1.892E-02	57.54	1.522E-01	1.497E-01	3.86	3.481E-02	3.999E-02	13.64	5.127E-02	5.019E-02	4.26	2.504E-02	2.504E-02	-
	1.102E-02			1.539E-01			3.947E-02			5.158E-02			NF		
	3.134E-02			1.431E-01			4.568E-02			4.773E-02			NF		
8	2.509E-02	2.416E-02	13.14	1.703E-01	1.713E-01	0.83	4.946E-02	4.235E-02	20.66	5.199E-02	5.615E-02	7.35	2.519E-02	2.587E-02	3.67
	2.678E-02			1.706E-01			4.500E-02			6.024E-02			NF		
	2.063E-02			1.729E-01			3.258E-02			5.622E-02			2.654E-02		
9	6.830E-02	6.096E-02	12.30	1.107E+00	8.536E-01	25.72	1.303E-01	9.896E-02	27.74	2.381E-01	1.788E-01	28.98	2.890E-02	2.757E-02	4.26
	6.127E-02			7.279E-01			8.741E-02			1.418E-01			2.713E-02		
	5.331E-02			7.259E-01			7.917E-02			1.566E-01			2.668E-02		
10	2.260E-02	2.220E-02	20.29	1.488E-01	1.500E-01	1.27	5.030E-02	6.182E-02	16.21	7.222E-02	7.191E-02	5.73	2.305E-02	2.305E-02	-
	2.649E-02			1.490E-01			6.657E-02			7.586E-02			NF		
	1.751E-02			1.522E-01			6.858E-02			6.764E-02			NF		
11	3.061E-02	2.521E-02	19.18	1.190E-01	1.154E-01	4.12	5.115E-02	4.493E-02	12.02	7.143E-02	6.609E-02	7.30	NF	2.459E-02	-
	2.130E-02			1.172E-01			4.147E-02			6.207E-02			2.459E-02		
	2.370E-02			1.100E-01			4.217E-02			6.476E-02			NF		
12	1.754E-02	2.190E-02	23.82	7.954E-02	7.795E-02	2.07	5.742E-02	5.542E-02	13.58	6.070E-02	5.560E-02	8.01	NF	-	-
	2.048E-02			7.632E-02			6.174E-02			5.365E-02			NF		
	2.768E-02			7.799E-02			4.709E-02			5.246E-02			NF		

Table A 7b: Measured concentrations (c), mean (x̄) and relative standard-deviation (RSD) of the last 5 eluting analytes LTB_4, 12-HEPE, 15-HETE, 12-HETE and 5-HETE from the sample pool of "Set12" (probes 6, 10, 11); concentration values were obtained via Thermo Xcalibur Quanbrowser software; to get the actual sample concentrations, and respective mean and standard-deviation, these values were multiplied by 2 regarding the applied sample volume (40 µl) and internal standard volume (20 µl)

	LTB_4			12-HEPE			15-HETE			12-HETE			5-HETE		
sampling	c [ng/ml]	x̄ [ng/ml]	RSD [%]	c [ng/ml]	x̄ [ng/ml]	RSD [%]	c [ng/ml]	x̄ (ng/ml]	RSD [%]	c [ng/ml]	x̄ [ng/ml]	RSD [%]	c [ng/ml]	x̄ [ng/ml]	RSD [%]
1	NF	1.495E-01	0.14	1.472E+00	1.475E+00	0.83	4.750E+00	4.762E+00	0.79	1.696E+01	1.717E+01	1.15	4.642E+00	4.674E+00	0.60
	1.494E-01			1.489E+00			4.732E+00			1.736E+01			4.687E+00		
	1.497E-01			1.465E+00			4.805E+00			1.719E+01			4.693E+00		
2	NF	1.546E-01	-	1.282E+00	1.269E+00	0.88	4.549E+00	4.555E+00	0.13	9.978E+00	9.916E+00	0.60	4.583E+00	4.623E+00	0.82
	NF			1.261E+00			4.558E+00			9.910E+00			4.628E+00		
	1.546E-01			1.264E+00			4.560E+00			9.859E+00			4.659E+00		
3	NF	1.492E-01	-	1.195E+00	1.203E+00	1.10	4.565E+00	4.623E+00	2.48	7.906E+00	8.048E+00	3.05	4.725E+00	4.761E+00	1.78
	NF			1.195E+00			4.549E+00			7.906E+00			4.701E+00		
	1.492E-01			1.218E+00			4.755E+00			8.331E+00			4.858E+00		
4	NF	1.492E-01	0.52	1.154E+00	1.159E+00	0.41	4.430E+00	4.422E+00	0.61	6.394E+00	6.396E+00	0.93	4.718E+00	4.684E+00	1.19
	1.497E-01			1.162E+00			4.444E+00			6.337E+00			4.714E+00		
	1.486E-01			1.162E+00			4.391E+00			6.457E+00			4.620E+00		
5	NF	1.491E-01	0.08	1.141E+00	1.141E+00	0.06	4.415E+00	4.418E+00	0.21	5.959E+00	5.901E+00	1.40	4.626E+00	4.636E+00	0.45
	1.492E-01			1.141E+00			4.410E+00			5.807E+00			4.660E+00		
	1.490E-01			1.142E+00			4.428E+00			5.938E+00			4.622E+00		
6	1.553E-01	1.563E-01	0.84	1.133E+00	1.132E+00	0.22	4.350E+00	4.383E+00	1.09	5.770E+00	5.859E+00	1.52	4.611E+00	4.629E+00	0.89
	1.572E-01			1.129E+00			4.360E+00			5.859E+00			4.600E+00		
	NF			1.133E+00			4.437E+00			5.947E+00			4.676E+00		
7	NF	1.489E-01	-	1.128E+00	1.124E+00	0.32	4.373E+00	4.363E+00	0.18	5.263E+00	5.307E+00	1.86	4.722E+00	4.696E+00	0.72
	NF			1.121E+00			4.360E+00			5.239E+00			4.657E+00		
	1.489E-01			1.124E+00			4.358E+00			5.421E+00			4.707E+00		
8	1.487E-01	1.487E-01	-	1.113E+00	1.111E+00	0.39	4.305E+00	4.302E+00	0.10	5.012E+00	5.013E+00	0.87	4.724E+00	4.719E+00	1.32
	NF			1.114E+00			4.297E+00			5.057E+00			4.654E+00		
	NF			1.106E+00			4.304E+00			4.969E+00			4.778E+00		
9	NF	1.500E-01	1.13	1.207E+00	1.169E+00	2.77	5.494E+00	4.940E+00	9.72	9.235E+00	7.692E+00	17.39	6.001E+00	5.205E+00	13.25
	1.512E-01			1.152E+00			4.642E+00			6.948E+00			4.816E+00		
	1.488E-01			1.149E+00			4.684E+00			6.891E+00			4.797E+00		
10	1.487E-01	1.487E-01	-	1.120E+00	1.118E+00	0.11	4.430E+00	4.421E+00	0.83	5.296E+00	5.275E+00	1.21	4.723E+00	4.716E+00	1.30
	NF			1.117E+00			4.381E+00			5.204E+00			4.651E+00		
	NF			1.118E+00			4.453E+00			5.326E+00			4.773E+00		
11	NF	-	-	1.109E+00	1.111E+00	0.22	4.341E+00	4.318E+00	0.86	4.970E+00	4.963E+00	1.23	4.665E+00	4.654E+00	0.49
	NF			1.114E+00			4.338E+00			5.020E+00			4.669E+00		
	NF			1.110E+00			4.275E+00			4.898E+00			4.628E+00		
12	NF	1.513E-01	0.22	1.113E+00	1.107E+00	0.49	4.390E+00	4.357E+00	0.66	4.769E+00	4.744E+00	1.03	4.611E+00	4.675E+00	1.20
	1.510E-01			1.106E+00			4.343E+00			4.688E+00			4.707E+00		
	1.515E-01			1.102E+00			4.337E+00			4.775E+00			4.708E+00		

Table A 8a: Measured concentrations (c), mean (x̄) and relative standard-deviation (RSD) of the first 5 eluting analytes 6-keto-$PGF_{1\alpha}$, TXB_2, $PGF_{2\alpha}$, PGE_2 and PGD_2 from the sample pool of "Set11" (probes 7, 9, 10); concentration values were obtained via Thermo Xcalibur Quanbrowser software; to get the actual sample concentrations, and respective mean and standard-deviation, these values were multiplied by 2 regarding the applied sample volume (40 µl) and internal standard volume (20 µl)

	6-keto-$PGF_{1\alpha}$			TXB_2			$PGF_{2\alpha}$			PGE_2			PGD_2		
sampling	c [ng/ml]	x̄ [ng/ml]	RSD [%]	c [ng/ml]	x̄ [ng/ml]	RSD [%]	c [ng/ml]	x̄ [ng/ml]	RSD [%]	c [ng/ml]	x̄ [ng/ml]	RSD [%]	c [ng/ml]	x̄ [ng/ml]	RSD [%]
1	3.199E-02	2.027E-02	51.01	2.464E-01	2.421E-01	1.54	3.760E-02	3.800E-02	9.01	3.036E-02	2.718E-02	11.46	2.320E-02	2.344E-02	2.98
	1.635E-02			2.394E-01			4.160E-02			2.704E-02			2.289E-02		
	1.246E-02			2.406E-01			3.479E-02			2.413E-02			2.422E-02		
2	1.583E-02	1.565E-02	6.69	1.155E-01	1.197E-01	3.50	3.320E-02	2.716E-02	19.31	2.249E-02	2.406E-02	15.17	2.301E-02	2.301E-02	-
	1.452E-02			1.239E-01			2.456E-02			2.146E-02			NF		
	1.659E-02			1.199E-01			2.373E-02			2.823E-02			NF		
3	1.303E-03	1.012E-02	77.37	1.024E-01	1.035E-01	0.97	1.817E-02	2.881E-02	34.56	2.208E-02	2.190E-02	3.57	2.402E-02	2.322E-02	3.00
	1.626E-02			1.038E-01			3.037E-02			2.259E-02			2.288E-02		
	1.280E-02			1.043E-01			3.789E-02			2.105E-02			2.276E-02		
4	6.294E-03	5.091E-03	28.31	5.696E-02	5.454E-02	7.10	2.646E-02	2.691E-02	36.76	2.221E-02	2.225E-02	5.10	NF	-	-
	5.485E-03			5.007E-02			3.701E-02			2.113E-02			NF		
	3.493E-03			5.658E-02			1.725E-02			2.340E-02			NF		
5	7.924E-03	1.298E-02	44.81	3.381E-02	3.229E-02	4.22	1.667E-02	2.304E-02	37.36	1.929E-02	1.969E-02	3.11	NF	2.278E-02	-
	1.933E-02			3.118E-02			3.283E-02			2.039E-02			2.278E-02		
	1.167E-02			3.187E-02			1.962E-02			1.938E-02			NF		
6	3.272E-03	2.984E-03	265.82	4.115E-02	3.800E-02	13.18	3.323E-02	2.912E-02	25.29	2.279E-02	2.033E-02	10.50	NF	2.278E-02	0.02
	-5.089E-03			3.222E-02			2.062E-02			1.916E-02			2.278E-02		
	1.077E-02			4.062E-02			3.351E-02			1.903E-02			2.279E-02		
7	1.282E-02	8.502E-03	84.97	3.720E-02	4.000E-02	9.43	2.463E-02	2.740E-02	18.97	2.207E-02	2.184E-02	3.61	2.289E-02	2.289E-02	-
	1.252E-02			3.852E-02			2.418E-02			2.248E-02			NF		
	1.619E-04			4.429E-02			3.340E-02			2.096E-02			NF		
8	9.468E-03	4.162E-03	180.26	9.672E-02	9.074E-02	9.32	2.086E-02	1.557E-02	48.06	2.391E-02	2.235E-02	9.87	NF	-	-
	-1.143E-03			8.476E-02			1.028E-02			2.079E-02			NF		
	NF			NF			NF			NF			NF		
9	4.213E-03	8.453E-03	45.86	5.034E-02	5.393E-02	8.93	4.323E-02	2.630E-02	58.27	2.233E-02	2.131E-02	5.68	NF	-	-
	1.182E-02			5.941E-02			1.336E-02			1.997E-02			NF		
	9.330E-03			5.206E-02			2.232E-02			2.161E-02			NF		
10	-4.278E-04	1.242E-03	374.25	2.883E-02	3.301E-02	13.36	1.850E-02	1.667E-02	72.78	1.503E-02	1.681E-02	11.55	NF	2.295E-02	-
	-2.340E-03			3.257E-02			2.778E-02			1.888E-02			2.295E-02		
	6.493E-03			3.762E-02			3.725E-03			1.653E-02			NF		
11	1.294E-02	4.693E-03	227.75	4.857E-02	4.745E-02	4.16	2.422E-02	3.114E-02	38.89	2.038E-02	1.904E-02	6.84	NF	2.282E-02	-
	-7.382E-03			4.862E-02			4.513E-02			1.898E-02			NF		
	8.520E-03			4.517E-02			2.408E-02			1.777E-02			2.282E-02		
12	-4.309E-03	1.001E-03	511.72	2.957E-02	3.214E-02	7.77	1.948E-02	2.780E-02	35.28	2.148E-02	1.978E-02	8.86	2.272E-02	2.284E-02	0.76
	1.402E-03			3.229E-02			2.531E-02			1.798E-02			NF		
	5.908E-03			3.456E-02			3.862E-02			1.989E-02			2.296E-02		

Table A 8b: Measured concentrations (c), mean (x̄) and relative standard-deviation (RSD) of the last 5 eluting analytes LTB_4, 12-HEPE, 15-HETE, 12-HETE and 5-HETE from the sample pool of "Set11" (probes 7, 9, 10); concentration values were obtained via Thermo Xcalibur Quanbrowser software; to get the actual sample concentrations, and respective mean and standard-deviation, these values were multiplied by 2 regarding the applied sample volume (40 µl) and internal standard volume (20 µl)

	LTB_4			12-HEPE			15-HETE			12-HETE			5-HETE		
sampling	c [ng/ml]	x̄ [ng/ml]	RSD [%]	c [ng/ml]	x̄ [ng/ml]	RSD [%]	c [ng/ml]	x̄ [ng/ml]	RSD [%]	c [ng/ml]	x̄ [ng/ml]	RSD [%]	c [ng/ml]	**x̄ [ng/ml]**	**RSD [%]**
1	1.649E-01	1.602E-01	2.53	1.139E+00	1.140E+00	0.15	5.315E+00	5.314E+00	0.35	6.654E+00	6.722E+00	1.84	4.731E+00	4.753E+00	0.95
	1.577E-01			1.142E+00			5.295E+00			6.647E+00			4.723E+00		
	1.579E-01			1.140E+00			5.332E+00			6.864E+00			4.805E+00		
2	NF	1.517E-01	0.51	1.091E+00	1.093E+00	0.24	4.543E+00	4.603E+00	1.14	4.827E+00	4.980E+00	2.92	4.726E+00	4.778E+00	2.49
	1.511E-01			1.096E+00			4.640E+00			5.116E+00			4.914E+00		
	1.522E-01			1.092E+00			4.626E+00			4.997E+00			4.693E+00		
3	1.494E-01	1.507E-01	1.63	1.101E+00	1.098E+00	0.38	4.762E+00	4.718E+00	1.13	5.140E+00	5.133E+00	0.97	4.803E+00	4.751E+00	1.01
	1.491E-01			1.094E+00			4.734E+00			5.178E+00			4.708E+00		
	1.535E-01			1.100E+00			4.659E+00			5.080E+00			4.742E+00		
4	NF	1.490E-01	-	1.089E+00	1.087E+00	0.12	4.430E+00	4.366E+00	1.27	4.530E+00	4.522E+00	0.65	4.716E+00	4.652E+00	1.23
	NF			1.086E+00			4.332E+00			4.547E+00			4.607E+00		
	1.490E-01			1.087E+00			4.335E+00			4.490E+00			4.632E+00		
5	1.488E-01	1.500E-01	1.34	1.087E+00	1.090E+00	0.23	4.215E+00	4.257E+00	1.08	4.309E+00	4.332E+00	0.56	4.530E+00	4.613E+00	1.56
	1.524E-01			1.092E+00			4.306E+00			4.330E+00			4.654E+00		
	1.490E-01			1.091E+00			4.249E+00			4.357E+00			4.655E+00		
6	1.499E-01	1.495E-01	0.31	1.085E+00	1.086E+00	0.07	4.242E+00	4.214E+00	0.61	4.354E+00	4.316E+00	1.33	4.729E+00	4.682E+00	1.43
	NF			1.086E+00			4.207E+00			4.250E+00			4.605E+00		
	1.492E-01			1.086E+00			4.192E+00			4.346E+00			4.710E+00		
7	NF	-	-	1.090E+00	1.089E+00	0.11	4.275E+00	4.335E+00	2.23	4.390E+00	4.445E+00	3.73	4.780E+00	4.878E+00	3.70
	NF			1.091E+00			4.283E+00			4.314E+00			4.768E+00		
	NF			1.088E+00			4.447E+00			4.632E+00			5.087E+00		
8	1.489E-01	1.494E-01	0.51	1.092E+00	1.088E+00	0.45	4.287E+00	4.272E+00	0.49	5.132E+00	5.062E+00	1.96	4.852E+00	4.771E+00	2.39
	1.500E-01			1.085E+00			4.257E+00			4.992E+00			4.690E+00		
	NF			NF			NF			NF			NF		
9	NF	1.586E-01	-	1.090E+00	1.090E+00	0.04	4.187E+00	4.203E+00	0.43	4.650E+00	4.669E+00	0.70	4.657E+00	4.676E+00	0.81
	1.586E-01			1.090E+00			4.198E+00			4.707E+00			4.720E+00		
	NF			1.089E+00			4.223E+00			4.651E+00			4.652E+00		
10	NF	1.489E-01	-	1.086E+00	1.087E+00	0.07	4.146E+00	4.165E+00	1.09	4.338E+00	4.361E+00	0.48	4.736E+00	4.699E+00	1.71
	1.489E-01			1.088E+00			4.132E+00			4.366E+00			4.607E+00		
	NF			1.087E+00			4.216E+00			4.379E+00			4.754E+00		
11	1.527E-01	1.541E-01	0.78	1.089E+00	1.087E+00	0.19	4.181E+00	4.184E+00	0.24	4.238E+00	4.243E+00	0.69	4.801E+00	4.770E+00	2.45
	1.548E-01			1.085E+00			4.195E+00			4.274E+00			4.869E+00		
	1.548E-01			1.087E+00			4.176E+00			4.216E+00			4.641E+00		
12	NF	-	-	1.084E+00	1.084E+00	0.03	4.168E+00	4.152E+00	0.46	4.168E+00	4.169E+00	0.46	4.722E+00	4.701E+00	0.55
	NF			1.084E+00			4.131E+00			4.150E+00			4.672E+00		
	NF			NF			4.157E+00			4.188E+00			4.708E+00		

Table A 9: Hemolytic impact on one sample pool has been divided into 2 aliquots; pool 1 was extracted directly (n=3), pool 2 was centrifuged and then extracted (n=3)

	x̄ direct [pg/ml]	RSD direct [%]	x̄ centrifuged [pg/ml]	RSD centrifuged [%]	x̄ difference [pg/ml]	RSD difference [%]
6-keto-$PGF_{1\alpha}$	1.126E+01	3.5	1.054E+01	37.3	7.141E-01	6.3
TXB_2	9.379E+02	1.4	9.466E+02	1.3	-8.697E+00	-0.9
$PGF_{2\alpha}$	2.926E+01	29.3	3.015E+01	18.1	-8.918E-01	-3.0
PGE_2	4.497E+01	9.7	4.572E+01	8.6	-7.434E-01	-1.7
PGD_2	2.076E+01	3.2	2.139E+01	7.0	-6.265E-01	-3.0
LTB_4	-	-	-	-	-	-
12-HEPE	6.248E+02	1.0	6.237E+02	1.0	1.088E+00	0.2
15-HETE	3.134E+03	1.0	3.106E+03	0.6	2.772E+01	0.9
12-HETE	1.156E+04	2.0	1.160E+04	1.6	-3.582E+01	-0.3
5-HETE	2.703E+03	1.9	2.631E+03	1.0	7.277E+01	2.7

Table A 10: Recovery of analytes after SPE; for calculation see Table A 16

	$area_{IS\ ex}$	$area_{IS\ dir}$	recovery [%]	x̄ [%]	RSD [%]
6-keto- $PGF_{1\alpha}$-d4	1186731	1185729	100.1	103.2	4.5
	1187325	1173136	101.2		
	1229002	1134249	108.4		
TXB_2-d4	2189550	2629386	83.3	85.1	2.4
	2153968	2553766	84.3		
	2204939	2511808	87.8		
$PGF_{2\alpha}$ -d4	643011	758958	84.7	87.1	3.8
	618486	726650	85.1		
	656883	717432	91.6		
PGE_2-d4	1242305	1440285	86.3	88.9	4.8
	1221551	1420936	86.0		
	1319313	1397861	94.4		
PGD_2-d4	297594	475708	62.6	71.6	8.9
	328190	456218	71.9		
	353953	440185	80.4		
LTB_4-d4	547038	1480735	36.9	37.7	1.5
	532347	1451755	36.7		
	546043	1385368	39.4		
15(S)-HETE-d8	443230	1525413	29.1	30.2	1.5
	441297	1482704	29.8		
	459678	1441084	31.9		
12(S)-HETE-d8	362817	1030770	35.2	36.7	2.1
	367530	1028830	35.7		
	381980	976686	39.1		
5(S)-HETE-d8	445259	1242589	35.8	37.6	2.8
	439049	1216488	36.1		
	468121	1146777	40.8		

Table A 11: Accuracy data and results; obtained at 10 ng/ml actual concentration; for calculation see Table A 16

	6k-$PGF_{1\alpha}$	TXB_2	$PGF_{2\alpha}$	PGE_2	PGD_2	LTB_4	12-HEPE	15-HETE	12-HETE	5-HETE
measured conc. [ng/ml]	9.79	9.78	10.16	10.18	9.83	10.21	6.37	12.39	12.63	13.14
	10.30	10.35	10.49	9.85	9.66	10.08	6.19	12.09	13.00	12.26
	10.22	10.27	10.37	10.11	9.86	9.94	6.15	12.05	12.75	12.20
	9.83	10.02	10.02	10.13	9.96	9.67	6.39	12.15	12.81	12.59
accuracy [%]	100.4	101.0	102.6	100.7	98.3	99.7	62.8	121.7	128.0	125.5
RSD [%]	2.6	2.6	2.1	1.5	1.2	2.3	1.2	1.5	1.5	4.3

Table A 12a: Inter -day precision data and results obtained at 1 ng/ml actual concentration; standard deviation resembles the method-precision; for calculation see Table A 16

	6k-$PGF_{1\alpha}$	TXB_2	$PGF_{2\alpha}$	PGE_2	PGD_2	LTB_4	12-HEPE	15-HETE	12-HETE	5-HETE
measured conc. day 1 [ng/ml]	1.03	0.99	1.01	0.99	0.77	1.05	1.56	4.74	4.83	4.65
	1.02	1.00	1.02	0.97	0.79	1.08	1.55	4.74	4.88	4.64
	1.02	0.96	1.03	0.97	0.80	1.06	1.76	4.75	4.76	4.65
measured conc. day 2 [ng/ml]	1.00	0.95	0.95	0.95	0.44	1.08	1.26	5.19	5.38	5.10
	1.03	0.96	0.98	0.92	0.45	1.10	1.28	5.28	5.52	5.20
	0.99	0.92	0.97	0.88	0.43	1.00	1.19	5.08	5.21	4.91
$\bar{x}$ [ng/ml]	1.01	0.96	0.99	0.95	0.61	1.06	1.43	4.96	5.10	4.86
RSD [%]	1.5	3.1	3.3	4.3	30.8	3.1	15.5	5.0	6.2	5.1

Table A 12b: Inter-day precision data and results obtained at 10 ng/ml actual concentration; standard deviation resembles the method-precision; for calculation see Table A 16

	6k-$PGF_{1\alpha}$	TXB_2	$PGF_{2\alpha}$	PGE_2	PGD_2	LTB_4	12-HEPE	15-HETE	12-HETE	5-HETE
measured conc. day 1 [ng/ml]	10.61	9.72	10.65	9.86	8.32	10.21	5.51	12.84	14.48	13.11
	10.21	9.73	10.41	9.87	8.61	10.39	5.71	12.47	15.13	13.09
	10.51	9.84	10.53	9.95	8.52	10.91	6.13	13.32	15.55	13.99
measured conc. day 2 [ng/ml]	10.58	10.04	10.33	10.29	7.62	11.08	6.52	14.54	16.42	14.95
	10.88	9.91	10.46	10.20	7.40	10.80	6.34	14.52	15.83	14.54
	10.45	9.57	10.16	10.26	7.41	10.71	6.15	14.24	16.11	14.55
$\bar{x}$ [ng/ml]	10.54	9.80	10.42	10.07	7.98	10.68	6.06	13.65	15.59	14.04
RSD [%]	2.1	1.7	1.6	2.0	7.1	3.1	6.3	6.6	4.5	5.6

Table A 14: Linear equations of calibration curves with weighing factor 1/x including coefficient of determination; obtained by Xcalibur analysis software

analyte	linear equation
6-keto-$PGF_{1\alpha}$	Y = 0.00746682+0.178438*X R^2 = 0.9996
TXB_2	Y = -0.000859495+0.11226*X R^2 = 0.9999
$PGF_{2\alpha}$	Y = 0.00455703+0.170042*X R^2 = 0.9994
PGE_2	Y = -0.00133101+0.10717*X R^2 = 0.9996
PGD_2	Y = -0.00290348+0.132503*X R^2 = 0.9996
LTB_4	Y = -0.0264739+0.179697*X R^2 = 0.9954
12-HEPE	Y = -0.322654+0.298295*X R^2 = 0.9789
15-HETE	Y = -0.368779+0.10844*X R^2 = 0.9863
12-HETE	Y = -0.483272+0.14636*X R^2 = 0.9876
5-HETE	Y = -0.373168+0.128995*X R^2 = 0.9616

Table A 13: Limit of detection and limit of quantification of the developed analytical method; for calculation see Table A 16

	LOD [pg/ml]	LOQ [pg/ml]
6-keto-$PGF_{1\alpha}$	4.4	13
TXB_2	4.4	13
$PGF_{2\alpha}$	6.3	19
PGE_2	4.4	13
PGD_2	6.3	19
LTB_4	217	650
12-HEPE	35.2	106
15-HETE	491	1484
12-HETE	491	1484
5-HETE	491	1484

Table A 15: Raw data of SPE extracted calibration solutions with respective concentration levels

cal. level [ng/ml]	area ratio analyte/internal standard [ ]									
	6-keto-$PGF_{1\alpha}$	TXB_2	$PGF_{2\alpha}$	PGE_2	PGD_2	LTB_4	12-HEPE	15-HETE	12-HETE	5-HETE
0.01	9.548E-03	4.840E-04	6.757E-03	3.218E-04	-	-	-	-	-	-
0.02	1.076E-02	1.446E-03	-	6.660E-04	7.253E-04	-	-	-	-	-
0.05	1.403E-02	4.502E-03	1.305E-02	3.930E-03	3.176E-03	-	-	-	-	-
0.1	2.440E-02	8.784E-03	2.141E-02	7.871E-03	9.025E-03	1.013E-02	-	-	-	-
0.50	1.009E-01	5.594E-02	8.676E-02	4.730E-02	6.296E-02	5.401E-02	-	-	-	-
0.75	1.526E-01	8.585E-02	1.271E-01	7.504E-02	9.304E-02	8.105E-02	2.506E-02	-	-	-
1	1.881E-01	1.048E-01	1.612E-01	9.885E-02	1.216E-01	9.482E-02	9.619E-02	-	-	-
5	9.461E-01	5.540E-01	8.134E-01	5.064E-01	6.271E-01	7.630E-01	9.225E-01	2.188E-01	3.859E-01	4.536E-01
7.5	1.383E+00	8.346E-01	1.261E+00	7.853E-01	9.783E-01	1.069E+00	1.083E+00	4.051E-01	5.689E-01	5.789E-01
10	1.825E+00	1.116E+00	1.626E+00	1.042E+00	1.258E+00	1.539E+00	1.608E+00	6.298E-01	7.479E-01	6.934E-01
25	4.352E+00	2.807E+00	4.043E+00	2.592E+00	3.302E+00	4.237E+00	5.220E+00	2.310E+00	2.939E+00	2.661E+00
50	9.189E+00	5.666E+00	8.627E+00	5.474E+00	6.809E+00	9.659E+00	1.588E+01	5.877E+00	7.910E+00	6.063E+00
75	1.322E+01	8.283E+00	1.270E+01	7.988E+00	1.001E+01	1.315E+01	2.360E+01	6.771E+00	9.534E+00	7.295E+00
100	1.775E+01	1.133E+01	1.732E+01	1.082E+01	1.312E+01	1.844E+01	3.047E+01	1.076E+01	1.442E+01	1.479E+01

Formulas used for calculation:

Table A 16: List of all formulas used for calculations

calculated value	formula			formula number
mean or average $\bar{x}$	$\bar{x} = \frac{\sum x_i}{n}$	x_i n	measured value number of values	(1)
standard deviation SD	$\mathrm{SD} = \sqrt{\frac{\sum (x_i - \bar{x})^2}{(n-1)}}$			(2)
relative standard deviation RSD [%]	$\mathrm{RSD} = \frac{\mathrm{SD}_{x_n}}{\bar{x}_n} * 100$	SD_{xn} $\bar{x}_n$	standard deviation of n measured values mean value of n measured values	(3)
recovery [%]	$\frac{area_{IS\,ex}}{area_{IS\,dir}} * 100$	$area_{IS\,ex}$ $area_{IS\,dir}$	area under the curve of the extracted IS area under the curve of the directly measured IS	(4)
accuracy [%]	$\frac{\sum \left(\frac{measured\ conc_i}{actual\ conc_i} * 100\right)}{n}$	measured $conc_i$ actual $conc_i$	concentration result obtained by MS –analysis actual concentration	(5)
inter-day precision (= RSD) [%]	$\frac{\mathrm{SD}_{x_{n(1+2)}}}{\bar{x}_{n(1+2)}} * 100$	$SD_{xn(1+2)}$ $\bar{x}_{n(1+2)}$	standard deviation of n measured concentrations of day 1 and 2 mean concentration of n measured concentrations of day 1 and 2	(6)
LOD x_{LOD}	$x_{LOD} = s_{x0} * t_{f,\alpha} * \sqrt{\frac{1}{m} + \frac{1}{n_{cal}} + \frac{\bar{x}_{cal}{}^2}{Q_x}}$	s_{x0} $t_{f,\alpha}$ f α m n_{cal} Q_x $\bar{x}_{cal}$	process standard deviation student factor degree of freedom; significance level; α=4% for HETEs &LTB_4; for PGs, HEPEs,TXs α=6% amount of measurements per calibration sample; m=1 amount of calibration samples deviance mean concentration	(ÖNORM-DIN-32645, 2011) (7)
LOQ x_{LOQ}	$x_{LOQ} = k * s_{x0} * t_{f,\alpha} * \sqrt{\frac{1}{m} + \frac{1}{n_{cal}} + \frac{((k * x_{LOD}) - \bar{x}_{cal})^2}{Q_x}}$	1/k	factor for relative uncertainty of the result; k=3	(ÖNORM-DIN-32645, 2011) (8)

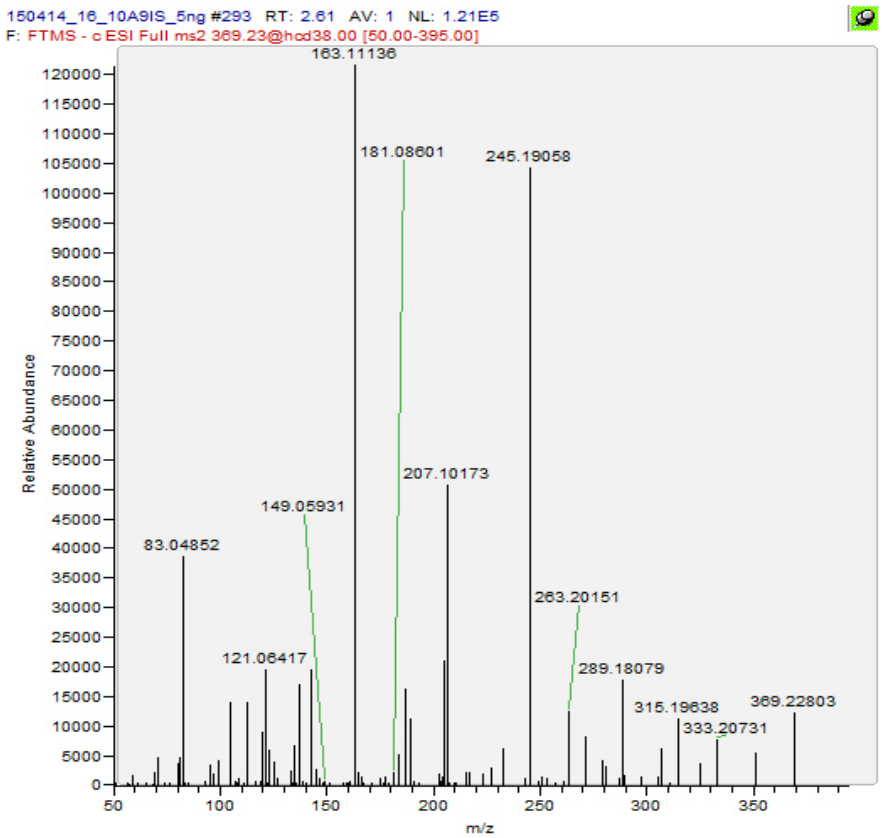

Figure A 1: Mass spectrum of 6-keto-PGF$_{1\alpha}$ in a 5 ng/ml analyte solution; obtained via targeted MS² in negative mode on a Q Exactive™ MS

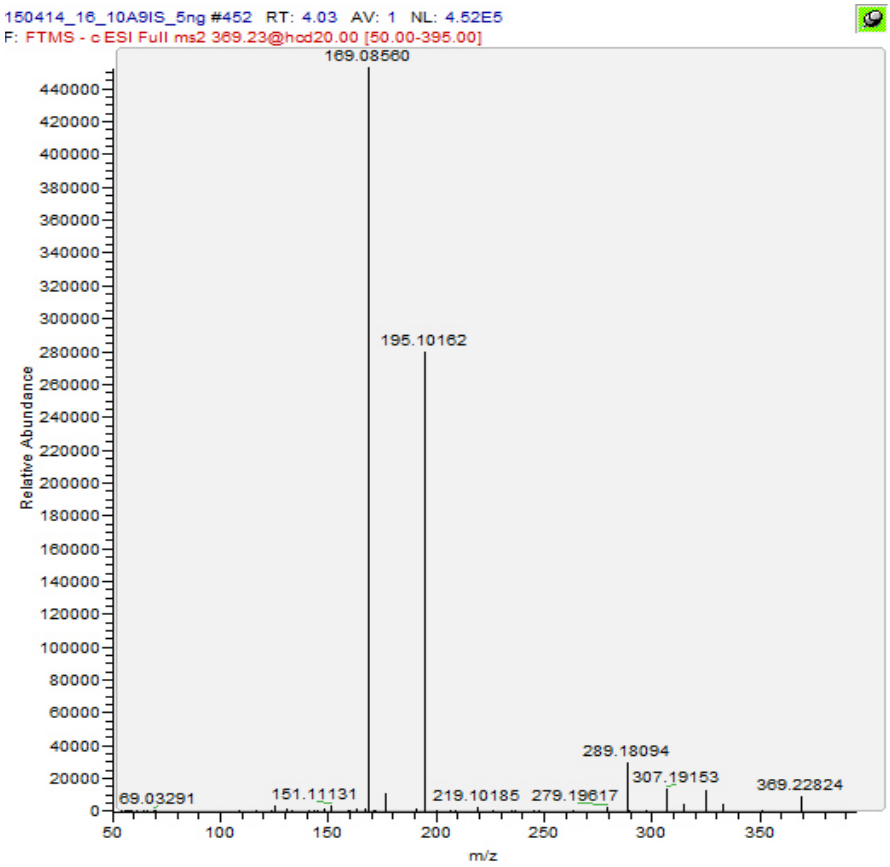

Figure A 2: Mass spectrum of spectrum of TXB$_2$ in a 5 ng/ml analyte solution; obtained via targeted MS² in negative mode on a Q Exactive™ MS

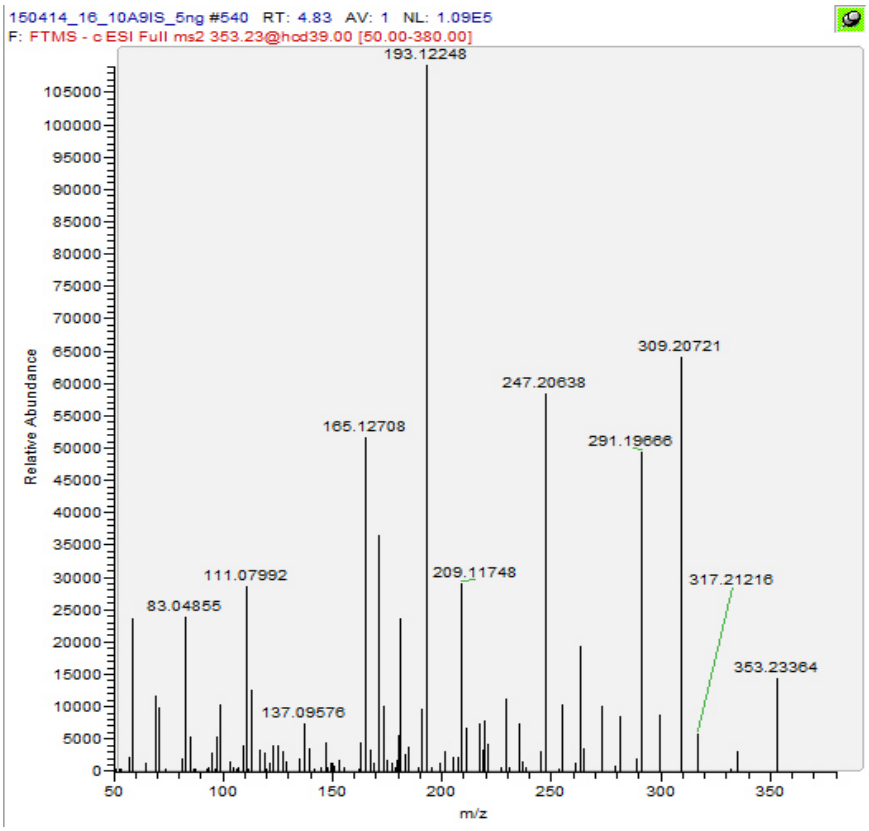

Figure A 3: Mass spectrum of $PGF_{2\alpha}$ in a 5 ng/ml analyte solution; obtained via targeted MS^2 in negative mode on a Q Exactive™ MS

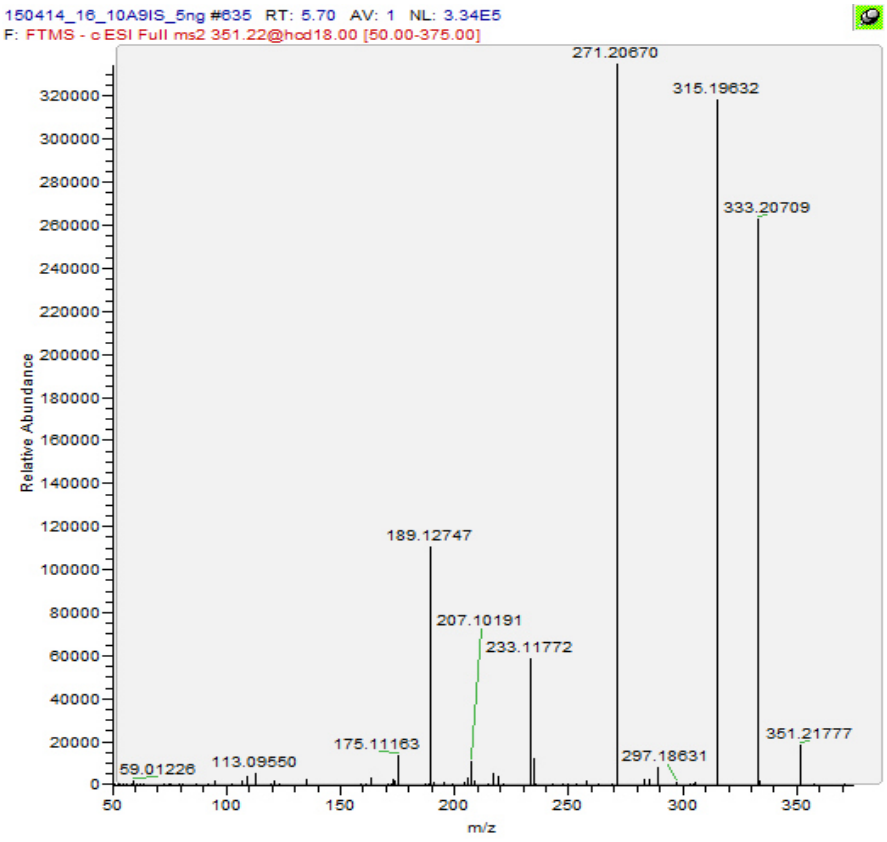

Figure A 4: Mass spectrum of PGE_2 in a 5 ng/ml analyte solution; obtained via targeted MS^2 in negative mode on a Q Exactive™ MS

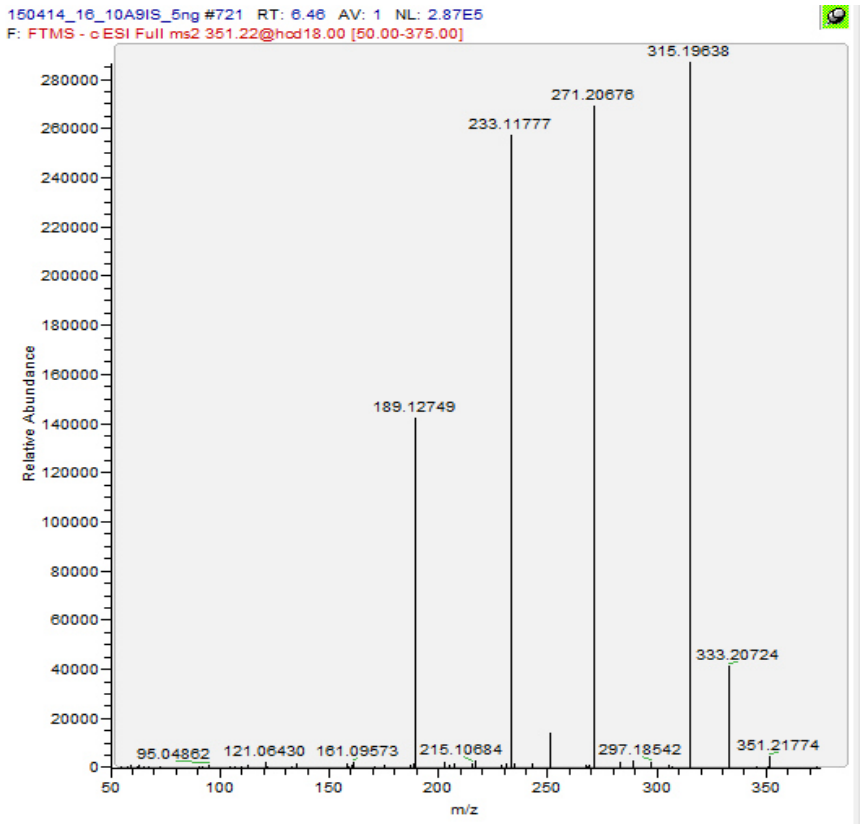

Figure A 5: Mass spectrum of PGD_2 in a 5 ng/ml analyte solution; obtained via targeted MS^2 in negative mode on a Q Exactive™ MS

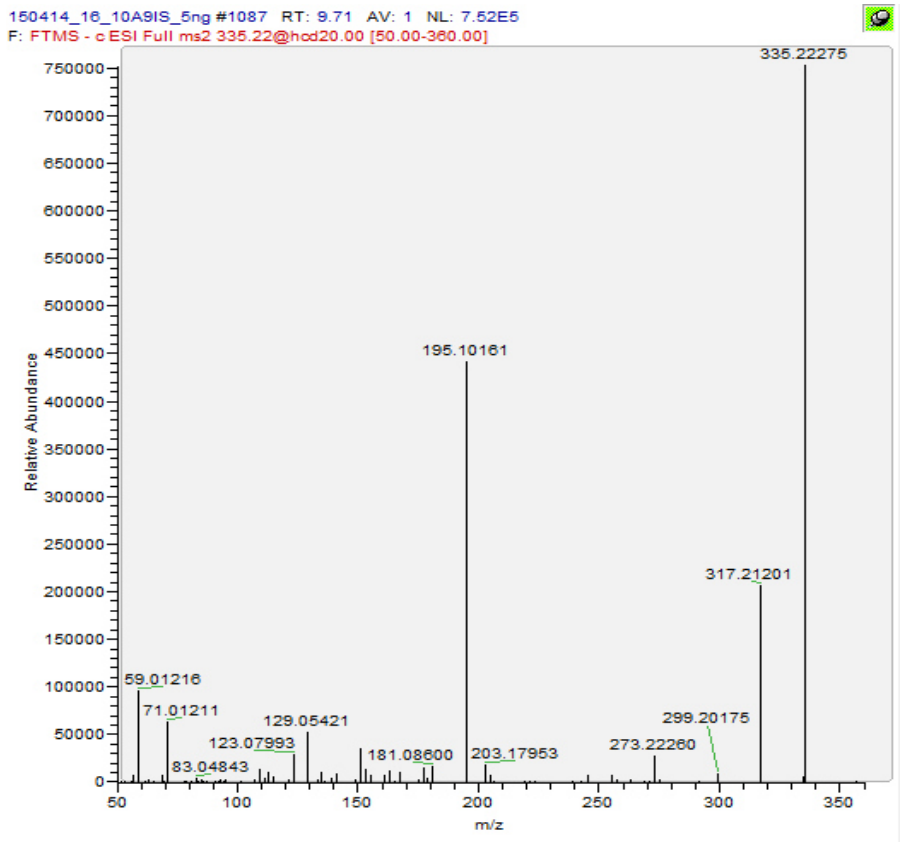

Figure A 6: Mass spectrum of LTB_4 in a 5 ng/ml analyte solution; obtained via targeted MS^2 in negative mode on a Q Exactive™ MS

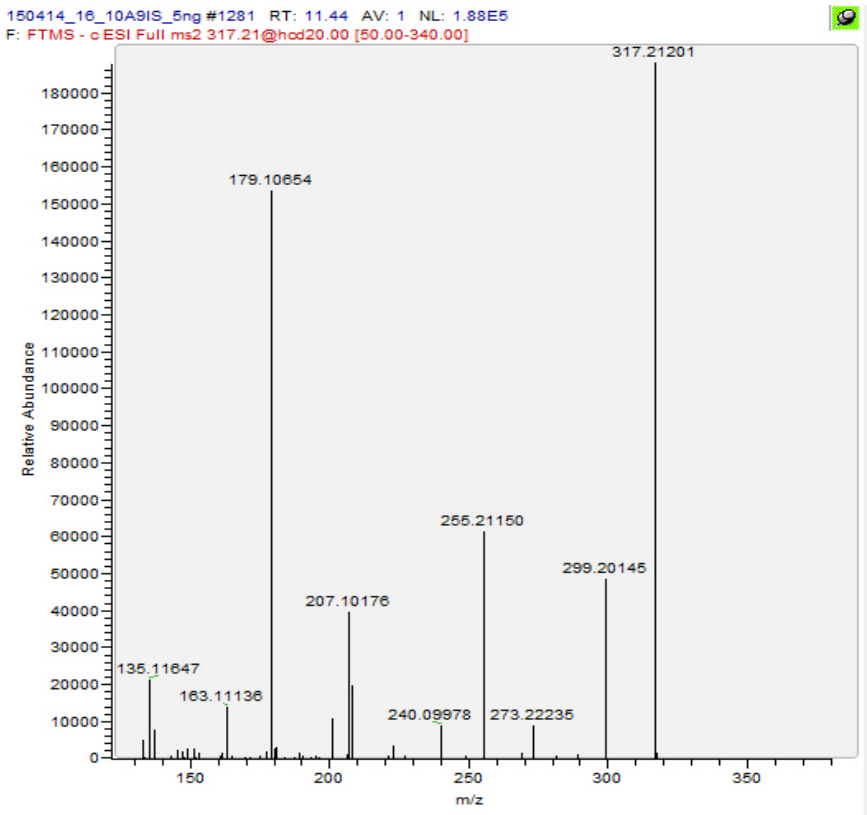

Figure A 7: Mass spectrum of 12-HEPE in a 5 ng/ml analyte solution; obtained via targeted MS² in negative mode on a Q Exactive™ MS

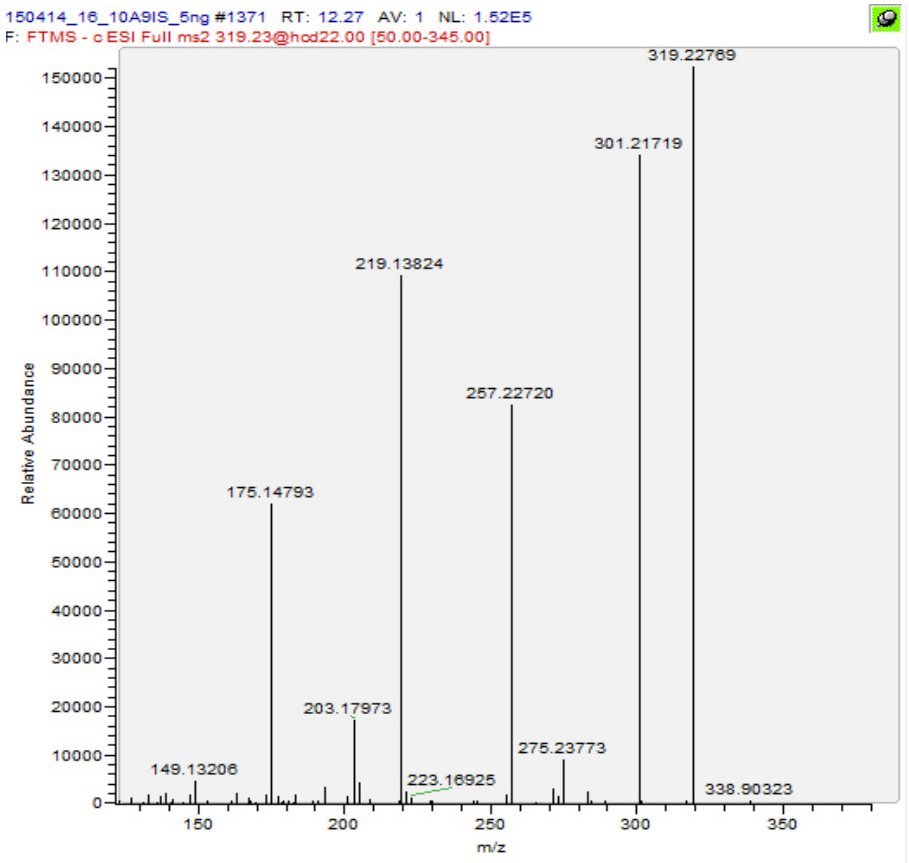

Figure A 8: Mass spectrum of 15-HETE in a 5 ng/ml analyte solution; obtained via targeted MS² in negative mode on a Q Exactive™ MS

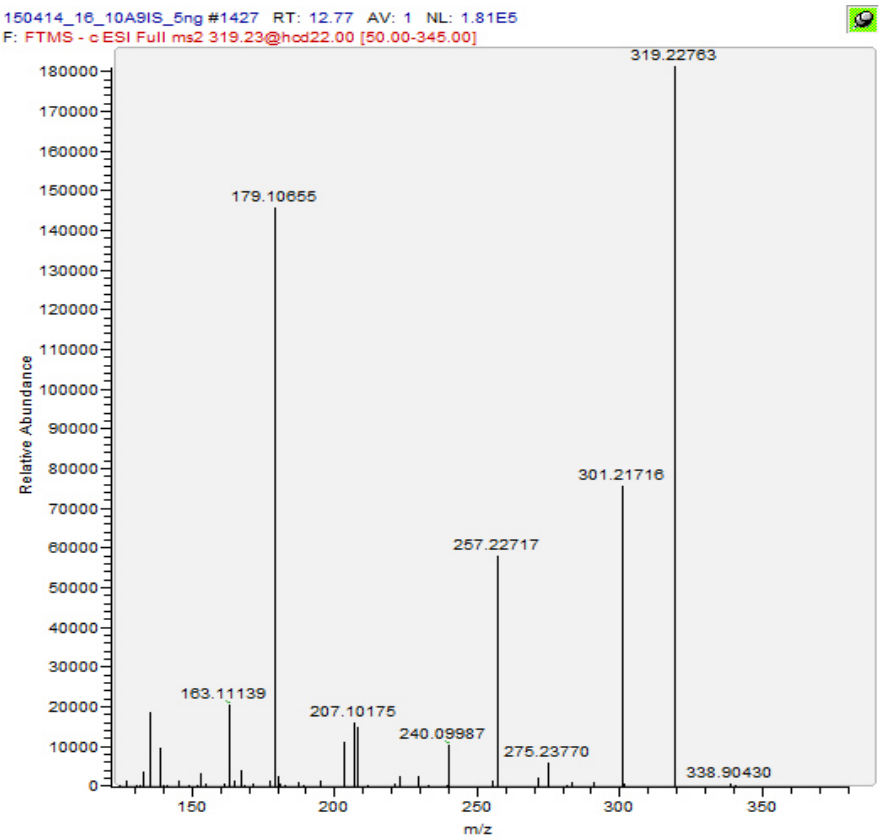

Figure A 9: Mass spectrum of 12-HETE in a 5 ng/ml analyte solution; obtained via targeted MS² in negative mode on a Q Exactive™ MS

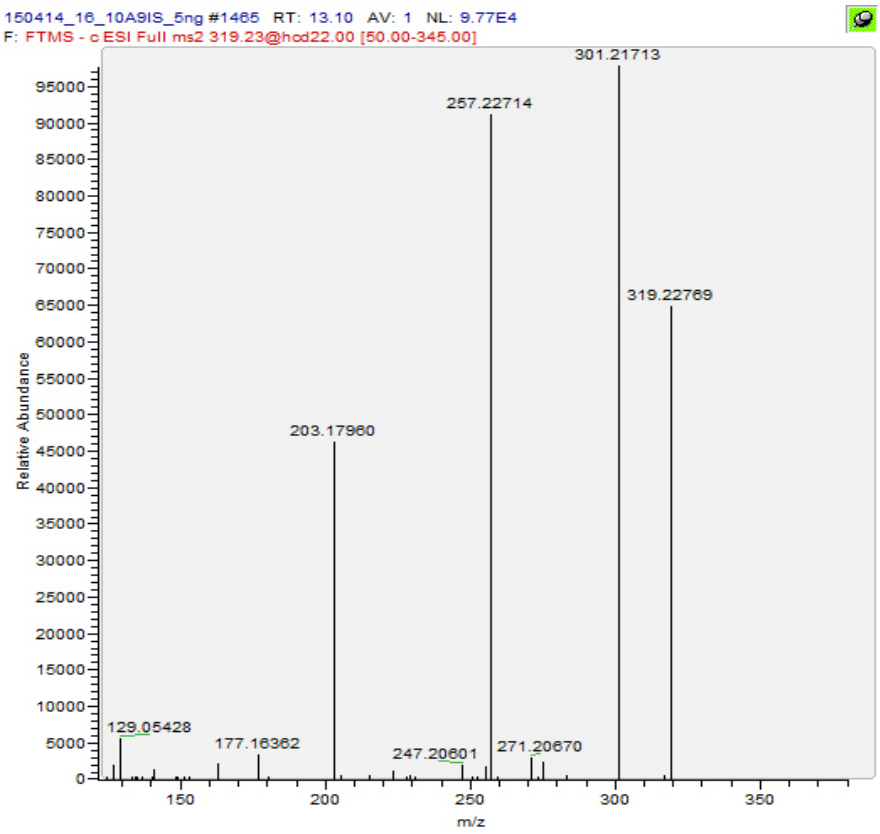

Figure A 10: Mass spectrum of 5-HETE in a 5 ng/ml analyte solution; obtained via targeted MS² in negative mode on a Q Exactive™ MS